NTNU – Trondheim
Norwegian University of
Science and Technology

Analysis of an Intermediate Band Solar Cell System

Based on Systems Engineering Principles

Anne Elisabeth
Thorstensen

Chemical Engineering and Biotechnology
Submission date: December 2013
Supervisor: Fride Vullum, IMTE
Co-supervisor: Annik Magerholm Fet, IØT
Turid Worren Reenaas, IFY

Norwegian University of Science and Technology
Department of Materials Science and Engineering

Preface

This report describes the master's thesis carried out in the course "TMT4900 Materials Chemistry and Energy Technology, Master Thesis". Fride Vullum-Bruer (Dep. of Materials Science and Engineering) has been the supervisor, and Turid Worren Reenaas (Dep. of Physics) and Annik Magerholm Fet (Dep. of Industrial Economics and Technology Management) have been co-supervisors during this work. They have guided me throughout this process, and contributed in different technology fields. I would like to express my thanks to them. Also, I would like to thank my fellow students who have helped me during the last preparations of the thesis.

By doing this master's thesis, I have been part of a new research activity on NTNU; the interdisciplinary project "Socially Robust Solar Cells (SoRoSol)" which deals with sustainable development of intermediate band solar cells (IBSCs), and has been carried out in the solar cell physics group at the Department of Physics at NTNU. In addition, as a chemist and materials engineer, it was a rewarding experience to study a completely new field for me; systems engineering, and I gathered knowledge outside the boarders of my study program.

I, Anne Elisabeth Thorstensen, declare that the work described in this report has been done in accordance with the regulations at NTNU.

Trondheim, December 2013.

Abstract

The intermediate band solar cell (IBSC) is a so-called third generation solar cell, based on a new type of semiconductor materials; the intermediate band (IB) materials. In IB materials there is an additional intermediate energy band in the band gap of the semiconductor. Solar cells using such materials have an efficiency limit of 63 % in comparison to 41 % for solar cells made of conventional semiconductors. IBSCs have been attempted realized since 2001, based on toxic or non-abundant materials only. For sustainable development of IBSCs, it is important to identify materials and production routes that result in minimized environmental impacts.

Two possible host materials for IBSCs were identified during a previous specialization project, and these were used as case materials to explore the challenges related to realization of sustainable IBSCs. This thesis describes the analysis of an IBSC system based on a ZnO/IB-Cu_2O/Cu_2O cell. The main objective was to analyze and optimize this intermediate band solar cell to determine if ZnO and Cu_2O are promising IBSC materials.

To get an overview of the functions and relationships of a complete IBSC system, a method combining the detailed materials technology field and holistic systems engineering process was utilized. This unusual combination and the fact that IBSCs are a relatively new and unexplored concept, resulted in a customized approach.

Sustainable solutions for large-scale production of the IBSC with focus on cell structure and materials were explored. Two cell cases were developed; an "advanced" cell with high quality materials and production, and one "simple" cell with a more conventional production route and less complex materials. The location of the desired IBSC system installation was set to a rooftop in Oslo, and a conventional photovoltaic (PV) system being planned there was the basis for a system example. Desired and location-based performance parameters for an IBSC system located in Oslo were identified.

A new approach that can solve combined materials technology and systems engineering assignments was developed. By utilizing this approach, challenges for ZnO and Cu_2O as IBSC host materials were identified. The material challenges proved to be comprehensive, but might be overcome by customized growth of Cu_2O single crystals to reduce resistivity, and tailoring the buffer layer and surface treatment at the ZnO/IB-Cu_2O junction to reduce unwanted interface defects. The findings in this thesis implied that the ZnO/IB-Cu_2O/Cu_2O IBSC could be manufactured for industrial purposes to compete with other PV technologies if the material challenges are overcome.

Sammendrag

Mellombåndsolcellen er en såkalt tredje generasjon solcelle, basert på en ny type halvledermaterialer; mellombåndsmaterialer, også kalt IB-materialer. I IB-materialer er det et ekstra energibånd i båndgapet til halvlederen. Solceller laget av slike materialer har en teoretisk effektivitetsgrense på 63 % sammenlignet med 41 % for solceller laget av konvensjonelle halvledere. Siden 2001 har det vært fler forsøk på å produsere mellombåndsolceller, men disse har kun basert seg på sjeldne eller giftige materialer. For bærekraftig utvikling av mellombåndsolceller er det viktig å identifisere materialer og produksjonsmetoder som fører til minimale miljøpåvirkninger.

To mulige vertsmaterialer for mellombåndsolceller ble identifisert under et tidligere spesialiseringsprosjekt. Disse ble brukt som case-materialer i denne oppgaven for å utforske utfordringer knyttet til realisering av bærekraftige mellombåndsolceller. Denne masteroppgaven beskriver analysen av et mellombåndsolcellesystem basert på en ZnO/IB-Cu_2O/Cu_2O celle. Hovedmålet var å analysere og optimalisere denne mellombåndsolcellen og avgjøre om ZnO og Cu_2O er lovende materialer for mellombåndsolceller.

For å få en oversikt over funksjoner og relasjoner mellom komponentene av et komplett mellombåndsolcellesystem, ble detaljert materialteknologi og den helhetlige systems engineering prosessen kombinert. Denne uvanlige kombinasjonen og det faktum at IBSCs er et relativt nytt og uutforsket konsept, resulterte i en ny og spesialtilpasset metode.

Bærekraftige løsninger for storskalaproduksjon av mellombåndsolceller med fokus på cellestruktur og materialer ble utforsket. To celle caser ble utviklet, en «avansert» celle med høykvalitetsmaterialer og -produksjon, og en «enkel» celle med en mer konvensjonelle produksjonsmetoder og mindre komplekse materialer. Plasseringen av det ønskede mellombåndssolcellesystemet ble valgt til et tak i Oslo, og et konvensjonelt krystallinsk solcellesystem som planlegges å installeres der dannet grunnlaget for et systemeksempel. Lokasjonsbaserte og spesifiserte ytelsesparametere for et mellombåndsystem med beliggenhet i Oslo-området ble identifisert på grunnlag av behov og krav bestemt tidligere i prosessen.

En ny tilnærming som kan løse kombinerte materialteknologi og systems engineering-baserte oppgaver ble utviklet gjennom denne masteroppgaven. Utfordringer vedrørende ZnO og Cu_2O som vertsmaterialer for mellombåndsolceller ble identifisert ved å benytte denne tilpassede metoden. De materielle utfordringene viste seg å være omfattende, men kan løses ved å tilpasse enkrystallveksten av Cu_2O som vil redusere resistiviteten, og skreddersy et bufferlag og overflatebehandling for ZnO/IB-Cu_2O-grenseflaten for å redusere uønskede defekter. Funnene i denne masteroppgaven antydet at ZnO/IB-Cu_2O/Cu_2O mellombåndsolcellen kan produseres for industrielle formål og konkurrere med andre PV teknologier dersom de materielle utfordringene blir løst.

Contents

List of abbreviations

3J	Three terminal multi-junction
AC	Alternating current
ALD	Atomic layer deposition
AM	Air mass
ARC	Anti-reflective coating
a-Si	Amorphous Silicon
AZO	Al-doped zinc oxide
a-ZTO	Amorphous zinc tin oxide
BIPV	Building integrated photovoltaics
BOS	Balance of system
BSF	Back surface field
CB	Conduction band
CED	Cumulative energy demand
CIGS	Copper indium gallium diselenide
c-Si	Crystalline Silicon
CVD	Chemical vapor deposition
CVT	Chemical vapor transport
DC	Direct current
DNI	Direct normal irradiation
DSSC	Dye-sensitised solar cell
EPBT	Energy pay-back time
EPIA	European Photovoltaic Industry Association
Eq.	Equivalents
EVA	Ethylene vinyl acetate
FSF	Front surface field
FU	Functional unit
FZ	Floating zone/float zone
GHG	Greenhouse gases
GWP	Global warming potential
GZO	Ga-doped ZnO
HMA	Highly mismatched alloys
I	Current
IB	Intermediate band
IBSC	Intermediate band solar cell
IR	Infrared
ISO	International Organization for Standardization
ITO	Indium tin oxide
I-V	Current-Voltage

LCA	Life cycle assessment
LCI	Life cycle inventory
LCIA	Life cycle impact assessment
MBE	Molecular beam epitaxy
mc-Si	Multicrystalline silicon
MJ	Multi-junction
mono-Si	Single/mono-crystalline Silicon
MOCVD	Metal-organic chemical vapor deposition
MPP	Maximum power point
MPPT	Maximum power point tracking
N.A/n.a.	Not available
NRR	Non-radiative recombination
NOCT	Nominal operating cell temperature
NTNU	Norwegian University of Science and Technology
P	Power
PCM	Potential for CO_2 mitigation
PECVD	Plasma-enhanced chemical vapor deposition
PLD	Pulsed laser deposition
PR	Performance ratio
PV	Photovoltaic
QD	Quantum dot
QFL	Quasi-Fermi level
R&D	Research and development
Rf	Radio frequency
sc-Cu_2O	Single crystal cuprous oxide
sc-Si	Single/mono-crystalline silicon
SE	Systems engineering
SENSE	Sustainability Evaluation of Solar Energy Systems
SEP	Systems engineering process
SoRoSol	Socially robust solar cells (project at NTNU)
STC	Standard conditions
TCO	Transparent conducting oxide
TF	Thin film
UHD	Ultra high doping
UV	Ultraviolet
V	Voltage
VAPE	Vacuum arc plasma evaporation
VB	Valence band
ZO	Un-doped zinc oxide
ZTO	Zinc tin oxide

1 Introduction

For a number of years, energy resources like coal, petroleum and natural gas have dominated the world's energy market. Refining and consumption of these fossil fuels contribute to global warming and air pollution, and are also harmful to the earth's ecosystem both on- and offshore. With regard to energy systems, many projects aimed at mitigating these problems, and also to fulfill the increasingly restrictive environmental laws are being planned. Many countries have introduced policies to promote the installation of new renewable source plants in order to reach the Kyoto protocol targets, and specific mention to photovoltaic plants is reported [1]. Photovoltaic energy conversion is widely considered as one of the more promising renewable energy technologies, which has the potential to contribute significantly to a sustainable energy supply and may help to mitigate greenhouse gas emissions [2].

The need for rational use of resources is rapidly increasing with population growth and increased quality of life, especially in the third world countries. An unlimited resource for energy can be the solution to all the energy-related problems mentioned above. The power the sun irradiates on our planet is estimated to be about 175,000 TW, four orders of magnitude more than the power used worldwide, even in the most energy intensive times [3]. In addition to being the most abundant energy source on earth, solar power is also considered one of the cleanest of renewable energy resources [4]. The public opinion, too, is particularly favorable to the use of solar energy, which seems to be without any environmental impact [5].

However, there are some challenges regarding the current photovoltaic (PV) technologies. The cost versus efficiency issue and the question if new PV technologies can be developed and operated with minimal environmental impacts are addressed below.

1.1 The efficiency and cost challenge

The high cost and relatively low efficiency of solar conversion technology is currently an essential problem to be resolved before solar energy can become a major contributor on the energy market. Green [6] has described the future trends in photovoltaics by defining three generations of solar cells, each with characteristic cell costs and efficiency. Figure 1.1 [7] illustrates these three generations. The first generation is crystalline cells primarily made of silicon (Si) that have become commercially available over the last decades. The installed solar cell capacity has grown by almost 60 % annually since 2006. The global cumulative solar cell capacity was 7.3 GW in 2006, and in 2011 it had increased to 71.3 GW [8]. For this growth to continue, costs must fall further. The second-generation solar cells have comparable and lower efficiency to first-generation cells, see Figure 1.1, but are cheaper to make. They consist of thin-films that contain less silicon, or alternative materials such as copper–indium–diselenide and cadmium-telluride. Green predicts further that 1st generation cells eventually will get as cheap to fabricate as the 2nd generation, and thus instead markedly higher efficiencies are needed; the third-generation cells. These have fundamentally different designs that the 1st and 2nd generation, each harvesting a larger fraction of the sunlight, and thus achieve efficiencies above 30 % [9]. They are currently too expensive to be used with normal sunlight intensity (1 sun illumination). To achieve the predicted cost reduction, they are mounted at the focus of cheap lenses or mirrors known as concentrators or collectors that maximize the amount of sunlight harvested by each cell, effectively increasing the cell efficiency. One can then allow for expensive solar cells, since a smaller cell area is needed.

One of the proposed third generation solar cell concepts are intermediate band solar cells (IBSCs), that is targeted in this master's thesis.

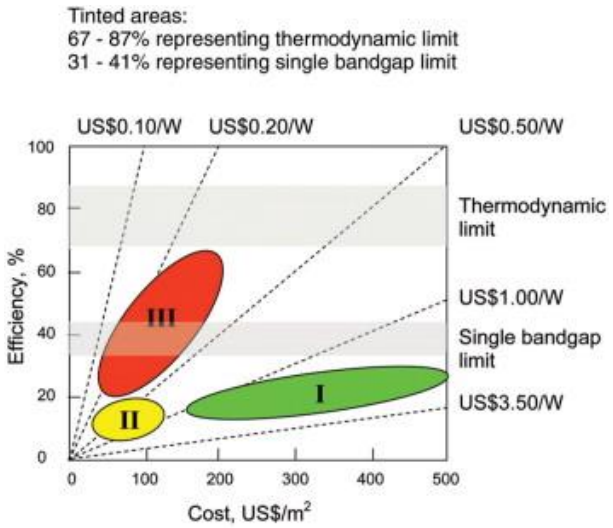

Figure 1.1: Efficiency versus cost for the three generations of solar cells; crystalline (1st generation), thin films (2nd generation), and new solar cell designs (3rd generation) [7].

1.2 The intermediate band solar cell (IBSC) concept

As early as 1960 Wolf proposed the use of energy levels situated in the forbidden gap of semiconductors to increase solar cell efficiency, by absorbing photons of energy below the band gap [10]. Several attempts were made to further develop this concept, and in 1997 Luque and Marti presented a more detailed theory on how introducing an intermediate energy level or band in the semiconductor band gap will increase the efficiency of solar cells significantly [11]. This technology was later labeled intermediate band solar cells (IBSCs) [12], and are, as already mentioned, part of the promising third generation PVs.

The IBSC is a novel photovoltaic converter with the possibility of exceeding the performance of conventional p-n solar cells [11], and lower the electricity cost [13]. There are primarily two types of intermediate band materials that are currently studied; quantum dot (QD) materials and bulk intermediate band materials. Luque and Marti describe these two concepts in a report from 2010 [13]. In the first concept, nano-crystal quantum dots are embedded in a semiconductor, or barrier material, and the intermediate band arises from the confined states of electrons in the conduction band potential wells. These wells originate from the conduction band offset between the dot and barrier material.

In the second concept, the intermediate band is formed by a high density (up to a few %) of individual atoms added to a *host* semiconductor to form an alloy or a highly doped material. These materials can support higher densities of intermediate band states than with quantum dots, and can thus achieve stronger absorption of below band gap photons than the first concept. The bulk intermediate band states can be formed by fabrication of so-called highly mismatched alloys (HMA), e.g. ZnTe:O, or ultrahigh doping (UDH) by dopants forming deep levels, e.g. GaAs:Ti.

Walukiewicz *et al.* was in 2000 the first to discover the new class of highly mismatched semiconductor alloys that later lead to the HM-IBSC concept [14]. These mismatched alloys' electronic properties are strongly dominated by a band anticrossing interaction between

localized states of isoelectronic impurities (e.g. oxygen) and the extended states of the semiconductor matrix, e.g. ZnTe, that lead to IB formation. The second bulk IB concept was presented by Luque *et al.* [15], where they show that non-radiative recombination can be suppressed in deep level-doped materials if the wave functions of the electrons trapped in the impurities become delocalized, as they are in the conduction and valence bands. This can occur if the impurity concentration is increased until the impurities are close enough to interact with each other.

The current challenge with IBSCs is to identify materials with suitable properties to approach the theoretical IBSCs efficiency potential of 63.1 % compared to a limit of 40.7 % for a conventional (first and second generation) solar cell under the same operating conditions [11]. The most studied IBSC concept is the QD-IBSC. The best success so far resulted in 18.7 % efficiency in an InAs/GaAs IBSC [16]. All of the three elements in this cell are either toxic or non-abundant, and so far no sustainable materials have been used in IBSCs [13].

At the Norwegian University of Science and Technology (NTNU), IBSCs have been studied since 2005. First, QD-IBSCs was in focus, but to move towards a sustainable realization of the IBSC technology, bulk materials are needed. In the Socially Robust Solar Cells (SoRoSol) project at NTNU, Cr-doped ZnS has been studied for a couple of years, but the band gap is not optimal for an IB material. A specialization project was therefore conducted to identify new IB materials with more suitable properties [17]. The objectives of the SoRoSol-project involve building a platform for socially robust development of high efficient IBSCs by (1) performing materials research that leads to robust innovation, (2) studying health, safety and environmental aspects of the life cycle of solar cells made of these materials and (3) studying the potential changes in technology design and values in the different disciplines.

One more step towards the SoRoSol-goal of introducing IBSCs on the market would be to evaluate the sustainability of a complete IBSC system from raw materials extraction to end of life. Life cycle assessment (LCA) would be a suitable method for this evaluation, and it was the initial goal for this thesis.

1.3 Life cycle assessment and systems engineering

The development of sustainable technologies requires an overall evaluation of the product's environmental impacts and benefits. During the operation phase, the photovoltaic technology can be considered almost absolutely clean. However, evaluating the production process of solar panels is important to consider the emissions and energy consumption during the whole panel life. For these reasons, only a deeper analysis can give a more correct basis to evaluate the real environmental sustainability of PV technology [5]. Traditional environmental impact analyses generally focus on a restricted number of life cycle steps. This approach is very narrow because it gives only a restricted picture of the effective environmental performances of the product. In renewable energy plants generally the largest environmental impacts occur during the manufacture and installation steps [18].

Life cycle assessment (LCA) is a tool for assessing the environmental impacts of a product or product system over its entire life cycle. This involves quantifying the inputs of materials and energy, and output of pollutants and waste during the life cycle stages of the system studied [19]. Every life cycle phase from resource extraction to end-of-life management is taken into account if a so called "cradle to grave" LCA is performed. If a shorter path of the life cycle is preferred, a "cradle to gate" or "gate to gate" LCA can be considered. The LCA approach

gives the possibility to compare the environmental performance of different product systems performing the same function. LCA is therefore a powerful tool to evaluate the environmental impact of different energy systems or alternatives of the same type of system, e.g. two different PV technologies, over their entire life cycle. See Chapter 3 for a short description of the LCA framework and a review of LCA performed on PV systems.

To conduct a LCA, the whole system with all processes and every energy and material flow within the system boundaries should be known. A new technology can therefore be difficult to evaluate through a LCA. First, the system parameters must carefully be selected, and a complete system design must be ready to undergo the extensive LCA evaluation.

The initial goal of doing a LCA for a complete IBSC system turned out to be unrealistic. Far out in the timeline for the thesis, the uncertainties, alternatives and choices needed to evaluate and design this system proved to be more than enough for a master's thesis itself. The holistic perspective required from the SoRoSol-project suggested that a top-down method would be appropriate for the new goals for the thesis, further explained in the next section.

Systems engineering (SE) is a management technology for designing or improving a system. The systems engineering process (SEP) approach involves transformation of needs and requirements into a set of system products and process descriptions, generation of information for decision makers and formulation of input for next level of development [20]. This methodology can be used to plan and develop a system based on technological and environmental needs and requirements, that later can be the basis for a complete LCA study of the IBSC system. Usually SEP requires attention to all parts of an integrated system, including technology, environment, bioware, software and economy, but regarding the goal of a specific system study, the focus can be put on the most important discipline(s) for achieving that goal. The SEP methodology based on a six steps sequential approach [21] that will be performed in this master's thesis is described in section 5.1 and 5.2, and conducted in the results Chapters 6 to 10.

1.4 Objectives and limitations

As a step towards the long term goal at NTNU of realizing large scale deployment of intermediate band solar cells, the challenges related to identifying a complete bulk IBSC system will here be analyzed by the systems engineering approach with focus on technology. The interactions with the environment will also be considered, to ensure a sustainable IBSC system.

The starting point for this master's thesis was the results from a specialization project [17] conducted for the same interdisciplinary project group; SoRoSol. During the specialization project called "New Materials for Intermediate Band Solar Cells", materials with the potential to satisfy IB host material requirements were identified. Two of the materials that exhibited these properties were the oxides Cu_2O and ZnO. These were chosen as case materials to study a heterostructure IBSC system based on sustainable host materials in this thesis.

Goals

As mentioned above, the initial goal for the thesis was to conduct a full LCA based on processes and flows that can be suitable for the new IBSC system. To manage this in a way that would be scientifically reliable, the system would first have to be described in detail

based on environmental and technological requirements. This can be done by combining the SE methodology (see section 5.1) and LCA. As might have been expected, the planning phase facilitated by the SEP turned out to be a complete master's thesis in itself. The detailed and holistic goals for the SEP approach conducted here were defined as:

- Identify needs and requirements regarding the complete IBSC system.
- Describe the desired performance of the IBSC system, including a functional analysis of the IBSC device.
- Investigate and choose compatible materials and production route(s) for the Cu_2O/ZnO-based IBSC.
- Perform an optimization phase to find the best alternatives for the IBSC.
- Look at a system example at a specified location.

The overall goal is to identify challenges regarding materials and production of an IBSC system based on a Cu_2O/IB-Cu_2O/ZnO heterojunction.

The total result was a number of choices and arguments for each part of the IBSC device and a case example of a complete IBSC system. These results will form the basis for an IBSC system that can be evaluated further by LCA or another environmental research tool. The location is set to Oslo to get an idea of how an IBSC system will operate on a building in this area.

Outline

In Chapter 2, photovoltaics, in particular the IBSC concept, and production methods for solar cell materials are first explained. In section 2.4 and 2.5 the module components and units added to make up a PV system are described, and parameters influencing PV systems are mentioned in section 2.6. Chapter 3 is a literary review of LCA studies of PV systems. This review was initially done to facilitate a LCA study of the IBSC system, and was kept for other purposes after the thesis objective was changed. Chapter 4 is a background literary review of heterostructure solar cells based on Cu_2O and ZnO and IBSC synthesis.

The steps 1-5 of the SEP described in Chapter 5 are conducted in Chapters 6 to 10, including some subchapters where important choices that influence the rest of the process are discussed.

In Chapter 11, the process used in this thesis with emphasis on challenges experiences during the new method are discussed, and a conclusion is given in Chapter 12.

Throughout this thesis, several terms and abbreviations related to the IBSC and IBSC system are used:

IB material/IB-layer = intermediate band material, e.g. Cu_2O:N
IBSC host material = intermediate band solar cell host material, e.g. Cu_2O
IBSC = intermediate band solar cell
IBSC device = intermediate band solar cell
IBSC module = intermediate band solar cell module
IBSC system = intermediate band solar cell system
PV system = photovoltaic system, can be the IBSC system depending on the context

2 From solar cell to photovoltaic (PV) system

A solar cell is essentially a p-n junction illuminated by solar radiation. A brief introduction to solar radiation, the basic operation of solar cells, and the major loss mechanisms in solar cells are described in this section. For a brief introduction in photovoltaic (PV) theory, please see Appendix A.

In this chapter, the parts of a solar cell system are explained, from concept and production of solar cells to a complete system. First, the three generations of solar cells are explained. The structures of different solar cells are then compared in section 2.2, including a more detailed description of intermediate band solar cells (IBSC). In section 2.3 possible routes to high quality solar cell production are described. Next, the parts added when connecting solar cells to form a module are described in section 2.4. To complete a PV system, electrical components and mounting structure for the modules are needed. These parts of the system are investigated in section 2.5, and different parameters influencing the system performance are addressed in section 2.6.

2.1 The three generations

As mentioned in the introduction, the different photovoltaic technologies can be divided into three generations [22]. The first generation includes single- and multicrystalline Si-wafers (sc- and mc-Si) and a few other crystalline wafers, like GaAs. Crystalline silicon (c-Si) has reached a record efficiency of 25 %, but most commercial c-Si modules have efficiencies in the range of 13-19 % [23]. Among the second generation PVs, some of the thin film (TF) technologies are available on the market, and other are still under development. Commercial TF modules offer efficiencies between 6-12 %, with a target of 12-16 % by 2020 [23]. The third generation of PVs is a compilation of all new concepts that aim for higher efficiency by capturing more photons than are available according to the Shockley limit (see section 2.6.1). The Technology Brief for Solar Photovoltaics by The International Renewable Energy Agency (IRENA) and International Energy Agency's Energy Technology Systems Analysis Programme (IEA-ETSAP), expects that solar cells based on novel active layers will have efficiencies above 25 % during the period 2015-2020 and up to 40 % by 2030 [23].

An overview of the different PV technologies belonging to the three generations is given in Figure 2.1.

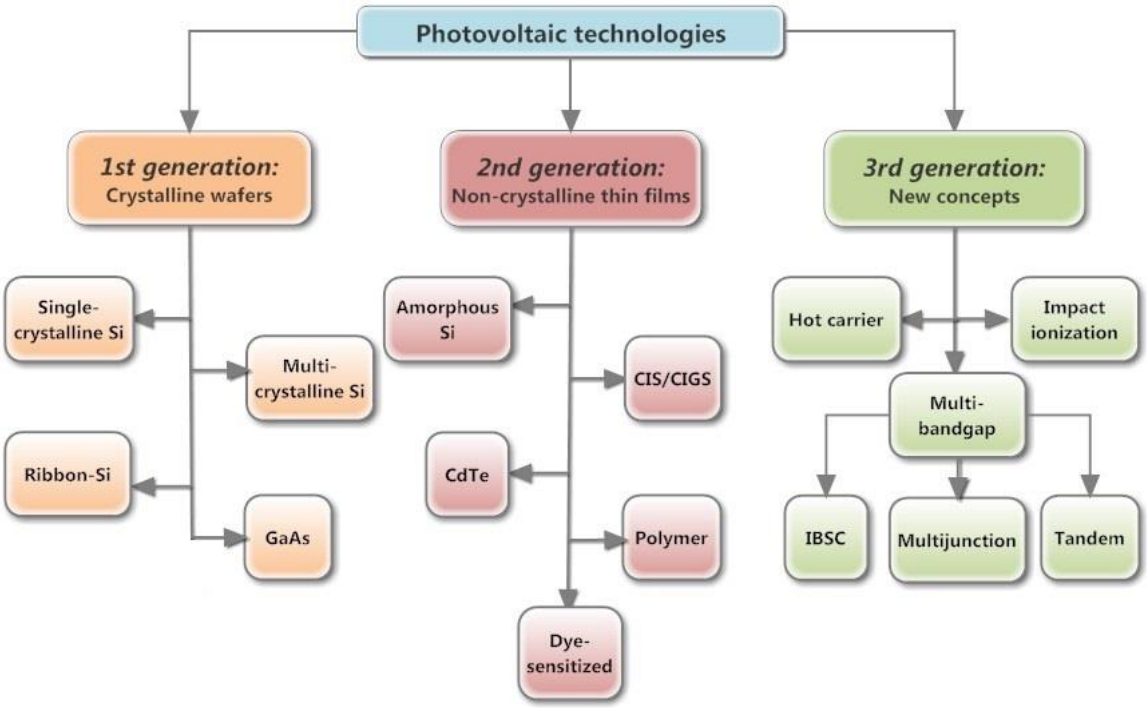

Figure 2.1: Overview of 1st generation; crystalline wafers, 2nd generation; thin films and the 3rd generation of new PV concepts under development.

Future outlook

Crystalline silicon technologies have dominated the PV market for the last 30 years [24]. According to the Photovoltaics Report by Fraunhofer Institute for Solar Energy Systems ISE (Fraunhofer ISE), bulk Si-wafer based PV technology accounted for about 86 % of the total shipments in 2011 and thin film technologies had a total share of 14 %. European Photovoltaic Industry Association (EPIA) expects that by 2020, a more balanced mix of existing PV technologies will be in place and new emerging technologies will be commercialized [24].

2.2 The solar cell

A typical solar cell exists of n-emitter, p-emitter, front- and back electrodes and an anti-reflective coating. The active n-emitter and p-emitter make up the p-n junction where electricity is generated, and the contacts carry this electricity to the electric circuit outside the cells.

To minimize light reflection at the surface of the solar cell, an anti-reflective coating (ARC) is applied. Crystalline silicon cells without ARC, e.g. in façade-integrated PV systems, are estimated to reflect up to 30 % of the sunlight [25]. The ARC should be transparent and have appropriate refractive index with regard to the surroundings, usually air or glass, and underlying layer.

In the case of multi-band gap cells, multiple layers (multi-junction) are added to the active layers. The conventional single junction silicon cell has a much simpler structure than the novel multi-junction cells of the third generation. Their two structures are shown in Figure 2.2 [26, 27].

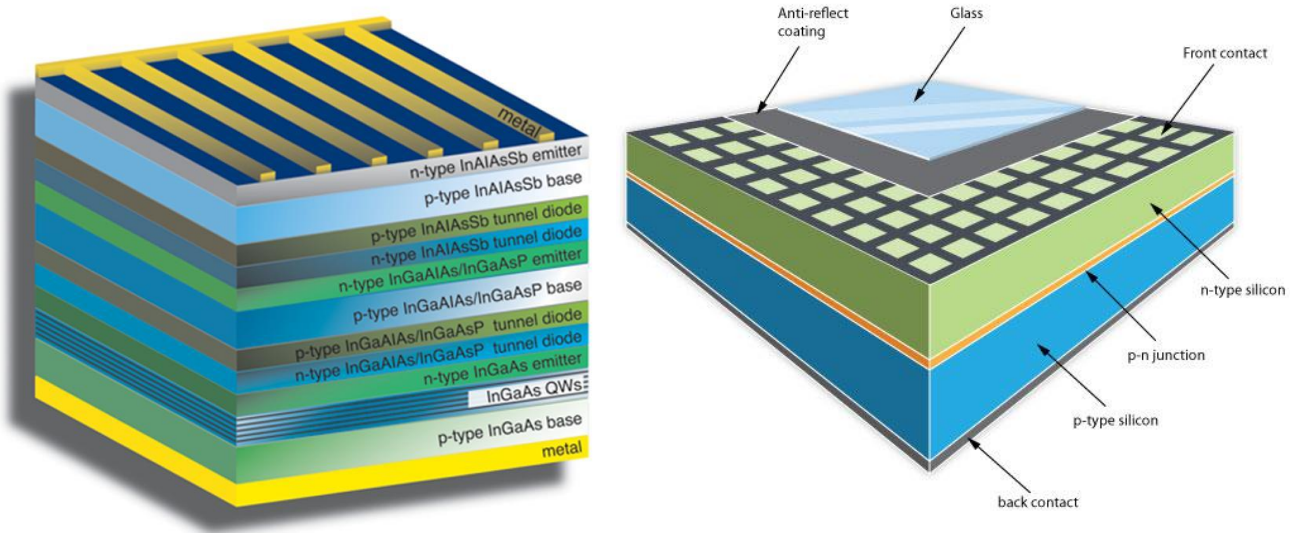

Figure 2.2: A multi-junction cell [26] to the left and a conventional Si-cell [27] to the right. The structures are shown to compare the complicity. The materials used are not of importance here.

The structures above should give a sense of the complicity of the multi-junction cells relative to the simple conventional cell. In the IBSC case, only one layer is added to the conventional solar cell structure, see Figure 2.3. This extra layer is the intermediate band layer, or IB-layer. The figure is not to scale, and the front contacts could be found under the anti-reflective coating, as seen for the Si-cell above.

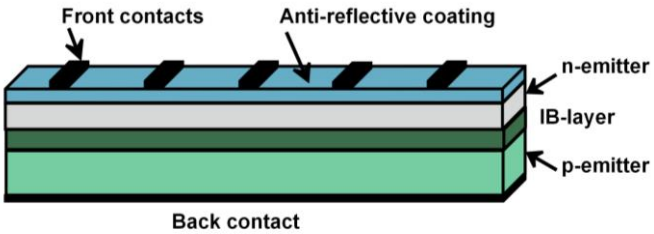

Figure 2.3: A schematic of a simple IBSC structure.

Intermediate band solar cells (IBSC) is a promising concept within the third generation of solar cells [11], [12]. The maximum efficiency of an IBSC is 63.1 % for maximum concentrated light, and 49 % for 1 sun, and equals that of a three-junction (3J) solar cell. A 3J cell and an IBSC both have three band gaps, but 3J cells are much more complex devices since they consist essentially of three cells, while IBSC is a single solar cell. Additionally, the IBSCs perform more stably in unsteady weather than 3J cells due to less severe constraints in current matching [28].

2.2.1 The intermediate band solar cell

There are some challenges concerning the realization of IBSCs. Some of these challenges will be outlined below, where the operation principle, cell geometry and material requirements of IBSCs are presented.

Operation principle

An intermediate energy band between the valence band and the conduction band of a semiconductor is what separates the IBSC from conventional solar cells. Figure 2.4 [29] shows a simplified band diagram of a material with an intermediate band (IB), also called host material, and the absorption processes that can take place in such a material.

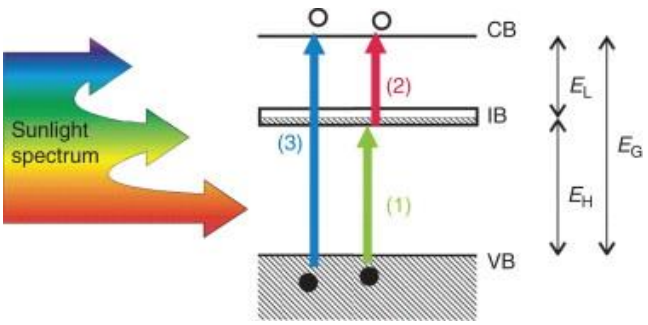

Figure 2.4: A simplified energy band diagram of an IB material. The main band gap, E_G, of the host material is split into two smaller band gaps; E_H and E_L. (1), (2) and (3) are the three possible absorption processes in the IBSC [29].

The IB divides the total band gap, E_G, into two smaller sub-band gaps, E_L and E_H, where $E_H > E_L$. Photons of energy below the main band gap can be absorbed by two transitions to and from the intermediate band (process (1) and (2) in Figure 2.4). Simultaneously, photons of energies higher than the main band gap (transition (3)) are also absorbed. Transition 1 and 2 allow a better exploitation of the solar spectrum, and thus increase the photocurrent compared to the case of a single-junction solar cell where only transition 3 is allowed.

The efficiency limit for a single IBSC is as high as 63.1 %, and is based on the following assumptions [11], [28]:

1. Only radiative recombination (no non-radiative recombination).
2. Infinite carrier mobilities.
3. Complete absorption of all photons with $E>E_L$ (no reflection).
4. No carriers extracted from the intermediate band, except for absorption and radiative recombination.
5. Optimal band gap of host material (1.9 eV), and the intermediate band is positioned 0.7 eV from the conduction band edge.

6. Fully concentrated black body radiation solar spectrum (6000 K).
7. Half-filled intermediate band.

As mentioned in the introduction, Luque and Marti first presented this efficiency limit for intermediate levels [11]. If however, the non-radiative recombination (NRR) is considered (assumption 1), the NRR will decrease the efficiency for IBSCs [12].

IBSC geometry

The geometry of an intermediate band solar cell first proposed by Luque and Marti is illustrated in Figure 2.5 [30].

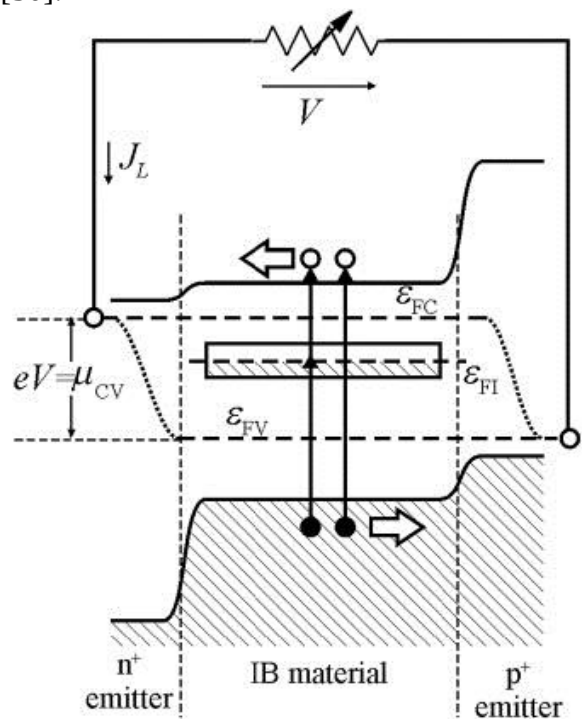

Figure 2.5: Top: A schematic drawing of the intermediate band solar cell, with an IB material sandwiched between n- and p-emitters. Bottom: Schematic band diagram of the IBSC in short-circuit. ε_{FC} is the QFL of the CB in the n-emitter, and ε_{FV} is the QFL in the VB of the p-emitter. E_{FI} is the QFL of the IB [30].

The semiconductor with an intermediate energy band within the forbidden gap is the IB material. It is situated between one strongly p-doped and one strongly n-doped semiconductor, the p-emitter and n-emitter, respectively. As with conventional solar cells, ohmic metallic contacts are attatched to the n- and p-emitters. The two emitters prevent the IB material from contacting the external electrodes, which would have led to a low cell voltage determined by E_H and not E_G (see also Figure 2.4).

Three separate quasi-Fermi levels (QFL) are assumed [11], labeled $\varepsilon_{CV,}$ ε_{IB} and ε_{FV} in the figure above. The output voltage, eV, is determined by the split between the conduction band (CB) and valence band (VB) quasi-Fermi levels, as for a conventional cell (see also Figure 2.4), and is equal to the chemical potential difference between the CB and VB QFLs in the n- and p-emitter, respectively. This voltage is limited by the main band gap of the semiconductor, E_G.

Material requirements and cell structure

For the intermediate band solar cell efficiency to approach its limit, certain material requirements must be fulfilled. The optical properties are most important for the IB material, and the electric properties for the p- and n-emitter, see Figure 2.6. The band gap and absorption spectra determine the optical properties, while the mobility, resistivity and effective charge carrier density determine the electronic properties. Ideally, one host material can be modified with three different dopants to function as both IB material and emitters, which results in the homostructure illustrated in the upper part of Figure 2.6. However, in case the host material cannot be both p- and n-doped, a second host material is needed for (at least) one of the emitters. This structure is called a heterostructure, and is illustrated in the lower part of Figure 2.6.

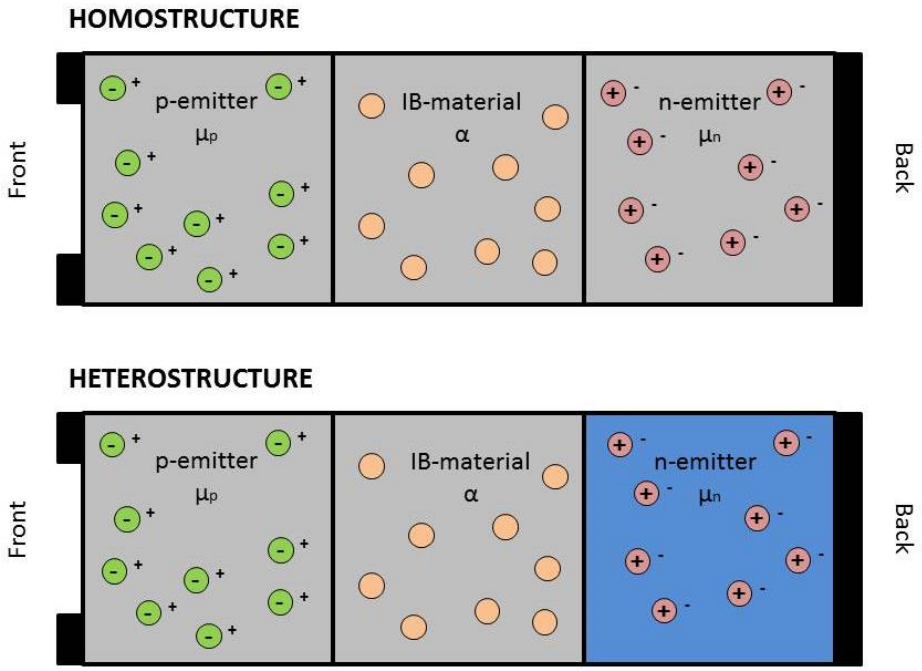

Figure 2.6: Homostructure (top) and heterostructure (bottom) IBSC with p-, IB-, and n-layers. The host materials are represented by grey and blue. Acceptors, IB forming dopants, and donors are green, orange, and red, respectively. The most important properties in each layer are indicated, where μ_p and μ_n are hole and electron mobilities, respectively, and α the absorption coefficient.

Some important material properties for IBSC host materials are described in Appendix B, and reference values as well as actual values for the most important parameters are found in Appendix C.

2.3 Preparation of solar cell materials

When planning and designing a solar cell, the preparation route for the active material(s) should be chosen early on. Conventional Si-cells are prepared as single crystalline or polycrystalline wafers, and in thin film solar cell production various deposition methods are used. Multi-junction cells can be manufactured with a combination of single crystalline and thin film materials.

Regarding IBSC production, several thin film deposition methods are possible, but higher crystalline quality is needed to approach desirable cell efficiency. Single crystal production is mentioned in section 2.3.1, and some high quality deposition methods are also described in section 2.3.2. Also, some lower quality deposition methods are mentioned at the end of section 2.3.2, to get an overview and understanding of previous attempts to produce Cu_2O/ZnO heterostructure cells (see section 4.3).

To obtain a high quality heterojunction cell, surface and interface effects and compatibility of different materials must be investigated, as described in section 2.3.3.

2.3.1 Single crystal production

In heterostructure solar cells, high material quality is crucial to achieve good electricity generation because of the many possible defects and non-optimal band matching in the junction caused by difference in band gap energy. Higher crystallinity means less grain boundaries, and thus less charge transport problems through the material. Also, the minority carrier lifetime in polycrystalline semiconductors decreases nonlinearly with increasing interface state density (lattice mismatch) at the grain boundaries, and decreases linearly with decreasing grain size [31], which indicates a higher and more stable minority carrier lifetime in single crystals. An example of a single crystal production method is the floating zone (FZ) melting technique where single crystal Cu_2O is prepared by using polycrystalline specimens of Cu_2O as "seed rods" for growing [32]. FZ silicon wafers are the preferred material for fabrication of high-efficiency mono-Si cells, and this technique is industrialized for silicon [33].

2.3.2 Deposition methods

Thin-films are two-dimensional materials of thickness ranging from nanometers to several micrometers. The deposition of thin films involves three steps; (1) creation of atomic, molecular or ionic species, (2) transport of these species through a medium, and (3) condensation of species on a substrate [34]. The techniques can be pure physical, pure chemical (gas- or liquid-phased), or based on a mix of physical and chemical reactions.

Physical methods

In evaporative methods, the source material is vaporized by heating/melting or sublimation, transported to, and eventually condensed on a substrate. A well-known example of evaporative techniques is Molecular Beam Epitaxy (MBE), a sophisticated, finely controlled method for growing single-crystal epitaxial films in an ultrahigh vacuum (10^{-11} torr) [35].

Another physical method is pulsed layer deposition (PLD) [36]. In this technique, a target material is ablated by a laser, leading to the formation of a plasma plume with high energy ions and electrons. The ablated material is then deposited on a heated substrate by nucleation

and growth. PLD is used to control stoichiometry of complex oxides, and results generally in high quality materials, such as single crystals.

Atomic layer deposition (ALD) has emerged as an important technique for depositing thin films [37]. No other thin film technique can approach the conformity achieved by ALD on high aspect structures. ALD is a gas phase technique based on sequential, self-limiting surface reactions. ALD processing is extendible to very large substrates and to parallel processing of multiple substrates.

Gas-phase chemical methods

Chemical processes in the gas phase include chemical vapor deposition (CVD), variants of CVD and thermal oxidation. These are described by Seshan [35]. CVD is a materials synthesis process whereby constituents of the vapor phase go through a chemical reaction near or on a substrate surface to form a solid product. The main feature of CVD is its versatility for synthesizing both simple and complex compounds with relative ease at generally low temperatures. In thermal oxidation, the substrate itself provides the source that is oxidized to the end product. This technique is more limited than CVD, but has extremely important applications in e.g. silicon device technology where very high purity oxide films are required.

Metal-organic chemical vapor deposition (MOCVD) is used for growing epitaxial films of compound semiconductors in the fabrication of optoelectronic devices. Composite layers of accurately controlled thickness and dopant profile are required to produce structures of optimal design for device fabrication.

Plasma deposition is a combination of a glow-discharge process and low-pressure chemical vapor deposition, and can be classified in either category. Since the plasma assists or enhances the chemical vapor deposition reaction, the process is called plasma-enhanced chemical vapor deposition (PECVD). Plasma deposition processes are used widely to produce films at lower substrate temperatures and in more energy-efficient fashion than can be produced by other techniques.

Lower quality deposition

Of electrochemical processes, electroplating is a well-known method where a metallic coating is electrodeposited on the cathode of an electrolytic cell [35].. Electrochemical processes are widely used in fabricating Cu_2O/ZnO heterostructure cells, where e.g. buffering methods can improve the interface challenges [38]. Physical-chemical methods combine both physical and chemical reactions, and are based on glow discharges or reactive sputtering. In sputtering techniques, thin-film deposition takes place by ejection of surface atoms from an electrode surface by momentum transfer from bombarding ions to surface atoms. However, these methods usually show poorer results than the physical and gas-phase chemical methods.

2.3.3 Compatibility of materials

The layers of a solar cell consist of different materials. Anti-reflective coating (ARC) and contacts should be chosen carefully to ensure they have the right properties. In a heterojunction solar cell, special attention should be paid to the interface of the two different active materials.

Light reflectance
The ARC must have appropriate refractive index relative to the layer underneath [39]. Reflection is minimized if the refractive index of the ARC is an intermediate value of the refractive indices of the materials on either side; that is, glass or air with refractive index n_0 and the semiconductor with refractive index n_2 [33]. This is expressed by:

$$n_1 = \sqrt{n_0 n_2} \tag{2.1}$$

The optimum thickness of the ARC is found at minimum reflectivity for the wavelength of the desired incoming photons, i.e. the wavelength that gives highest absorption. For an ARC of a transparent material with refractive index n_1, the ARC thickness d_1 which causes minimum reflection is calculated by:

$$d_1 = \frac{\lambda_0}{4n_1} \tag{2.2}$$

The work function
The work function is defined as the energy required to remove an electron located at the Fermi level from the semiconductor [39]. The work function of the p- and n-emitter of a heterostructure cell is important for a well-functioning interface, and varies for different materials and also by doping. However, here only the work functions of contacts of the emitters are explored in this work, since compatibility of the contacts is crucial for good charge transport in the cell.

Ideally, a metal-semiconductor junction results in an ohmic behavior if the barrier formed by the contact is zero. The carriers are then free to flow in or out of the semiconductor with minimal resistance across the contact [40, 41]. According to Streetman and Banerjee [42], the work function of the metal should be lower than that of the semiconductor, $\Phi_m < \Phi_n$, to form an ohmic contact for the n-type semiconductor-metal junction. For the p-type semiconductor-metal junction, it is the opposite case; $\Phi_m > \Phi_p$. A practical method for forming ohmic contacts is by doping the semiconductor heavily in the contact region. Thus, if a barrier exists at the interface, the depletion width is small enough to allow carriers to tunnel through the barrier. For example, when an Al-contact is formed on p-type Si, the metal contact provides the acceptor dopant, and the required p^+ surface layer is formed during heat treatment.

Lattice matching
For heterojunction solar cells, the compatibility of materials are extremely important for achieving the desired performance. Martin Green [39] explains that when the p- and n-emitter are joined together in the junction at thermal equilibrium, the difference in electron affinity and band gap energy create a displacement of the band edges of the two materials. However, if these parameters do not create “spikes” that block the photocurrent as a result of the mentioned displacement, another parameter is still essential to investigate in order to give a heterojunction with good properties; the lattice structure.

Green explains further that the defects due to mismatch at the interface between two lattices of different lattice constants create allowed energy states in the forbidden gap. These levels within the depletion region act as very efficient recombination states. In addition, they can facilitate tunneling processes for current transport from one side of the junction to the other.

Interface defects resulting in degraded cell performance are found at the Cu_2O/ZnO junction, see section 4.4.

Surface treatment

To minimize the interfacial defects in heterostructures, the layers could be surface treated before next layer is deposited. This can be done by etching, e.g. wet chemical etching, adding a buffer layer between two layers of different materials, or nanoscale structuring. Different surface treatments suitable for the Cu_2O/ZnO interface are described in section 4.5.1.

2.4 The PV module

A photovoltaic (PV) module consists of several solar cells combined inside an encapsulant between a protective front and back sheet. The anatomy of a typical PV module is shown in Figure 2.7 [43].

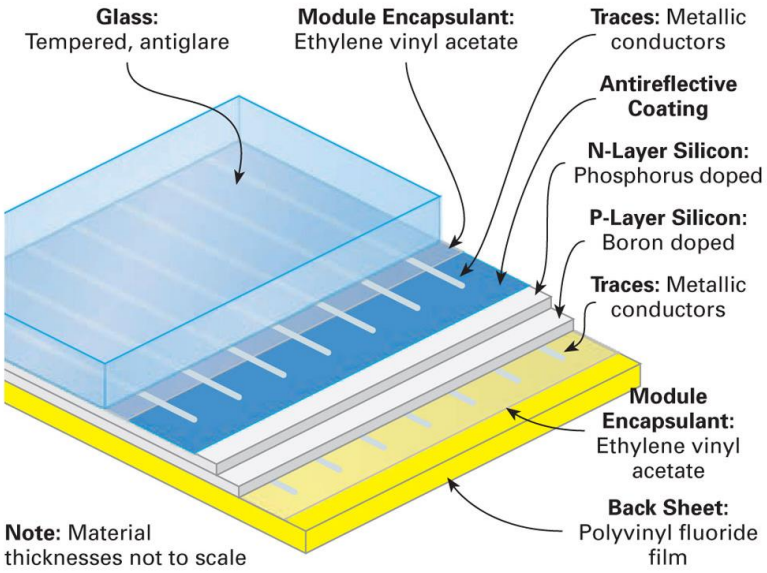

Figure 2.7: The different parts of a typical photovoltaic module [43].

Solar cells are connected in series to increase the total output [25]. The interconnected cells are called cell strings. To protect the solar cells against mechanical stress, weathering and humidity, the cell strings are embedded in a transparent bonding material that also isolates the cells electrically. The bonding system is applied to a substrate; usually glass, but acrylic plastic, metal or plastic sheeting can also be used. The solar cells can lie on top of, between or under substrate(s), depending on the process. The covering on the light-sensitive side of the solar cells must be highly transparent. Low-iron solar glass, also called white glass, is often used for this purpose, with up to 91 % light penetration. The solar glass is tempered to withstand thermal stress, and anti-reflective coating can be added to increase the light transmission up to 96 %.

2.4.1 Cell encapsulation

Three types of encapsulation for solar cells are described in [25]:

- EVA (ethylene vinyl acetate) encapsulation
- Teflon encapsulation
- Casting-resin encapsulation

Encapsulation with EVA involves lamination of the cell strings in vacuum chamber by applying negative and positive pressure at increased temperature. During this process the EVA melts and surrounds the cells on all sides. This encapsulation requires UV-resistant weatherproofing, usually solar glass, on the front side. Large module size is possible with EVA, and different lamination configurations can be fabricated with the use of various substrates. With large modules it is possible that the cells begin to float during encapsulation, which can lead to unequal gaps between the cells.

Encapsulation in Teflon involves the solar cells being enclosed in a special fluoropolymer similar to the EVA process described above. Teflon-encapsulated solar cells lie on a substrate plate and require no covering on the front. This encapsulation is mostly used for small-scale special modules, like solar roof tiles.

In casting-resin encapsulation, the solar cells are fixed between two glass sheets using adhesive pads. The front sheet is highly transparent, hardened solar glass, while the rear sheet can be any kind of hardened glass. The cavity between the glass sheets is filled with a casting resin, which surrounds the solar cells and hardens. An advantage with this encapsulation is the exact placing of the cells during the whole process. Even large modules are possible without the possibility of uneven gaps between the cells. This encapsulation is frequently used for integration in buildings, e.g. in facades, transparent roofs and solar shading devices.

2.4.2 Framing and protecting sheets

A crystalline module encapsulated in EVA is illustrated in Figure 2.7. Solar glass with antiglare is used as the top protection material, while the back material is the widely used polyvinyl fluoride (tedlar) film.

After the front and back protections are added, the modules are framed to protect the fragile glass edges and to facilitate the mounting. The frames are usually aluminum, but steel is also used. The frame is clamped on the frameless module using silicon or rubber seal [44].

2.4.3 Types of modules

Solar cell modules can generally be divided into three categories; standard modules, special modules and custom-made modules [25]. Special modules are mass-produced modules for special purposes, including all small-scale applications and lightweight modules used for solar vehicles, boats, camping and solar tiles. Custom-made modules are specially fabricated for a specific location, like a cold or warm façade, a glazed roof or a shading device.

Modules with the aim of achieving maximum energy yields per square meter at as little cost as possible are called standard modules. A typical standard module is glass-film laminates encapsulated in EVA, with or without aluminum frames. These modules are prepared with no special demands on the modules regarding shape or size. They are either attached standard base-frames or building-integrated with special profile systems.

Typically 36-216 crystalline cells are assembled into a standard module with a power output of 100 to 300 W_p for crystalline cells, with for example dimensions of 1.6 x 1.0 m [44].

2.5 The PV system

A photovoltaic (PV) system is composed of PV modules, often both series and parallel-connected, and the balance of system (BOS). BOS includes inverter(s), energy storage devices (if used), power control systems, mounting structure, and the energy network [23, 45]. A PV system can either be grid-connected or stand-alone. In the latter system, the storage devices and charge controller have the function of storing the generated electricity for as long as needed, while in grid-connected systems these components are not needed [25]. When interconnecting PV modules, the voltages can be added up at constant current if the modules are electrically identical [44].

This thesis focuses on designing a *grid-connected rooftop* intermediate band solar cell (IBSC) system, and the following description of the electrical components in section 2.5.1, and mounting structure in section 2.5.2, will reflect this system choice.

2.5.1 Electrical components

The energy network includes the power-conditioning equipment for converting the generated direct current (DC) into alternate current (AC) with the proper form and magnitude required by the power grid [46]. At the component level, BOS components for grid-connected applications are not yet sufficiently developed to match the lifetime of PV modules [45].

The German Solar Energy Society [44] describes how a typical module can be installed. The PV modules are combined by series and parallel connection to form an electrically and mechanically larger unit; the PV array. The series-connected modules are described as a string. The individual strings are connected in the array junction box. The string cables, the DC main cable and the equipotential bonding conductor (if used) are connected. The generator junction box contains supply terminals, isolation points and if required, string fuses and string diodes. The DC main disconnect/isolator switch is also sometimes found in the junction box. In larger systems, string monitoring elements have recently been implemented. They are connected to a data monitoring system and will be able to notify of any fault in the module string. String fuses protect the wiring from overloading, and to decouple individual module strings.

For electrical installation of a PV system, both AC and DC cabling are needed, as well as metering. Depending on the system's size and purpose, a PV feed-in meter or a bidirectional meter is required. The inverter, being an important electrical component in PV systems, which influences the power output to a great extent, is further explained below.

Inverter

The German Solar Energy Society [25] explains that the solar inverter is the link between the PV generator and the AC grid. The main task of the inverter is to convert the generated DC electricity into AC electricity and, if grid-connected, to adjust the electricity to the frequency of the grid. With coupling to a building's grid, the power can be consumed in the building before the surplus power is fed to the grid.

Solar inverters can perform the following functions [44]:

- Conversion of DC current from the PV modules into standard AC current.
- Adjustment of inverters' operating point to the maximum power point (MPP) of the modules, see section 2.6.1 about I-V characteristics.

- Recording of the operating data and signaling.
- Establishment of DC and AC protective devices.
- Grid monitoring or grid management.

Below are the three main inverter concepts explained, to be able to select the appropriate inverter concept for a specific PV system [25, 44]:

Central inverter concept
Three different central inverter concepts exist. The low-voltage range concept for $V_{DC} \leq 120$ V involves only few modules in each string, and needs high cable cross-sections to reduce the ohmic losses. Longer strings and higher voltage of $V_{DC} \geq 120$ V concepts need smaller cable cross-sections, but greater shading loss is possible because of the longer strings. The master-slave concept uses several central inverters. The "master" inverter operates in lower irradiance ranges. When the power limit is reached, one of the "slave" inverters takes over.

Multiple MPP regulator concept
With different irradiance, shading conditions or differently oriented arrays for a system, modules with similar ambient conditions could be connected in separate strings. Each string can be connected to a maximum power point tracking (MPPT) input of a multiple MPPT inverter to operate each string independently. Different number of modules and even different types of modules can also be stringed together in this concept.

Module inverter concept
To achieve high system efficiency the inverters should be optimally adjusted to the PV modules. In the ideal case every module should be operated at MPP. To pursue MPP for every module, each module should be pared with an inverter. Partial shading by surroundings will not affect more than the exact module(s) that loses sunlight. This concept allows for easily extension of the PV system, but the cost is higher than in the inverter concepts described above.

2.5.2 Mounting structure

Multiple interconnected PV modules make up a PV array that can be mounted on roofs of buildings, integrated in building facades or ground mounted into large power plants. A typical PV system consists of PV modules connected together in an array with the balance of system (BOS) [47].

All building surfaces exposed to direct solar radiation can be considered as suitable for installations of PV systems. Sloped roof, flat roof and facades can be sites for additive or integrative PV installations. Additive installations are added to an already existing building structure, while integrated installations are built in the building's roof or facade under construction or by replacing (part of) the building components [47]. When planning a PV system for an inclined roof, the angle and orientation of the modules are set as the angle and orientation of the roof. Not all such roofs are therefore suitable for PV installation. With flat roofs however, the planner has more freedom regarding the design and orientation of the modules to ensure best match for maximum incoming sunlight. Summarized from Reference [47], the next paragraphs address the four main methods of installing PV systems on and in roofs.

Inclined roof: Additive systems
As mentioned above, additive PV systems are added to the existing roof covering, and the modules are assembled with a metal grid. With this mounting method the roof covering remains unchanged and retains its waterproofing function. Also, the assembly and material costs are relatively low compared to the in-roof method when retrofitting existing roofs. All components, including the electrical connectors and cables, are usually exposed to weather. This must be taken into account when choosing the electrical components. The support structure must be able to absorb the mechanical and thermal stresses occurring at the generator, that otherwise would be transferred to the roof structure. Good air ventilation between the modules and roof covering gives optimal operation temperature.

Inclined roof: Integrated systems
The modules replace the conventional roof covering in the same plane, resulting in a more homogeneous surface. The mounting effort for retrofitting existing roofs can be high, whereas new building projects can benefit from savings in roofing costs. The mounting structure must maintain waterproofing between, underneath and in the areas surrounding the generator. To avoid moisture damage, sufficient air circulation must be ensured behind the modules. This air vent will also be advantages for cooling of the modules at high temperatures. The thermal stresses for in-roof modules because of poorer rear ventilation will lead to higher thermal loss compared to on-roof systems.

Flat roof: Additive systems
The modules are mounted on a metal framework above the existing roof skin, as with additive mounting on inclined roofs. Tilting of the modules by a support frame is done to achieve optimal angle for incoming sunlight. Opposed to inclined roofs, the considerable wind forces on the exposed areas of PV arrays on flat roofs need to be accounted for. As a positive consequence, the modules are usually well vented resulting in less performance loss.

The allowed load on top of a building can limit the choice of mounting structure, and the weight of the structure needs special attention. The module row spacing on the roof is chosen in accordance with the construction height to prevent the rows from shading one another. In snowy regions, the modules should be mounted with sufficient spacing. Also, a minimum distance to the roof edge is typical.

Flat roof: Integrated systems
PV installation on flat roofs are usually not favorable considering power output, because of the higher module temperatures and flat tilt angles. Temperature losses and less incoming sunlight due to the non-optimal angles and orientation, lead to lower yields than on-roof mounting. The self-cleaning ability is also poorer, since dirt cannot slide off easily. From an architecture point of view, however, the flat integrated PV systems can be favorable regarding design and aesthetics. Also, building costs can be saved because no support frames are needed, and the modules can act as cover for heat insulation.

2.6 Parameters influencing system performance

To ensure high performance of solar cells, there are certain parameters that should be optimized. From an environmental perspective, Pacca *et al.* [48] stated that there are four main factors affecting the environmental performance of PV modules: conversion efficiency, lifetime, solar irradiation and fuel mix employed in the manufacturing process. From a pure performance perspective, the I-V characteristics with emphasis on the performance ratio should also be mentioned.

First, the efficiency, lifetime and typical I-V characteristics are described in section 2.6.1, and the performance ratio is explained in section 2.6.2. The location influenced parameters are explained in section 2.6.3, and performance related to dimensions of a PV system and temperature is mentioned in section 2.6.4.

2.6.1 Efficiency

The conversion efficiency, η, of solar cells is related to the amount of work done per incoming photon, and is defined as:

$$\eta = \frac{P_{out}}{P_{in}} \tag{2.3}$$

P_{out} is the electric power delivered by the cell, and P_{in} is the incoming power from the solar radiation. In 1961 Shockley and Queisser derived a detailed balance limit of the efficiency of p-n junction solar cells [49]. The maximum efficiency was found to be 41 % for maximum concentrated light (46050 suns) and energy gap of 1.1 eV, and 30 % for 1 sun and a band gap of 1.3 eV. Both efficiencies were calculated assuming black body radiation. The only recombination loss process considered was radiative recombination, i.e. spontaneous emission of photons, and all photogenerated carriers are collected. All photon energies higher than the band gap energy were considered absorbed [13]. Other assumptions are described in reference [49].

As mentioned earlier, third generation solar cells aim at higher efficiency, and are designed in various ways to increase the amount of work generated. Reducing the transparency loss and lattice thermalization losses, or adding band gaps in multi-junction cells make this possible. To increase the efficiency of a solar cell implies generally that the amount of electrical work extracted from the cell per photon supplied must increase [50].

The defined efficiency value of a solar cell is found from the current-voltage (I-V) characteristics of the specific cell [33], see paragraph below about I-V characteristics. However, real-life efficiencies are always lower than those attainable with single cells in laboratory conditions [51]. The losses found in PV systems can be aggregated in the performance ratio (PR) that takes all system losses into account (see section 2.6.2 below), and the lifetime of the solar cell system must also be considered when evaluating the system performance.

Lifetime

For conventional PV technologies 80 % of the initial efficiency is usually guarantied up to 25 years. However, most LCA studies neglect efficiency degradation [52]. Many lifetimes ranging from 10 to 30 years are used in LCA studies, see section 3.2, but 25 years is a widely

used as an assumption for new PV technologies being developed [52]. The electrical components often have shorter lifetimes than the PV modules, and replacement of some of the materials needed in the electrical components every 10 years can be used as an assumption [53]

I-V characteristics

As mentioned above, the defined efficiency value of a solar cell is found from the I-V characteristics. No power is generated in the cell under short or open circuit. The maximum power P_{max} produced by the device is reached when the product of current (I) and voltage (V) is maximum [33]. This current-voltage relationship is illustrated in Figure 2.8 [54], where I_{sc} is the short circuit current, V_{oc} is the open circuit voltage, and V_{mp} and I_{mp} are the voltage and current at maximum power, respectively.

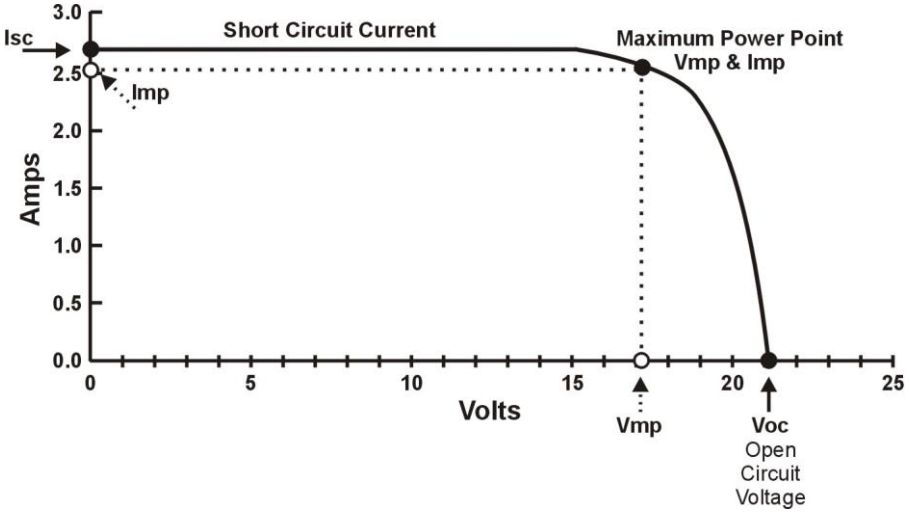

Figure 2.8 The I-V characteristics of a solar cell with maximum power point [54].

The defined efficiency of solar cells is the power at maximum power point (MPP) under standard test conditions, divided by the power of the radiation incident upon the cell [33].

2.6.2 Performance ratio

According to SMA Solar Technology AG [55], the performance ratio (PR) is one of the most important variables for evaluating the efficiency of a PV plant. PR is the ratio of the actual and theoretically possible energy outputs, and is largely independent of the orientation and incoming irradiation of a PV plant. Thus, PR is a great quality factor for comparing PV systems supplying the grid at different locations all over the world.

The PR expresses the proportion of the energy that is actually available for export to the grid after deduction of energy loss (e.g. due to thermal losses and conduction losses) and of energy consumption for operation. High-performance PV plants can reach a performance ratio of up to 80 %.

To calculate the PR for a specific PV system, there are some important variables that must be determined. The solar-irradiation values for the site of the PV plant can be determined using a measuring gage (e.g. Sunny SensorBox) that measures the incident solar irradiation at the PV plant. Also, a factor of the modular area of the PV plant and the relative efficiency of the

modules are needed. The optimum analysis period for calculating the performance ratio is one year

A simplified formula can be used for calculating the performance ratio:

$$PR = \frac{\text{Actual reading of plant output in kWh p.a.}}{\text{Calculated,nominal plant output in kWh p.a.}} \quad (2.4)$$

PV system losses due to balance of systems (BOS) and other indirect losses are often assumed to be 25 % if precise calculation is not possible. This gives PR = 0.75, and is the mean of common values varying from 0.65 to 0.95 in previous LCA studies [52]. In addition to the losses mentioned above, the PR also accounts for the effects of shading, snow cover, heat loss and DC–AC conversion loss [56].

2.6.3 Location

The irradiance and weather of a specific location will affect the performance of the PV system. With respect to the irradiance, the tilt angle of the solar panels is also important to optimize to achieve high output. The temperature of the surroundings will also influence the performance of the PV system. The environmental performance related to the location is most influenced by the energy mix used in the fabrication of the system.

Irradiance

The electrical performance and the characteristic curves of the PV module are heavily dependent on the irradiance. Therefore modules usually run in partial load operation [25]. When the irradiance drops by half, the electricity generated also reduces by half.

The irradiance is directly dependent on the location of the PV system. If a PV system is evaluated without knowing the exact location of the planned PV system, an average value for irradiation can be found. The average Middle Europe and Southern European yearly irradiation are 1000 and 1700 kWh/m^2, respectively [57]. Average annual irradiation, i.e. irradiance over time, for countries and some areas are given in Appendix D.

If the modules are tilted to optimize the incoming sunlight, the irradiation values can increase significantly.

Tilt angle

The tilt angle of fixed modules can be optimized according to seasonal or annual performance. The optimum tilt angle, B_{opt}, is the tilt angle of highest annual irradiation, and depends on the latitude, ϕ, and the local climate. Higher latitudes mean larger difference between summer and winter orientation of the sun and irradiation. This gives rise to the assumption that optimum summer parameters should have priority over the winter parameters in northern countries. According to Lorenzo [58], an approximate for the optimal module tilt can be calculated by:

$$B_{opt} = 3.7 + 0.69\,|\phi| \quad (2.5)$$

Environmental performance
Environmental performance of a solar cell system is directly linked to the electricity mix of the specific location. Stoppato [5] investigated the electricity mix of 26 countries in four different continents, and concluded that Norway has the cleanest energy mix of almost only hydro. However, Norway also has the lowest potential for CO_2 mitigation (PCM).

Weather and pollution
The electrical performance and the characteristic curves of the PV module are dependent on the temperature. This is explained in reference [25]. The module voltage is affected most of all by the module temperature. The voltage deviation of a ventilated 50 W module at standard conditions (STC) can amount to -8 V in summer and + 10 V in winter. The change in voltage of the module determines the system voltage, and therefore the design of the entire PV system. When several modules are connected in series, the increase in voltage at low temperatures can amount to more than 100 V, and may even exceed the voltage limit of downstream devices. The current however, hardly changes with the module temperature; just a slight increase with increased temperature. Increased voltage results in increased power output, see I-V characteristics above, and PV installation in colder weather can therefore be beneficial.

The degree of clean air at the location of the PV system is also a factor influencing the performance [59]. The more air pollution, the more "shadowing" effect the modules will feel. This effect will not be present in areas with clean air. An example location where this effect is minimized is hydro-based Norway with little air pollution, and also cold temperature most of the year that provides the voltage effect explained above.

2.6.4 Dimensions and temperature
The size of the modules and number of modules, as well as the mounting structure of the modules can also influence the system efficiency, especially at different temperatures, as described below.

When several modules are connected in series, the increase in voltage at low temperatures can, as mentioned above, amount to more than 100 V, and may even exceed the voltage limit of downstream devices. When sizing PV systems, therefore, particular attention must be paid to this situation, with the rule of thumb: 1 kW_p = 10 m^2 of PV area [25]. This number may have changed however, since this was published in 2005, but the reasoning is still valid.

In summer, the power reduction of high temperature modules should be considered when choosing the mounting structure. The power loss can be up to 35 % compared to STC if the PV is not able to emit heat easily to the surroundings through sufficient ventilation.

3 Review of PV system life cycle assessments

This chapter is a review of LCA studies conducted of PV systems. Comparison between PV studies is difficult since investigations employ different methods, use various data sources, replace unknown data with similar ones and take into account different levels of irradiation, operational periods and other assumptions for future technology enhancement [52]. However, the review on LCAs of PV systems was conducted to identify correlations between the parameters influencing system performance (see section 2.6), and more importantly, to identify the environmental impact found for existing PV systems.

First, an overview of the LCA methodology is given to guide the reader through the LCA review of PV systems and the discussion of results below. In section 3.3 some observations based on this review that may be helpful for the investigation of the IBSC system are done.

3.1 The life cycle assessment (LCA) methodology

The purpose of a LCA can be: (1) comparison of alternative products, processes or services; (2) comparison of alternative life cycles for a certain product or service, or (3) identification of parts of the life cycle where the greatest improvements can be made [60]. The LCA methodology is rapidly developing into an important tool for authorities, industries, and individuals in environmental sciences. The rest of this section will explain the four stages of LCA shown in Figure 3.1 [61], based on ISO14040 [19] and Roy [60].

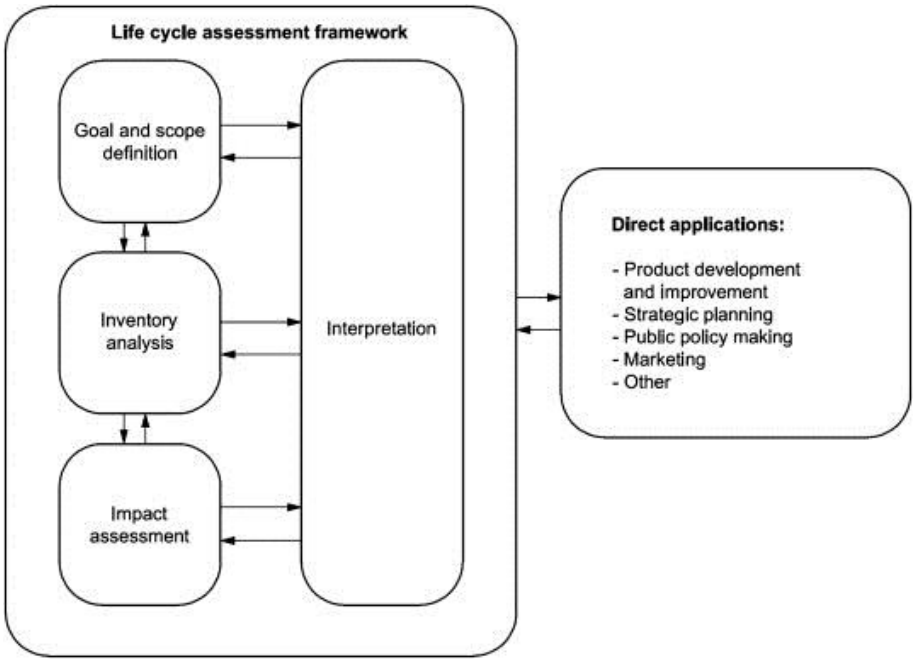

Figure 3.1: The four stages of life cycle assessment [61].

Goal and scope

Goal and scope definition may be the most important component of a LCA because this phase sets the parameters for the rest of the study. This first stage defines the purpose of the study, the expected product of the study, system boundaries, functional unit (FU) and assumptions. Depending on the extent and purpose of the study, different variants of LCA can be chosen;

e.g. “cradle to grave”, “cradle to gate”, “gate to gate” and “cradle to cradle”. The difference between these is primarily how many phases of the product or service life cycle that contributes to the research. A typical product life cycle is illustrated in Figure 3.2 [62].

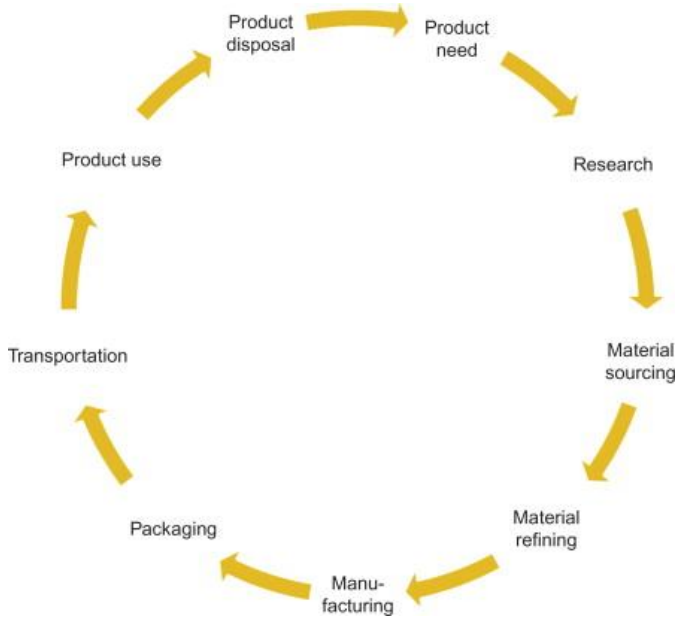

Figure 3.2: A typical product life cycle with nine phases [62].

The FU is a quantitative description of the service performance of the investigated product system(s) [63], and should provide a reference unit to which the inventory data are normalized. The definition of the FU depends on the environmental impact category and the aims of the investigation. It can be based on the mass of the product under study, energy consumption during the life cycle, economic values, or land area, among others.

Life cycle inventory (LCI) analysis

The inventory phase is the most work intensive and time consuming phase. There are many LCA databases, such as Franklin US98, Idemat 2005, Buwal 250, ETH-ESU 96 and Ecoinvent [64]. Data on transport, extraction of raw materials, processing of materials, production of well-known products, and disposal processes can normally be found in a LCA database. For product-specific data, the data should also be site-specific. The final collection of data should include all inputs and outputs from all the processes in the system in question.

Life cycle impact assessment (LCIA)

The life cycle impact assessment (LCIA) aims to understand and evaluate environmental impacts based on the LCI analysis. The inventory results are assigned to different impact categories based on the expected types of impacts on the environment. Impact assessment in LCA generally consists of the following elements: classification, characterization, normalization and valuation.

The impact categories can include global effects (e.g. global warming, ozone depletion); regional effects (e.g. acidification, eutrophication); and local effects (e.g. working conditions,

effects of hazardous and solid waste). For example, the cumulative energy demand (CED) can be used to calculate the energy payback time (EPTB) that often is used to evaluate the energy profitability of PV systems.

The calculated impact category indicators from the characterization step are used to directly compare the LCI results within each category. Normalization of the results will express potential impacts in ways that can be compared, by calculating category indicator results relative to reference value(s) [63]. Valuation, or weighting, is the assessment of the relative importance of environmental loads identified in the classification, characterization, and normalization stages. The environmental loads are weighted and compared or aggregated, e.g. global warming potential (GWP).

Interpretation

The purpose of a LCA is to draw conclusions that can support a decision, or provide a result for environmental issues that people without the knowledge of LCA methodology can understand. Issues concerning emissions, material use, energy use, etc., are identified for conclusions and recommendations consistent with the goal and scope of the study. The information from the LCI and LCIA phases are identified, quantified, checked, and evaluated. The results can then be communicated to decision makers, consumers, researchers or others involved. Quantitative and qualitative measures for improvements can include changes in product, process and activity design, concerning life cycle phases like raw material use, industrial processing, consumer use and waste management.

3.2 Published LCAs of PV systems

The environmental impacts of competing PV technologies were mapped through this review of LCA studies of PV systems. Even though no LCA was done for the IBSC system in this thesis, some of the performance parameters from the LCA review were valuable for specifying the system performance in Chapter 8.

Assumptions beyond what is listed in Table 3.1 are given in the respective references. Irradiation at different locations is given in Appendix D. The energy mix is another important parameter for the specific location. Different material amounts and energy consumption during production and application (roof, ground, tilt etc.) are the main reasons for diverging values when the location, performance ratio (PR), lifetime and conversion efficiency are the same for a specific technology. The different PV technologies are as follows:

mc-Si = Multi/poly-crystalline silicon
sc-Si = Single/mono-crystalline silicon
a-Si = Amorphous silicon
DSC = Dye sensitized
CIS = Copper indium diselenide
CIGS = Copper indium gallium diselenide
CdTe = Cadmium telluride cell
a-Si/sc-Si = Amorphous/mono-crystalline silicon
a-Si/μc-Si = Amorphous/micromorph silicon
TF Si = Thin film silicon
μm-Si = Micromorphous silicon

Table 3.1: Published carbon dioxide emissions per kWh for PV systems. The locations are provided to give an idea of the solar radiation and energy-mix assumed in the specific LCA study.

Year	Author	Location	PV techn.	PR	Life [yr]	η [%]	GWP [gCO_2-eq/kWh]	Ref.
1996	Nieuwlaar *et al.*	Netherlands	a-Si	n.a.	20	10	47.0	[65]
1996	Komiyama *et al.*	Japan, Indonesia	mc-Si	0.72	30	15	143.6, 132	[66]
1997	Kato *et al.*	Japan	sc-Si	0.81	20		91.0	[67]
1998	Dones *et al.*	Switzerland	mc-Si sc-Si	n.a.	30	14 16.5	189 114	[68]
1998	Kato *et al.*	Japan	a-Si mc-Si sc-Si	0.81	20	8.0 11.6 12.2	17 20 83	[69]
1998	Frankl and Gamberale	Italy	sc-Si	0.9	25	11.2/ 14.5	200	[70]
2000	Alsema	Netherlands	a-Si mc-Si	0.75	30	7.0 13	50 60	[71]
2000	Oliver and Jackson	Europe	mc-Si	n.a.	n.a.	12	120, 170	[72]
2001	Greijer *et al.*	Sweden	DSC	n.a.	20	7.0 12 9.0	19 22 25	[73]
2001	Kato *et al.*	Japan	CdS/CdTe	0.81	20	10.3 11.2 12.4	14.0 11.4 8.9 gC/kWh	[74]

2002	Meier	United States	a-Si	n.a.	30	5.7	39.0	[75]
2003	Ito *et al.*	China, Gobi Dessert	mc-Si	0.78	30	12.8	44	[76]
2005	Jungbluth	Switzerland	mc-Si sc-Si	n.a.	30	14.8 16.5	79 (Average)	[77]
2005	Battisti *et al.*	Italy	mc-Si	n.a.	20	10.7	26.4	[78]
2005	Hondo	Japan	mc-Si	n.a.	30	10.0	53.4	[79]
2005	Tripanagnostopoulos *et al.*	Greece	mc-Si	n.a.	20	10.5	104	[80]
2005	Raugei *et al.*	Italy	CdTe CIS	0.80	20	8.0 10	53 85	[81]
2006	Fthenakis and Alsema	Southern Europe	mc-Si CdTe CdTe	0.75 0.75 0.80	30	13.2 8.0 9.0	37 21 25	[82]
2006	Alsema *et al.*	Southern Europe	ribbon-Si mc-Si sc-Si	0.75	30	11.5 13.2 14.0	29.8 32.5 35.0	[57]
2006	de Wild-Scholten *et al.*	Southern Europe	mc-Si	0.75	30	13.2	34-42	[83]
2006	Veltkamp and de Wild-Scholten	Netherlands	DSC	0.75	5 10 30	8.0	107 54 18	[84]
2006	Muneer *et al.*	United Kingdom	sc-Si	n.a.	30	11.5	44	[85]
2006	Kannan *et al.*	Singapore	sc-Si	n.a.	25	7.3-8.9 10.6	217 165	[86]
2007	Raugei *et al.*	Italy	CdTe CIS mc-Si	0.75	20	9.0 11 14	48 95 57	[51]
2007	Pacca *et al.*	United States	a-Si mc-Si	0.95	20	6.3 12.9	34.3 72.4	[48]
2007	Fthenakis and Kim	United States and Europe	Ribbon-Si mc-Si sc-Si CdTe	0.75-0.80	30	11.5 13.2 14.0 9.0	25-32 30-38 45-48 16-22	[87]
2008	Ito *et al.*	China, Gobi Dessert	mc-Si mc-Si** a-Si CdTe CIS	0.78 0.78 0.77 0.77 0.78	30	12.8 15.8 6.9 9.0 11.0	12.1 9.4 15.6 12.8 10.5 (gC/kWh)	[88]
2008	SENSE report	Frankfurt, Rome and Solar belt	a-Si CdTe CIGS	All: 0.84-0.93	20	5.5 10.0 11.5	n.a. 36-66 33-61	[89]
2008	Stoppato	Different locations	mc-Si	0.80	28	16	123 $kgCO_2/m^2$	[5]
2008	Fthenakis et al.	Southern Europe	Ribbon-Si mc-Si sc-Si CdTe	0.80	30	11.5 13.2 14.0 9.0	29, 35, 44 32, 42, 52 35, 44, 55 -, 21, 26	[90]
2009	Ito *et al.*	China (Gobi Desert)	mc-Si sc-Si a-Si/sc-Si Thin-film Si CIS CdTe	0.77	n.a.	13.9 14.3 16.6 8.6 10.1 9.0	51.5 61.6 52.8 71.0 58.8 66.5	[91]

2009	de Wild-Scholten and Schottler	Southern Europe	a-Si/µc-Si CdTe CIS	n.a.	30	8.5 10.7 11.0	23.5 15.5 21.0	[92]
2009	Fthenakis *et al.*	Southern Europe	CdTe	0.80	30	10.9	19	[93]
2010	Ito *et al.*	China (Gobi Desert)	mc-Si sc-Si a-Si/sc-Si TF Si CIS CdTe	0.78	n.a.	n.a	42 51 43 56 45 51	[94]
2010	Filippidou *et al.*	Greece (Xanthi)	mc-Si CdTe	n.a.	n.a.	14 9.0	317 137 $kgCO_2/m^2$	[95]
2010	Dominguez-Ramos and Held	Spain	mc-Si sc-Si Ribbon-Si a-Si CdTe CIGS	0.78	30	13 15 12 7 9 10	31 33 28 26 17 31	[96]
2011	Ito *et al.*	Japan, Hokuto	mc-Si sc-Si a-Si/sc-Si a-Si µc-Si/a-Si TF CIS	n.a.	30	12.3-14.0 11.8-13.2 15.9 6.1 8.3, 8.8 8.8, 11.2	38-46 52-67 41 52 44, 46 36, 31	[97]
2011	de Wild-Scholten	Southern Europe	mc-Si sc-Si µm-Si CdTe CIGS	0.75	30	14.1 14.4 10.0 11.3 11.0	34 34 21 19 31	[98]
2011	Held and Ilg	Spain/Portugal, Italy and Germany	CdTe	0.80	30	10.9	18.7, 20.9 and 29.5	[99]
2012	de Wild-Scholten and Gløckner	Southern Europe	mc-Si	0.75	30	14.3	29	[100]
2012	Westgaard *et al.*	Southern Europe	mc-Si	0.84	30	n.a.	18, 21	[101]

**High efficiency mc-Si PV modules may use CF4, which is a strong greenhouse gas. The paper does not calculate this.

The energy bay-back time (EPBT) was also calculated in most of these LCA studies. The EPBT is the time it takes for the PV panel to generate the same amount of energy required for its manufacture. For verification of the IBSC system, this value would be helpful to compare the IBSC technology with competing PV technologies.

3.3 LCA review related to the IBSC system

As mentioned earlier, this LCA review was originally conducted as a preparation for the LCA study that was the initial goal of this thesis. Some observations from the LCA review can benefit the further research on IBSC system. The environmental results from different locations can imply where it would be environmentally beneficial to install a new PV system, and the LCA studies also gives an idea of the environmentally crucial phase(s) of a PV system's lifetime that most likely can be translated directly to the IBSC system.

Location

The location of the present study of an IBSC system was initially set to Europe, and average values for irradiation and electricity mix could then be used to discuss the technology and environmental performance. However, to examine the possibility of developing PV systems for use in Norway, the location was later chosen to be Oslo. Values for irradiation of different locations can be found in Appendix D.

From the LCA review it was found that Oslo was the cleanest location based on the hydro-electricity mix in Norway [5]. Production of solar cell systems in Norway could therefore seem environmentally friendly compared to other countries.

Production phase

In the reported LCA studies on PV systems, it is emphasized that the production phase is the most energy and material consuming phase. It follows that this is also the phase that has the largest impact on the total results from the LCA. Both the GWP and EPBT are highly dependent on this phase of the life cycle.

The materials and production route used in the PV system are therefore of great importance when the environmental impacts are evaluated through a LCA study.

From system to cell

LCAs are conducted with a holistic view of a system and its lifetime phases. However, to prepare a new system for a LCA study, the most challenging part(s) of the system with respect to potentially environmentally damaging materials and production choices should be prioritized. As mentioned in the introduction, the focus here will be on the IBSC cell based on a Cu_2O-ZnO heterostructure.

The cell will by far be the most innovative system unit, and the choices made for this unit probably have the highest potential to influence the environment with respect to other system parts. To study the challenges regarding a new IBSC cell, keeping the rest of the system parts conventional can be a great way to compare the novel technology to competing and existing technologies. Also, this makes it possible to plunge deeper into the cell materials from a materials technology perspective.

4 Background for Cu_2O/ZnO-based IBSCs

The host materials for the intermediate band solar cell will be Cu_2O and ZnO, as mentioned in Chapter 1. To collect information about these materials an extensive literary search was performed focusing on challenges related to heterojunction cells of these materials. It has been reported that Cu_2O is a good candidate for low cost solar cell realization [102], with ZnO as a promising n-emitter for heterostructured cells.

It is assumed that the reader has knowledge about materials science, basic solar cell theory and solar cell production methods. A short introduction on production methods was given in section 2.3, and solar cell theory and important material properties for solar cell applications are briefly explained in Appendix A and B, respectively.

A short overview of typical material properties of ZnO and Cu_2O are summarized in section 4.1 and 4.2, while various production routes of Cu_2O-ZnO heterojunctions are described in section 4.3, including the progress in cell performance. The challenges with the heterostructure cell are investigated in section 4.4 and possible improvements in section 4.5. The experimental values found in these sections are highly dependent on the experimental conditions and the methods used in all processes from raw material extraction to cell manufacturing. Also worth mentioning, is that both these materials are relatively unexplored compared to e.g. silicon, and the challenges discovered in this literary search should not limit further research.

In section 4.6, methods that might be suitable for synthesis of Cu_2O/ZnO-based bulk IBSCs are mentioned.

4.1 ZnO as solar cell material

Zinc oxide (ZnO) with bandgap energy of around 3.3 eV, see Appendix C, has attracted much attention as a future solar cell material. This is due to the theoretical conversion efficiency of around 18 % [103] and an absorption coefficient higher than that of a single crystal Si [104]. The intrinsic n-type behavior of ZnO is either due to oxygen vacancies or unintentional hydrogen incorporation [105]. A potentially low transmittance at the wavelength of light (45 % at 600 nm) has been reported for ZnO [106].

4.2 Cu_2O as solar cell material

Cu_2O has a direct band gap of 2.17 eV [107], high room-temperature mobility [108] and a reasonable minority carrier diffusion length (as single crystal) for solar cell applications [109]. Theoretical efficiency of solar cells based on Cu_2O is approximately 20 % [103]. The intrinsic p-type conductivity of cuprous oxide is usually attributed to Cu vacancies [110]. In spite of the promising theoretical efficiency and high mobility, poor cell performance is found in Cu_2O heterojunctions [111]. The cell efficiency is strictly limited by the resistance which is mainly due to the high resistivity of Cu_2O [102].

4.3 Production of Cu_2O/ZnO heterojunctions

According to Katayama *et al*. [106], the Cu_2O/ZnO heterojunction should be formed at low temperatures to avoid thermal reaction resulting in copper-rich regions at the Cu_2O/ZnO interface. They further suggest that electrodeposition, which can be performed at low temperature, is the most suitable method for producing high-quality heterojunction solar cells. The solar cells they produced by a two-step electrodeposition had a short-circuit photocurrent density of 2.08 mA cm^{-2}, an open-circuit voltage of 0.19 V and a conversion efficiency of 0.117 % under AM1.5 conditions.

The Cu_2O/ZnO junction can also be formed in a two-step hybrid process, by radio frequency (rf) magnetron sputtering of ZnO followed by electrodeposition of Cu_2O, giving a conversion efficiency of 0.24 % [112]. Another production route could be rf magnetron sputtering of ZnO can also be followed by low-pressure metal organic chemical vapor deposition (MOCVD) of Cu_2O to achieve epitaxial growth on the c-axis-oriented polycrystalline ZnO film [113]. The ZnO-layer can also be deposited on Cu_2O, as Akimoto *et. al* [114] reported, but the crystallographic orientation and current-voltage characteristics were far superior for the heterojunction with structure Cu_2O on ZnO than for the inverse structure. Under AM1.5 conditions, their best thin film p-Cu_2O/n-ZnO heterostructure showed a short-circuit photocurrent density of 2.8 mA cm^{-2}, an open-circuit voltage of 0.26 V and a conversion efficiency of 0.4 %.

Deposition methods that successfully increased the conversion efficiency above 1 % were performed by Minami *et al*. [108]: efficiencies of 1.52 and 1.42 % using AM2 solar illumination were obtained in a Ga-doped ZnO(GZO)-Cu_2O heterojunction solar cell fabricated using a ZnO thin film prepared by vacuum arc plasma evaporation (VAPE) and in a Al-doped ZnO(AZO)-Cu_2O device fabricated using pulsed laser deposition (PLD), respectively.

To improve the results by Minami *et al.*, transparent conducting oxide (TCO) deposition technology and the copper oxidation process were investigated by Mittiga *et al.* [102] to obtain better substrates. TCO films were ion beam sputtered onto Cu_2O substrates. The TCO films, both In_2O_3 doped with tin (ITO) and ZnO were grown by ion beam sputtering on good quality Cu_2O sheets prepared by oxidizing copper at a high temperature. The resulting ITO/ZnO/Cu_2O cell had an open-circuit voltage of 0.595 V, a short-circuit current density of 6.78 mA/cm^2 and a conversion efficiency of 2.01 % under simulated AM1.5 illumination. This was the highest reported conversion efficiency of a ZnO/Cu_2O heterojunction until Minami *et al.* in 2011 [115] achieved a conversion efficiency of 3.83 % in an AZO/ZO (un-doped ZnO)/Cu_2O cell prepared by ZO buffer layer and AZO n-emitter deposited by PLD on polycrystalline Cu_2O sheets made by oxidation of Cu sheets.

The high efficiency heterostructure by Minami *et al.* was based on the same materials as the cell examined by Jeong *et al.*, see Figure 4.1 [105]. Here, gold is used as the back contact, and indium-doped tin oxide (ITO) as the front contact.

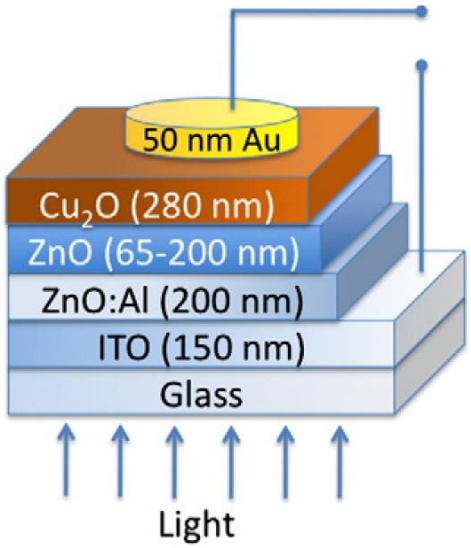

Figure 4.1: A heterostructure Cu_2O/ZO/AZO cell [105].

Recently, Nishi *et al.* [116] reported an even higher value than the previously reported 3.83 % efficiency for AZO/ZO/Cu_2O cells. They reached a promising 4.12 % by depositing AZO and ZO films by PLD at room temperature onto thermally oxidized Cu_2O sheets. The AZO layer served as a transparent electrode, and gold was used as the Cu_2O ohmic contact.

4.4 Challenges with Cu_2O/ZnO heterojunctions

The conversion efficiency of Cu_2O-ZnO heterostructures is normally between 1-4 % in recent literature (see section 4.3). In theory it should be possible to further improve the conversion efficiency of this heterojunction cell, considering that the theoretical limits of Cu_2O and ZnO are 20 and 18 %, respectively [103].

Interface states are known to influence the built-in potential of a diode, and hence its photovoltaic properties [117]. Poor interface quality and interface defects in ZnO/Cu_2O heterostructures have been blamed for poor solar cell performance [118, 119]. Abdu and Musa [111] state that the ZnO/Cu_2O heterojunction is essentially a Cu/Cu_2O Schottky cell, since Zn reduces Cu_2O to Cu. As a result, the photovoltaic properties of Cu_2O solar cells are markedly affected. Therefore, the ZnO deposition method and conditions as well as the surface treatment of Cu_2O are important parameters [120]. The interface lattice matching and factors leading to poor carrier transport across the junction should also be looked into.

4.4.1 Lattice matching

It is considered that defects induced by mismatch between the lattice parameters of the Cu_2O and ZnO films at the heterojunction may be responsible for low efficiency in these solar cells [106].

Akimoto *et al.* [114] described that the two stacking sequences, ZnO layer deposited on Cu_2O and Cu_2O layer deposited on ZnO, were not equivalent, and the second sequence resulted in significantly better I-V characteristics. The difference was ascribed to a smaller lattice mismatch due to the spontaneous orientation of the ZnO crystals that induced the growth of Cu_2O crystals with the preferential orientation. Since ZnO is hexagonal (wurtzite) while Cu_2O is cubic (cuprite), this matching gives a similar hexagonal atomic arrangement at the interface with a lattice mismatch of only 7.1 %.

However, to optimize the material properties of Cu_2O, it may be necessary to start with a high quality Cu_2O substrate and epitacially grow ZnO on top. This stacking sequence has been proved advantageous with respect to increased efficiency [115].

4.4.2 Transport across the junction

Jeong *et al.* [105] investigated the carrier transport and recombination mechanisms in Cu_2O-ZnO heterojunction thin film solar cells prepared by MOCVD of Cu_2O on sputtered ZnO film. They drew several conclusions about recombination and transport across the heterojunction, and summarized the findings in three categories; interfacial recombination, tunneling and Auger depth profile. The following paragraphs are based on this summary of unwanted transport across the junction as shown in Figure 4.2.

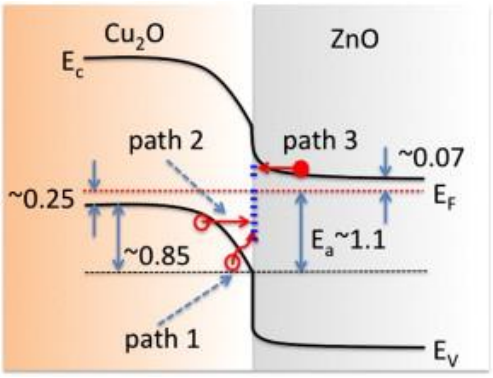

Figure 4.2: Band diagram of the Cu_2O/ZnO heterojunction. E_C, E_V, E_F, and E_a are the conduction band edge, valence band edge, Fermi level and activation energiey, respectively. Most of the band bending is on the Cu_2O side because of lower doping in Cu_2O compared to the ZnO side. Paths 1 and 2 indicate possible hole recombination pathways through interface defects. Activation energy, E_a, is the barrier that the holes have to overcome to recombine. Path 3 shows tunneling of electrons from the ZnO conduction band into interfacial trap states [105].

Interfacial recombination

The activation energy, E_a, is the barrier that the holes have to overcome to recombine. In the analysis done by Jeong *et al*. [105], the activation energies ranged from 0.99 to 1.34 eV, which are much smaller than the band gap of the Cu_2O absorber layer with E_g = 2.2 eV. This clearly indicates that current transport across the Cu_2O-ZnO interface must involve electron-hole recombination at interfacial states in the band gap [121]. The measured activation energy is the energy difference between the Fermi level and the valence band (VB) edge at the interface as shown in Figure 4.2. Indeed, assuming that the Cu_2O-ZnO junction is an ideal heterojunction at thermal equilibrium, and using literature values for electrical properties in the ZnO and Cu_2O films, E_a is estimated to be approximately 1-1.1 eV as shown in the figure above. Further, the Cu_2O region may be fully depleted, and the barrier is in this case the difference between the gold contact work function and the VB edge at the interface, which also gives a value of about 1-1.1 eV. Thus, Jeong et al. concluded that the interface recombination is the dominant current flow mechanism across the Cu_2O-ZnO heterojunction. The rate limiting step is diffusion of holes against the barrier established in the Cu_2O to recombine with electrons trapped at interfacial states. This mechanism is shown as path 1 in Figure 4.2.

Tunneling

One possible tunneling mechanism is depicted as path 2 in Figure 4.2, where a hole tunnels across the barrier due to band bending to recombine with a trapped electron. Recombination via tunneling is reduced in presence of the buffer layer so that, at high temperature, activated surface recombination becomes dominant. As the temperature is lowered, the activated recombination process slows down and tunneling becomes important again. The two processes, recombination via tunneling and activated recombination, can occur together and exist in parallel across the junction region. Either there is a region of very high acceptor density near the Cu_2O-ZnO interfacial region or tunneling is on the ZnO side where the donor densities are higher. This would be consistent with Zhang *et al.*'s [122] proposal that the recombination current in Cu_2O-ZnO flows by tunneling of electrons from the ZnO conduction band into interfacial trap states (path 3 in Figure 4.2). Presence of tunneling depends on the ZnO film thickness, which supports the previous conclusion that the tunneling is on the ZnO side. The tunneling is eliminated under illumination, which is consistent with the proposal

that the tunneling is into interfacial traps: under illumination interfacial traps are filled which would eliminate tunneling.

Auger depth profile

It is well known that copper can diffuse readily even at low temperature. To evaluate possible metal interdiffusion at the Cu_2O-ZnO interfaces, Jeong *et al*. measured the variation of Cu and Zn throughout the solar cell film stack using depth profiling by Auger spectroscopy. There is significant interdiffusion of Zn and Cu at the Cu_2O-ZnO interface. While it may seem that the Cu is diffusing up a concentration gradient into ZnO this is likely due to differences in the partition coefficient for Cu in ZnO and Cu_2O, i.e., chemical potential gradients drive the diffusion of Cu into ZnO. Clearly, we find Cu-atoms throughout the ZnO film. Copper can be a p-type dopant and diffusion of Cu into ZnO can compensate the n-type ZnO film. Also, Zn can act as an n-type dopant in Cu_2O, and thus compensate the p-type film. This interdiffusion and compensation may be responsible for the low open circuit voltages observed in Cu_2O-ZnO heterojunction solar cells.

Jeong *et al*. concludes that Cu_2O/ZnO interface recombination is the dominant carrier transport mechanism. Tunneling across an interfacial barrier also plays an important role in current flow, and a thin TiO_2 buffer layer reduces tunneling. A high open circuit voltage at low temperature (~ 0.9 V at around 100 K) indicates that Cu_2O-ZnO heterojunction solar cells have high potential as solar cells if the recombination and tunneling at the interface can be suppressed at room temperature.

4.4.3 Material properties

The quality and crystallinity of the Cu_2O and ZnO layers influences the performance of the heterostructure significantly. For high efficiency solar cells based on these materials, single crystal production should be investigated for the active substrate, and also high quality deposition techniques of the layer(s) grown on this substrate. As mentioned, the Cu_2O-ZnO heterostructures have been produced with both the Cu_2O and ZnO as the active substrate.

Cu_2O

Hussain *et al.* [112] argued that particle size, crystal faces and crystallinity of Cu_2O are important factors that determine the p-n junction interface, and consequently have an effect on the performance of the heterojunction solar cell. The crystal face of the p-Cu_2O film exposed at the p-n junction contains different atomic arrangement depending on which plane is exposed at the surface [123]. The energy level, density, and distribution of interface states at the p–n junction can be affected by that difference and, therefore, also the unwanted recombination losses at the interface [112].

According to Mittiga *et al.* [102], the cell performance of a Cu_2O-ZnO heterojunction solar cell is strictly limited by the resistance which is mainly due to the high resistivity of the Cu_2O substrate.

Li *et al.* [124] prepared high-quality Cu_2O thin film by introducing a low-temperature buffer layer (LTB-Cu_2O) on the Cu_2O films. The resistivity, carrier density and Hall mobility were measured. The Au metal electrodes were thermally evaporated onto the film. The ohmic

contact at the Cu_2O/Au interface was confirmed by liner dependence of I-V characteristics. Electrical transport properties of Cu_2O thin films are summarized in Figure 4.3 [124].

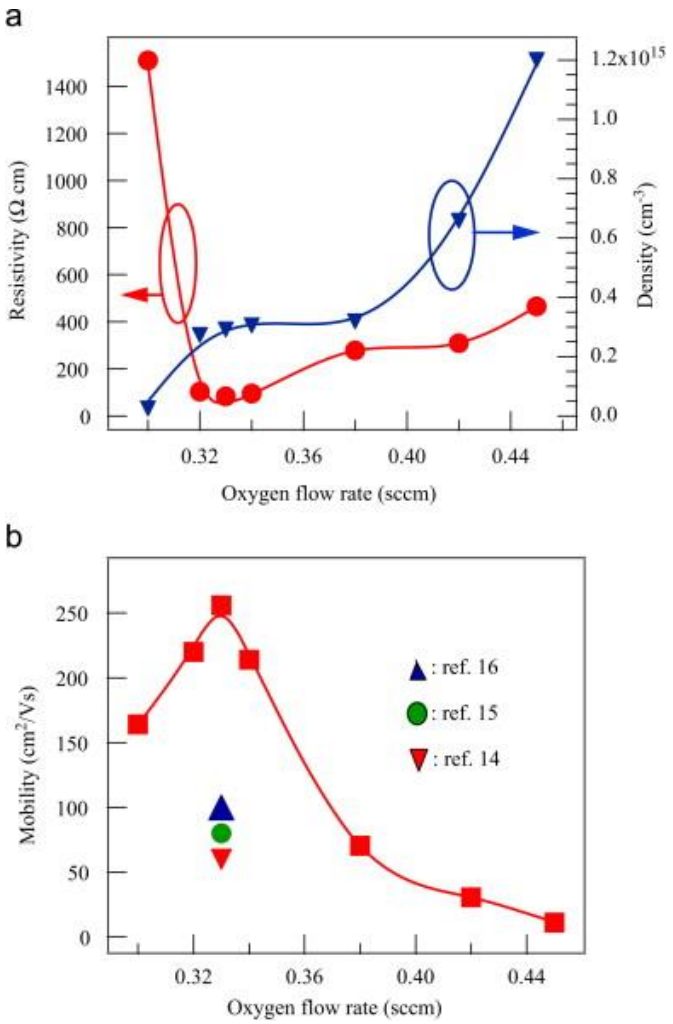

Figure 4.3: (a) Resistivity and hole density and (b) mobility of Cu_2O thin films with LTB-Cu_2O as a function of oxygen flow rates. Figure adapted from Li *et al.* [124].

The increase in hole concentration from 2.5 x 10^{13} to 1.2 x 10^{15} cm^{-3} when the oxygen flow rate increased was probably due to the increase of Cu vacancies with increasing oxygen flow rate [125]. The hole mobility reached as high as 256 $cm^2V^{-1}s^{-1}$ with a hole density of 1x10^{14} cm^{-3}, see Figure 4.3. The high hole mobility is probably mainly due to the improved crystalline quality. However, the resistivity is still quite high, see Figure 4.3a. High mobility and high resistivity at the same time might sound strange, but the correlation between the resistivity and hole density in Figure 4.3a at same oxygen flow rates shows that the resistivity is highly dependent on the amount of charge carriers. At the low oxygen flow rates the resistivitiy is high and the number of charge carriers low, and comparing Figure 4.3a and b, it seems unlikely that the mobilities should be high (> 150 $cm^2V^{-1}s^{-1}$) at the same time. However, there is a possibility that the low amount of charge carriers actually have very high mobilities. A low amount of holes should be able to move more freely and thus have high mobilities. This emphasizes the importance of the charge carrier density in IBSC host materials, see Appendix B and Navrus and Saritas [126].

ZnO

According to Katayama [106], ZnO has low transmittance at the wavelength of light. For solar energy utilization, given that the solar spectrum is in the 250-2500 nm region at sea level, the light in the infrared region (780-2500 nm) has considerable energy percentage that should be maximized [127]. Generally ZnO is a high performance material when it comes to easy deposition to high qualities, low resistivity, high mobility and generally few challenges regarding solar cell applications.

4.4.4 Most prominent challenges

The focus of improvement of these heterostructures should be at the most prominent challenges. Based on the literary review of material challenges, the two challenges worth improving are the resistivity of Cu_2O and the interface quality at the Cu_2O/ZnO junction.

To find solutions to these material problems, a starting point can be to look at the crystallinity of Cu_2O and the p-n interface. First, increasing the crystalline quality of the Cu_2O layer will lead to better transport properties, and looking at different ways to optimize the Cu_2O/ZnO interface may decrease band bending and the amount of defects.

4.5 Possible improvements of the Cu_2O/ZnO heterojunctions

Improvements of the conversion efficiency is expected to be possible by eliminating lattice-mismatch defects, which acts as recombination centers, and by increasing the transmittivity of ZnO film and reducing the resistance of Cu_2O [106]. No solution to increase the transmittivity of ZnO is proposed, but the possible issue is acknowledged.

A Cu metal thin film is easily created at the interface of AZO/Cu_2O heterojunctions by reducing the Cu_2O [120]. As a result, the photovoltaic properties of Cu_2O solar cells are markedly affected. Therefore, the AZO deposition method and conditions as well as the surface treatment of Cu_2O are important parameters.

4.5.1 Minimizing interface problems

The interface defects can be minimized by several techniques, such as; wet chemical etching, nanoscale structuring and inserting a buffer layer between the p- and n-layer.

Wet chemical etching

The three highest efficiency cells found in literature [102, 115, 116] were all fabricated by depositing layers on Cu_2O wafer-like polycrystalline sheets. A wet etching procedure was used to remove any trace of CuO from the Cu_2O surfaces before the ZnO films were deposited. For device fabrication, the CuO surface layer of the oxidized Cu_2O sheets can be removed by etching in three solutions: first, a solution of iron chloride ($FeCl_3$) and hydrochloric acid (HCl) followed by a solution of nitric acid (HNO_3) and sodium chloride (NaCl) and, finally, an ammonium persulfate ($(NH_4)_2S_2O_8$) solution in order to obtain a smooth surface [120].

Nanoscale structuring

According to Musselman *et al.* [38], nanoscale structuring of the Cu_2O/ZnO interface could be introduced to minimize electron transport lengths. Electrodeposition of Cu_2O was found to result in complete filling of self-assembling ZnO nanowire arrays to produce continuous junctions with abrupt interfaces. The nanowire architecture reduced the optical depth of the absorbing layer by scattering the incident light and collected charges from further within the absorbing layer. This technique was further investigated by Lee [128], which reported that a spatially controlled vertical ZnO nanowire array to overcome the short minority carrier diffusion length in Cu_2O. A scalable fabrication process was also developed using colloidal lithography and hydrothermal growth of ZnO nanowires. Figure 4.4 shows a nanowire Cu_2O-ZnO heterojunction solar cell [38].

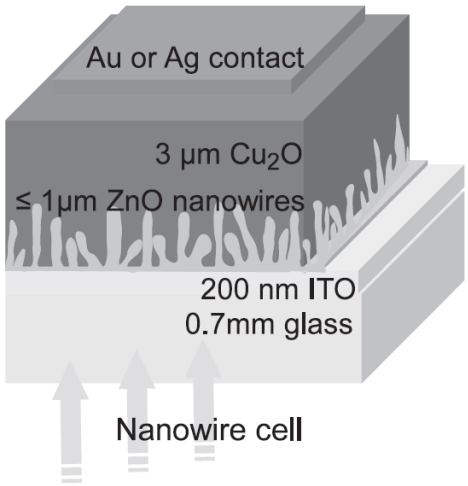

Figure 4.4: Nanowires of ZnO can minimize the electron transport lengths [38].

Nanostructured Cu_2O/ZnO heterojunction solar cell can also be fabricated by electrodeposition of Cu_2O into ordered ZnO cavity-like nanopatterns [129]. Significant increase in performance was observed in the cavity-like cell due to increased p-n heterojunction area and enhanced charge carriers collection ability. These results showed a simple and economic approach to fabricate electrodeposited nanostructure Cu_2O/ZnO solar cells.

Buffer layer

Inserting of a buffer layer at the heterojunction between Cu_2O and ZnO films will improve the performance of the cells by eliminating the mismatch defects which act as recombination centers, and protection of reduction processes that may exist between ZnO and Cu_2O [130]. Recombination via tunneling can also be reduced in presence of a buffer layer [105]. Among the proposed buffer layer materials are TiO_2 [105], $Zn_{1-x}Mg_xO$ [120], ZnO-In_2O_3 [120], amorphous $Zn_{1-x}Sn_xO$ (a-ZTO) [128] and un-doped ZnO (ZO) [116]. Of these materials, the a-ZTO buffer layer led to the highest reported conversion efficiency for thin film Cu_2O-ZnO cells of 2.65 % [128], and a ZO buffer layer was used in the Cu_2O wafer based cell with the efficiency record of 4.12 % [116].

4.5.2 Improve material properties

In particular, a substrate having large grains, high mobility and low resistivity is preferable for heterostructure cell growth [102]. The most efficient way to improve material properties for solar cell application might therefore be to increase the crystallinity. As mentioned in section 2.3.1, single crystal production results in high quality materials with improvements properties.

Single crystal production of Cu_2O

Using single crystal Cu_2O can reduce the resistivity significantly. Papadimitriou and Economou [131] mentioned three well known method to prepare these single crystals. First, Toth *et al.* [132] used a grain growth method to prepare thin plates of single crystals, but this method has two disadvantages. The orientation of these plates was not controllable, and secondly, during the oxidation a depleted interfacial region was formed. Therefore, in order to obtain a single crystal, half of the plate had to be removed by mechanical polishing. By

oxidation of single oriented crystals of Cu at variable oxygen pressure and temperature, Ebisuzaki [133] prepared single crystals and relatively thick disks of Cu_2O. The thickness of these disks was approximately 3.2 mm and the diameter about 18 mm.

For most applications, bulk single crystals are wanted. Usually bulk single crystals are grown from melts that requires crucibles. In the case of cuprous oxide however, the conventional bulk single crystal growth methods are challenging because molten Cu_2O is highly reactive with most crucible materials [134]. Therefore, the crucible free floating zone (FZ) method is ideal for growing high purity bulk cuprous oxide crystals [135].

Trivich and Pollack [136] may have been the first to explore a FZ-similar method to produce single crystals of Cu_2O. They used polycrystalline rods of Cu_2O to prepared single crystals in an arc-image furnace. Decades later, Ito *et al.* [32] used the floating zone melting technique for growing single crystals of cuprous oxide. Polycrystalline specimens of Cu_2O were used as "seed rods" for growing single crystal Cu_2O in an imaging furnace. The single crystals were cut as discs, and polished mechanically using Al_2O_3 powders and etched chemically. Ito *et al.* recognized that single crystals prepared by this method in air were of the best quality both considering concentration of defects and transport properties. This method was also successfully used by Chang *et al.* [135], where the feed and seed rods were prepared by thermal oxidation of copper metal rods of three different purity ratings; 99.9, 99.99 and 99.999 % pure Cu. The higher purity samples contained fewer copper vacancies because impurities can raise the activation energy of Cu_2O oxidation. However, for solar cell applications, a favorable higher number of copper vacancies would increase the hole concentration and mobility.

It took almost 50 years of research and financing to grow very high quality, large single crystals of Si by the FZ method, but today it is possible to simulate numerically the growth situations to improve the quality of even large diameter single crystals [137]. The FZ method has not yet been developed for large diameter bulk cuprous oxides, but it seems likely that the large FZ mono-Si technique can help further research of large Cu_2O single crystal wafers. However, continuous cooperation between crystal grower and crystal user and good crystal characterization is necessary to achieve the same research growth for other technological important materials than Si [137].

Reducing the resistivity of Cu_2O

The resistivity in Cu_2O can be greatly reduced by growing single crystals as opposed to polycrystals. To reduce the resistivity even further, careful doping of the material can be a solution. For Cu_2O substrates slowly cooled to room temperature resistivities greater than 22000 Ω cm were found by Mittiga *et al.* [102], and dopants such as F, P, N, Cl, In, Mg, Si, and Na were introduced to reduce this value. A clear resistivity reduction was reached only with Cl doping, but a strong reduction of the diffusion length also occurred.

High quality production of ZnO

Although not equally important as the crystalline quality in Cu_2O, single crystals of ZnO can also reduce some of the challenges resulting in poor cell performance in Cu_2O/ZnO heterostructures. According to Ohshima *et al.* [138], ZnO single crystal growth has mainly been carried out by three methods; the flux method [139, 140], the chemical vapor transport (CVT) method [141-144] and the hydrothermal method [145, 146]. The hydrothermal method

is known as a method to grow highly crystalline and large-sized crystals at relatively low temperatures [147].

If the ZnO emitter is a window layer on top of the Cu_2O, single crystallinity might be difficult to achieve by deposition on single crystal Cu_2O. High quality deposition of ZnO on Cu_2O leading to large grain polycrystallinity can probably be achieved by a high quality physical deposition techniques, such as MBE, PLD or MOCVD as decribed in section 2.3.2.

4.5.3 Low resistivity contact formation

As discussed earlier, the resistivity of Cu_2O is a great issue that must be solved before high solar cell efficiencies can be reached. An important step in this realization is to optimize the Cu_2O ohmic contact formation. Most metals reduce cuprous oxide to form a copper enriched region or a large surface density of states, except non-reacting gold [148]. Gold is the most reported ohmic contact for the Cu_2O layer in solar cells [149], but Tl is also reported not to reduce Cu_2O [118]. The necessity of further research towards reduction of the contact resistance is needed, and one solution may be a degenerate layer between the Cu_2O and metal contact [149].

In order to form an ohmic contact to n-type ZnO, the work function of the contact metal should be less than that of ZnO's electron affinity (4.2–4.35 eV) [41]. Therefore, Al and Ti have been used for ohmic contacts to n-ZnO as their work functions to ZnO are 4.28 and 4.33 eV, respectively [150].

4.6 Synthesis of Cu_2O/ZnO-based IBSCs

Quantum dot intermediate band solar cells have been studied for some time, but their weak sub-bandgap absorption results in low efficiencies [13]. Bulk intermediate band solar cells were initially considered improbable, but Luque and Marti describe four approaches for synthesizing bulk IBSCs [13]:

- Highly mismatched alloys
- Transition metals derived from Ab Initio calculations
- Thin film technology for IBSC
- Intermediate bands generated from deep levels

The latter approach is further studied here, as a p-Cu_2O/IB-Cu_2O/n-ZnO heterojunction. Some experimental and calculated procedures to form deep levels can be found in section 4.6.1. Cu_2O as an IB material is proposed in section 4.6.2, and optimum IB material parameters are discussed by Navrus and Saritaz [151] and in the specialization project conducted in the SoRoSol-group [17].

4.6.1 Bulk IBSC based on deep levels

Ion implantation is a promising method to form an intermediate band based on deep levels through high doping. Samples of Si that are heavily doped with Ti have been prepared by ion implantation with densities above $2x10^{21}$ cm^{-3} [152]. A following pulsed-laser melting process can restore the high quality of the crystal. At low temperatures, a rectifying junction is formed between the Ti-doped layer and the highly resistive n-substrate, which can be interpreted as an IB–nSi junction [13, 153]. The Ti-doped layer becomes electrically isolated from the substrate, and seems to show p-mobility, which is attributed to the almost electron-filled Ti level that would act as an intermediate band [13]. The Ti-doped layer seems to present a reduced non-radiative recombination due to high concentration of Ti [154]. Recently, it was confirmed that the recombination was suppressed at high enough Ti concentration [155]. It was suggested that the concentration of recombinant deep level reached a saturation value, in this case at 10^{13} or 10^{14} cm^{-2} implantation doses, and that the remaining implanted atoms had no recombinant nature.

4.6.2 N-doped Cu_2O as IB material

It has been proposed that nitrogen doped Cu_2O can be a possible intermediate band material [156]. They found that Cu_2O samples doped with nitrogen in the 1.15-2.54 at% range show clear absorption bands below the fundamental optical band gap. The intensity of the intermediate bands is correlated with the nitrogen concentration, and the energy of one of the two levels (0.72 eV) corresponds exactly to the optimal value for an IB device. The most heavily doped Cu_2O sample shows a resistivity value as low as 1.14 Ω cm, which is the lowest value ever reported for Cu_2O.

The doping effects of nitrogen on the crystal structure, electronic structure, and optical properties of Cu_2O have also been studied by first-principles calculations by Zhao *et al.* [157]. The results showed that nitrogen doping slightly widens the band gap of Cu_2O, and form an intermediate band located at about 0.9 eV from the valence (or conduction) band. N-doped Cu_2O is very likely to absorb at a maximum across the solar light spectrum, from the near infrared region to the ultraviolet region. Based on these results, N-doped Cu_2O was considered to be a perfect intermediate band material by Zhao *et al.*.

Cu_2O also possess near optimal material properties for IBSCs except for the high resistivity [17, 126]. See Appendix B for theory of IBSC material properties and Appendix C for reference values for high performance IB materials.

5 The method based on systems engineering

The systems engineering process (SEP) is explained below. The SEP-based method used in this thesis is explained in section 5.2.

5.1 Systems engineering process

The management technology called systems engineering (SE) can assist and support policy making, planning, decision making and associated resource allocation or action deployment [158]. The systems engineering process (SEP) is a comprehensive, iterative and recursive problem solving process, applied sequentially top-down by integrated teams [20]. From a life cycle perspective, the phases of a system included in systems engineering are given in Figure 5.1 (modified after Fet [21]). SEP is a process of bringing a system into being, and included in the process are; project planning, design, construction and production, see the two top boxes in the figure. These processes are explained more detailed in blue text in the figure. The SEP only deals with the first part of the system's life cycle, as seen from the figure.

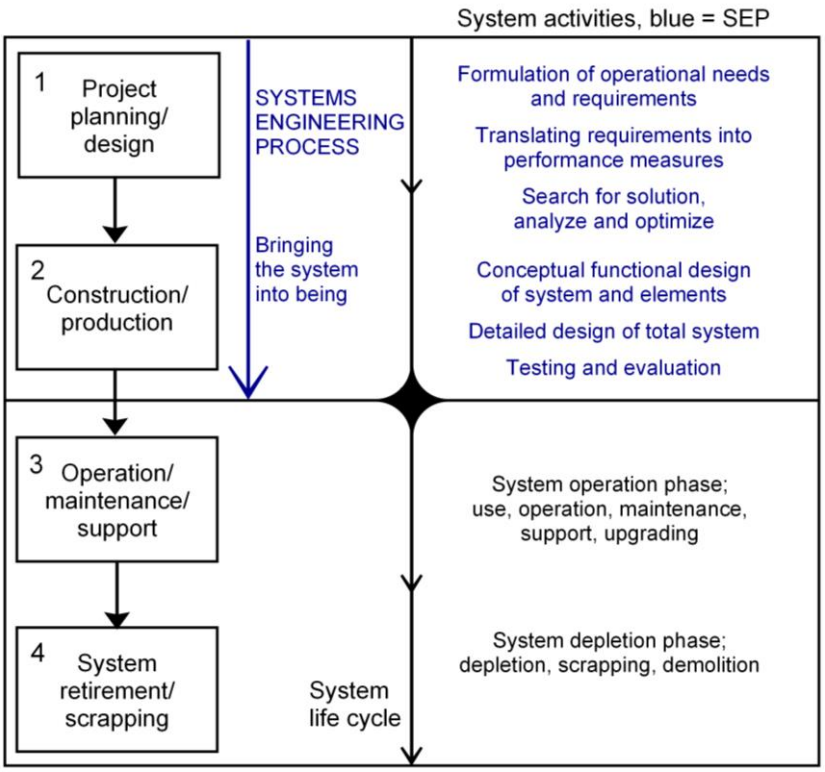

Figure 5.1: The systems engineering process in a system life cycle perspective, where the four process boxes constitute the system life cycle, and SEP is the process of bringing the system into being; box 1 and 2, with more detailed description of activities in blue. Figure modified after Fet [21].

There are generally three phases of systems engineering management; Development Phasing, The Systems Engineering Process and Life Cycle Integration. The SEP is the middle activity as described in Figure 5.2 [20], where "Process input" is the input from the initial phase "Development Phasing" and "Process output" is the input to the next phase; "Life Cycle Integration". The SEP activities defined by Leonard [20] are compiled into three main processes; "Requirements Analysis", "Functional Analysis and Allocation" and "Design Synthesis". The "System Analysis and Control" phase applies to all three processes, and

includes technical management activities required to measure progress, evaluate and select alternatives and document data and decisions. The three processes are summarized in Table 5.1.

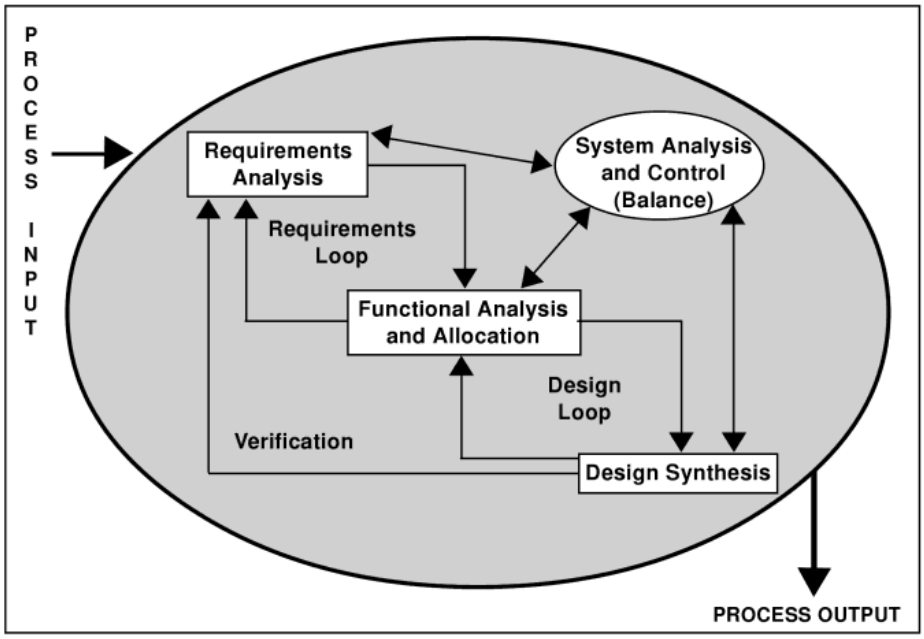

Figure 5.2: The systems engineering process [20].

Table 5.1: Summary points from the three main processes in the systems engineering process [20].

Requirements analysis	- Three requirement perspectives: Operational, functional and physical - Collaboration between various life cycle stakeholders necessary to produce acceptable requirements document - Requirements are a statement of the problem to be solved - Constrained and integrated requirements are required - Trade studies must be accomplished to select a balanced set of requirements that provide feasible solutions to customer needs
Functional analysis and allocation	Translating system-level requirements into detailed functional and performance design criteria: - Identifying at successively lower levels what actions the system has to do - Define task sequences and relationships between functional elements - Define process and data flows - Define the time sequence of time-critical functions - Allocate performance and establish traceability of performance requirements
Design synthesis	Translate the functional architecture from the previous process to a physical architecture by defining physical components needed to perform the functions: - Allocate functions and constraints to system elements - Synthesis technology elements and alternatives, and assess technology alternatives - Define physical interfaces and system product work breakdown structure (WBS) - Develop life cycle techniques and procedures - Integrate system elements and select preferred concept/design

By using a systems engineering process it is possible to systematically view the elements of the system, assess their contributions to the problem, and establish a framework for the environmental assessment [159] of the system. The approach illustrated in Figure 5.2 can be divided into the six steps shown in Figure 5.3, as explained by Fet [21]. These six steps are described more detailed in the following sections.

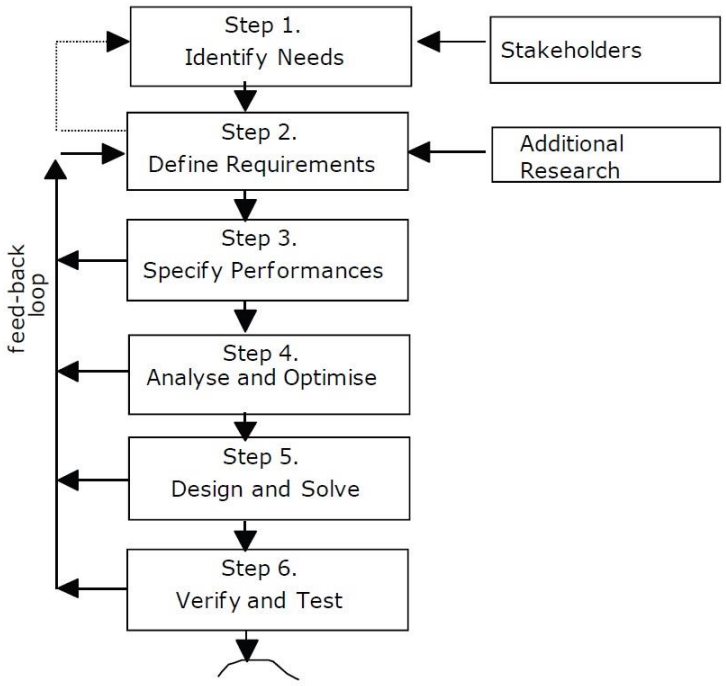

Figure 5.3: The six steps in the systems engineering process [21].

5.1.1 Step 1: Identify needs

As described by Fet [21], the needs or desires for one or more system results are identified in this first step. The most important stakeholders within the system's life cycle who provide this system are also identified.

When identifying the needs for improvements, the stakeholder's requirements must be known, see Figure 5.3. The requirements to environmental performances of a system can be set by the international and national authorities. The requirements can be based on knowledge about the condition of the environment, about economic interests, and/or the need for new or improved technologies. The needs must be identified in accordance to these requirements from the stakeholder(s).

These following three questions are useful to identify the needs [21]:

1. What is needed? (Statement of needs)
2. Why is it needed? (The logic)
3. How may the needs be satisfied? (Search for technical solutions)

The "statement of needs" should be presented in specific qualitative and quantitative terms, in enough detail to provide a foundation for further activity. Step 2 in this systems engineering process is defining the requirements. These first two steps are repeated until all needs and requirements are defined and quantified.

5.1.2 Step 2: Define requirements

In this step, Fet [21] explains that the operational, physical and functional requirements are defined. Requirements regarding the actions and functions to be carried out during the operation of the system are called *operational performance requirements*. These requirements reflect the stakeholder's needs relative to utilization and achievement of a mission, and are thus related to the useful life of the system. The operational requirements can be answers to the second question in step 1; the "whys".

The *functional performance requirements* describe the system's ability to carry out work, and involve breaking down the system into convenient parts. The life cycle activities are described here, and the functional requirements are the answer to the "what" question in step 1.

The *physical performance requirements* reflect the need for physical interactions between different sub-systems, system elements, and interaction with the environment. These requirements are related to a specific location, environment and application, and may be an answer the "how" question in step 1.

The requirements should address all stages of the system life cycle within the system boundaries, and must be set to each part of the integrated system, as seen from Figure 5.4, modified after Fet [21]. The bioware, economics and software of the system make up the management area, and the hardware, or technology, is the operational area.

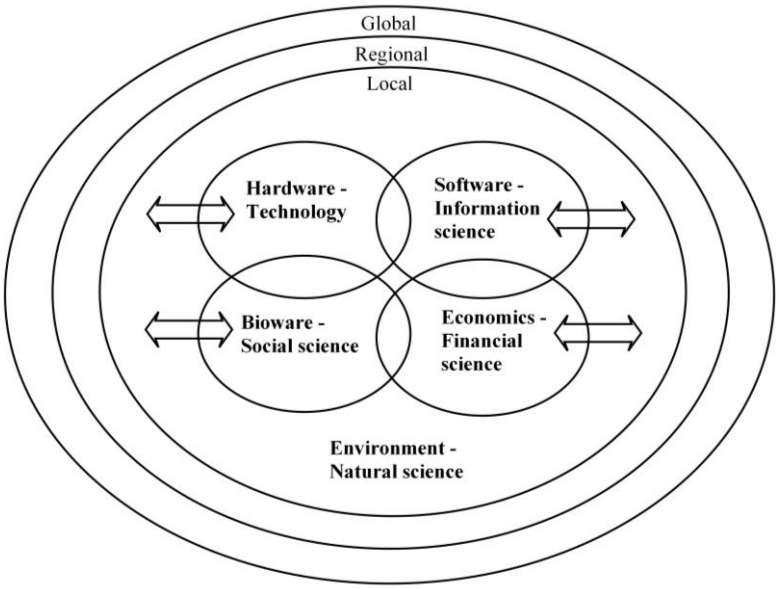

Figure 5.4: An integrated system including the four disciplines; technology, financial science, information science and social science, that interacts with the environment (natural science). The figure is modified after Fet [21].

When defining requirements for a system, the choice of discipline(s) included in the study should be defined. The system boarders and possibility for interactions with the environment are also described as a result of this system analysis limitation.

5.1.3 Step 3: Specify performance

The requirements are translated into well-defined and measurable criteria for the total system and its subsystems to specify the system performance [21]. The system should be subdivided into convenient parts, and a functional analysis related to subsystems, system elements and integrated parts of the system must be performed. The life cycle activities must also be described in this step.

A process flow chart is made in this step to create an overview of the life cycle of the system. This flow chart is a sequence of processes linked together by material flows, including transportation of material.

This step should include a functional analysis where requirements are broken down from the system level to the subsystem level, and as far down in the system hierarchy necessary to identify criteria and constrains for system components. All facts of system design and development, production, operation and demolition and support should be covered. This way all significant activities during the system's life cycle are taken into account, and at the same time all system elements and integrated parts (hardware, software, bioware and economy) are recognized and defined.

Measures and conditions for measurements should also be included in the specified performance. The full range of physical and regulatory constraints under which the system operates is also recognized in this step. All these performance measurements should verify the requirements set in step 2, and at the same time the needs from step 1 are met. Regarding system requirements that only ask for performance of the total system, the system designer can distribute or allocate specifications to the subsystems and individual elements.

The performance specification should be a result of an iterative loop of step 1, 2 and 3, see Figure 5.3 [21]. The Requirements from step 2 are usually set within acceptable tolerances, and the performance description is only accepted if the requirements are satisfied within these tolerances. The output of both step 2 and step 3 must satisfy the needs stated in step 1.

5.1.4 Step 4: Analyze and optimize

Different options for a solution can be analyzed based on the performance specification [21]. This step includes evaluating various system design alternatives. Conflicting interests are identified and balanced, and may lead to the need for prioritizing the requirements.

Trade-off and specification of system performance are repeated in an iterative process until the potential for a satisfactory system design or solution is found. To perform a fair and objective evaluation of the system, a reproducible way of testing and evaluating is required. Sometimes an important performance requirement for one system element must be prioritized, and then the rest of the system is optimized with this constraint.

To sum up this step: searching for a configuration, finding principles and technologies to meet specifications conceptually, selection or discrimination between system alternatives and optimizing by trade-off analysis.

5.1.5 Step 5: Design and solve

This step involves designing a system that satisfies the needs of the stakeholders [21]. An interdisciplinary team is often required to secure the best solution. Subsystems, elements, components and even processes/activities should be defined. This detailed design phase begins with the configuration or concept derived from step 1-4.

When an accepted conceptual design is established, further definitions leading to realization of hardware, software, bioware and economics, and their relation to the environment from a life cycle perspective, should be made. Performance of the system during its entire life cycle is important here, and this will particularly be of interest when environmental impacts are evaluated.

5.1.6 Step 6: Verify and test

After this step the system can be produced, and all interests regarding the system have been dealt with [21]. During the construction of the system, it should be verified by terms of the needs and requirements identified in step 1 and 2. This can be done by simulation or rapid prototyping compared to known reference systems. The system should in particular satisfy the requirements set by the stakeholders and users of the system. With a test program, a performed test phase with feedback should be registered and evaluated.

By writing a final report with all data, test conditions and procedures, the process behind the development of the solution can be verified and replicated for new problems. Testing of the system can continue long after the SEP is completed. Different types of testing during the system life cycle are illustrated in Figure 5.5 [160].

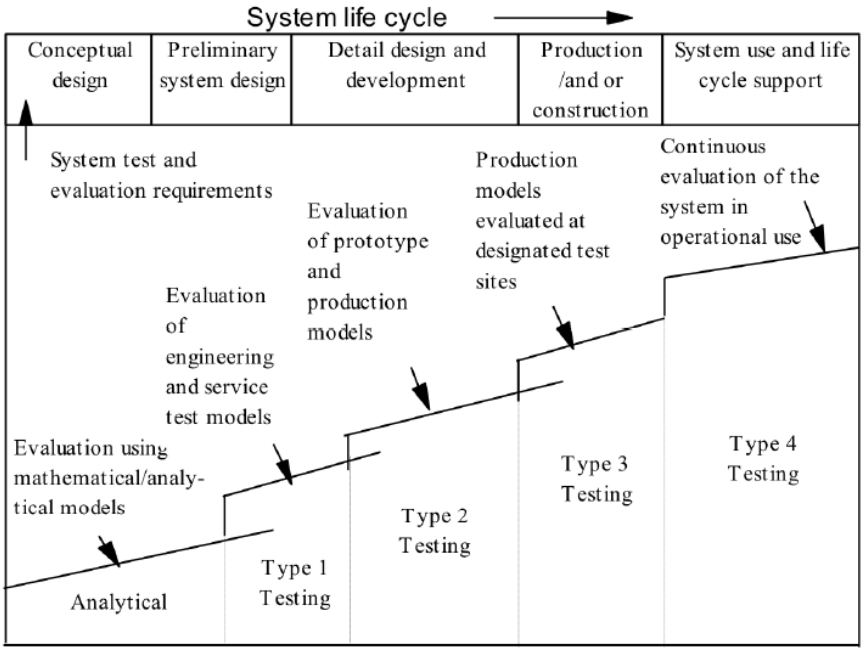

Figure 5.5: System evaluation during the system life cycle [160].

5.2 The method used in this thesis

The SEP described above is a holistic methodology that might work best with systems that are already developed to some extent and possible to describe, or systems that can be planned based on knowledge of similar systems with the same technology and/or materials. The non-technological disciplines; economy, bioware and software, see Figure 5.4, usually require an interdisciplinary team to identify a new or improved design from a holistic system perspective.

5.2.1 How to reach the goals

A complete SEP regarding all system disciplines for an immature system like the IBSC system turned out to be too time demanding for a master's thesis in materials technology. The combination of the systems engineering way of thinking with a top-down holistic approach, and a bottom-up lab-oriented field like material science, was challenging and an individual method for this kind of assignment had to be designed.

The work carried out in this thesis included planning of an intermediate band solar cell using the SEP methodology, with the whole IBSC system as a starting point and driving force to develop solar cells ready for PV system installation. This was done with two main goals in mind:

1. Map the challenges regarding Cu_2O and ZnO as host materials in an IBSC with emphasis on cell material selections and production route.
2. Describe requirements and specified performance for a complete IBSC system, and at the same time prepare for a LCA.

A simplified SEP was used to obtain the main goals above in an efficient and realistic way. The available literature to aid the design of the materials science-SEP combination method was limited, since SEP probably has never been used for a PV system with material focus. The new method combines material analysis and product design by identifying a suitable IBSC production route conducted in the SEP steps 1-5. Step 6 was not performed, since no lab work or other form for testing of the imagined IBSC cell production and IBSC system was possible during the limited time.

5.2.2 Overview of the process

First, the needs were identified from an overall perspective down to the main subsystems of the IBSC system in Chapter 6, where the system structure also is explained. Next, the requirements of the system and subsystems based on the needs can be found in Chapter 7. In Chapter 8 the system performance is specified - first from a system perspective, and then broken down to the intermediate band solar cell subsystem and its system elements. This IBSC subsystem, meaning only the IBSC device, is further investigated in Chapter 9, from a detailed material perspective. A production method for the IBSC is selected in Chapter 10, where also a possible design of the whole PV system is given as a case example of an IBSC system in Oslo.

Some of the choices made for the IBSC system throughout these results chapters will influence the rest of the process, and are given a section in the end of the chapters for justification and eventual alternatives that could have been chosen.

The resulting method was a dynamic materials science-based systems engineering process where mainly materials and production route choices, as well as some PV system aspects, were analyzed and discussed.

6 Step 1: System needs

This is the first step in the systems engineering process, as described in section 5.1. First, the needs for a general PV system are defined, before the interested parties and technology needs of an IBSC system are stated. The IBSC subsystem needs are further explained in section 6.2.

6.1 Identify the needs

The overall needs of an integrated system of photovoltaic technology are found for different disciplines in section 6.1.1 to get an idea of how wide the system boarders for photovoltaic systems can be. In section 6.1.2, the parties interested in an IBSC system are identified. The hardware, or technology, discipline from Figure 5.4 is then chosen for further development of the intermediate band solar cell system, whose technological needs are found in section 6.1.3.

6.1.1 The overall needs

The customer of a future PV system is the society, or everyone using electricity. The need for electricity generated from renewable energy resources, like the sun, will be more and more evident in the future. Thus, the overall need for this PV system can be formulated like "High efficiency electricity generation from solar radiation".

To get an overview of the needs for every part of the integrated system, the three questions described in section 5.1.1 are first answered for all the disciplines in Figure 5.4. To do this on a higher, general level of the renewable energy system, the reader is asked to take some steps back from the specific IBSC concept.

Table 6.1: The overall needs for the whole integrated system of photovoltaics.

	Environment	**Hardware**	**Bioware**	**Economics**	**Software**
What is needed?	- Renewable electricity generation - Less emissions during whole lifetime	- Higher efficiency electricity generation - Less maintenance - New PV systems	- Easier access to renewable energy sources - Encourage the public to use PV systems	- Cheaper electricity generation - Financing and demand for new PV technology	- Transparent information to gain trust - Smart Home and other IT solutions
Why is it needed?	- To phase out environmentally damaging and limited fossil fuels - Environmental restrictions/laws	- Most existing energy technologies focus on fossil fuels - Higher efficiency and lower cost	- Higher standard of living → increased energy demand - All people do not think green	- Less area used; save money - Affordable in developing countries	- Easier - More control and user-friendly solutions
How may the needs be satisfied?	- Wind, sun, waves and other renewable energy sources - The suns energy is clean and limitless	- PV technology can cover the future energy need - Longer lifetime and better performance - R&D: New PVs	- Encourage people to use environmentally friendly electricity generating products, like PV systems	- More funding for research and technology development - Cheaper production (e.g. solar cells)	- Research and development of PV-IT systems - Knowledge level of the public - Marketing of solar cells

Regarding the need to encourage people to use environmentally friendly PV systems, it is important to keep in mind that simple and cost-effective solutions are needed to reach out to people with varying standards of living. Today's PV systems are fully competitive for off-grid electricity generation and can be delivered with diesel-based on-grid systems in countries with good solar resources [23]. PV technology can thus be an important step towards greener energy in developing countries.

In developed countries, grid-connected systems are beneficial because of the easy access to the grid. However, the variable nature of the solar source, especially in northern countries, means that appropriate grid management and technology (e.g. smart grids) and energy storage are required for maximum utilization of the PV system [23]. As an example of a system that consists of all the integrated parts and disciplines of systems engineering, a future grid-connected Smart Home PV scenario with user-friendly solutions is shown in Figure 6.1 [161].

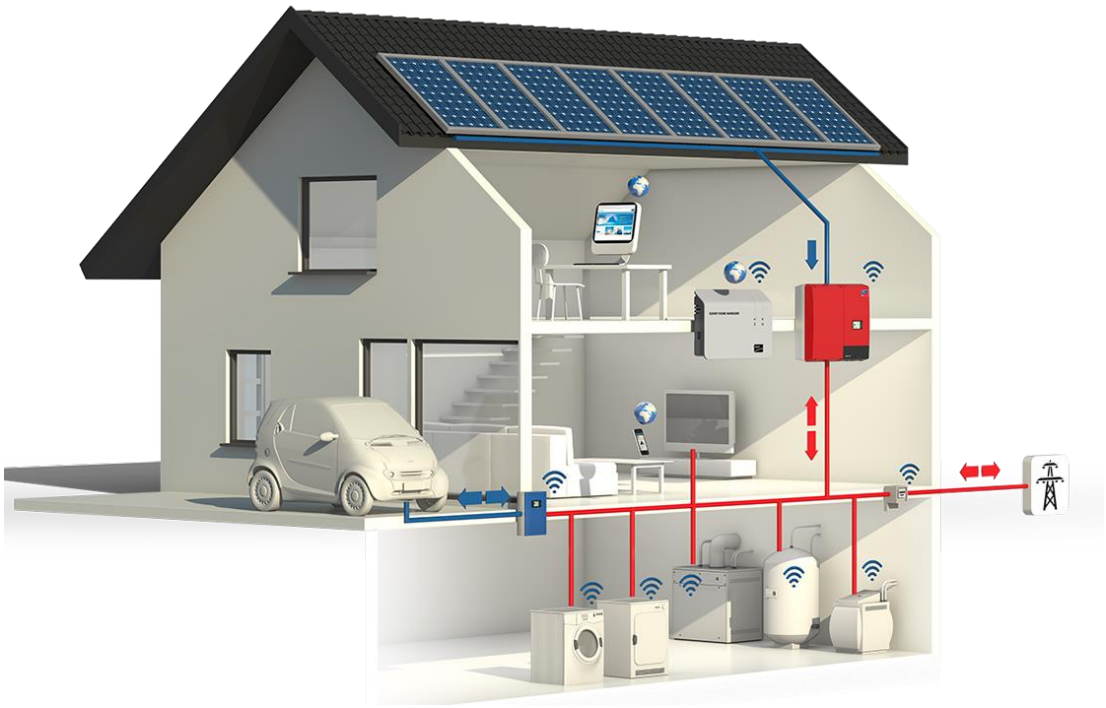

Figure 6.1: A Smart Home solution with an integrated energy system of different disciplines [161].

The Sunny Home Manager is the central controller in the SMA Smart Home in Figure 6.1 [161]. It is connected to the PV inverter called "Sunny Boy 5000 Smart Energy" through a communication system, and allows connections to household appliances. Based on the production and consumption forecast, current output and the desires of the user, the Sunny Home Manager controls household appliances so that self-produced power is delivered whenever needed.

Based on the examples above, new PV technology can both be user friendly and implemented in existing and new energy markets. An important step towards implementation of both simple systems to improve the living standard of low-requirement customers and more complex systems for e.g. the industry or high-standard customers is to increase the efficiency of the solar cells.

6.1.2 Parties interested in an IBSC system

There are many interested parties in a potential well-functioning intermediate band solar cell system that in theory can give 50 % higher efficiency than conventional Si-based systems. Based on the three time perspectives; short term, medium term and long term, and different geographical scales, proposed interested parties are outlined in Table 6.2. In a PV system life cycle, short term will mainly be related to planning and selecting materials, production route for laboratory and industry, and give examples of a designed PV system. The medium term perspective can be related to testing of the solar cells and further development in the industry, and finally, the long term perspective can be thought of as the utilization phase and further down the system's life cycle.

Table 6.2: Interested parties for a new intermediate band solar cell PV system in three different time perspectives and geographical extent.

	Local	**Regional/ national**	**Global**
Short term perspective	- SoRoSol-group - Solar cell researchers at NTNU in general	- Solar cell researchers (Norwegian universities) - Norwegian solar cell industry	- Solar cell researchers worldwide - Environmental organizations
Medium term perspective	- Further development and improvement at NTNU - Possible cooperation between NTNU and solar cell industry	- Solar cell industry in Norway - Norwegian environmental organizations	- Solar cell industry worldwide - Environmental organizations - The public
Long term perspective	- Citizens of Trondheim - Companies with building projects in Trondheim - ZERO emission buildings	- Norwegian public; rooftop, building integrated PV systems - Norwegian industry and building companies - Norwegian environmental organizations - National authorities; regulations for use, end of life, recycling, etc.	- Citizens word-wide - Development aid; give people of need cheap and easy electricity - Building companies - Environmental organizations

Exact goals for designing the system will vary depending on who is describing the goal. As seen from Table 6.2, the many interested parties may have different focus, and may also be related to different subsystems of the total PV system. A bottom-up approach will be used to attempt to reach the goals. This approach is based on needs and requirements which are set in cooperation with the interested parties in the chosen time and geographical zone.

In this thesis, the initial focus will be the local short term perspective, and the interested parties regarded will mainly be the SoRoSol-project members. When the system performance is specified, materials selected and production methods identified in Chapters 8, 9 and 10, however, the long term global perspective will be kept in mind. That way, the designed IBSCs can be competitive on the PV market in the future.

6.1.3 Hardware needs for the IBSC system

This work is a material's science thesis, and should therefore focus on the technology part of an integrated system, and in particular the materials. As already stated in the Chapter 1, an intermediate band solar cell system will be outlined to locate challenges regarding the implementation of a sustainable IBSC technology based on Cu_2O and ZnO. The goal is to investigate whether the chosen IBSC host materials are good candidates, and select the remaining materials in an IBSC, as well as a suitable production method for future industry purposes. An extended goal is to prepare for a LCA of the whole IBSC system.

To identify the "statement of needs" for the IBSC system, discussions with the main stakeholder, Associate Professor Turid Worren Reenaas, and literary search and processing were repeated in an iterative loop until the descriptions of needs were satisfactory for the further activities in this thesis. Table 6.3 describes the needs for the entire IBSC system as answers to the three needs questions.

A more detailed statement of needs is given during the presentation of the whole system in section 6.2.

Table 6.3: Identified hardware needs related to the whole IBSC system.

What is needed?	- A grid-connected intermediate band solar cell system, made with sustainable materials and production, with approx. 50 % higher module efficiency than Si-modules.
Why is it needed?	- High efficiency PV systems contribute to the battle against fossil fuels. - Existing high-efficiency PV systems are made with toxic and/or expensive materials and production routes. - Simpler technology than multi-junction cells (competition). - Reduce area need compared to conventional cells.
How may the needs be satisfied?	- Environmentally friendly (non-toxic, abundant) and high quality materials. - High quality, sustainable production route that preferably is available at NTNU; both equipment and the competence, and more importantly ready for large scale production. - Socially robust solar cells, sustainability verified by a LCA and/or other analyses.

6.2 The subsystems and needs

The system consists of a PV module that can be divided into two subsystems; the balance of systems (BOS) and the photovoltaic (PV) module, see Figure 6.2. The levels in the figure are shown in order to facilitate navigation in the system diagram which may be handy when the needs and requirements are defined in this chapter and Chapter 7.

The BOS subsystem needs are addressed in section 6.2.1, and the PV subsystem needs are stated more detailed in section 6.2.2.

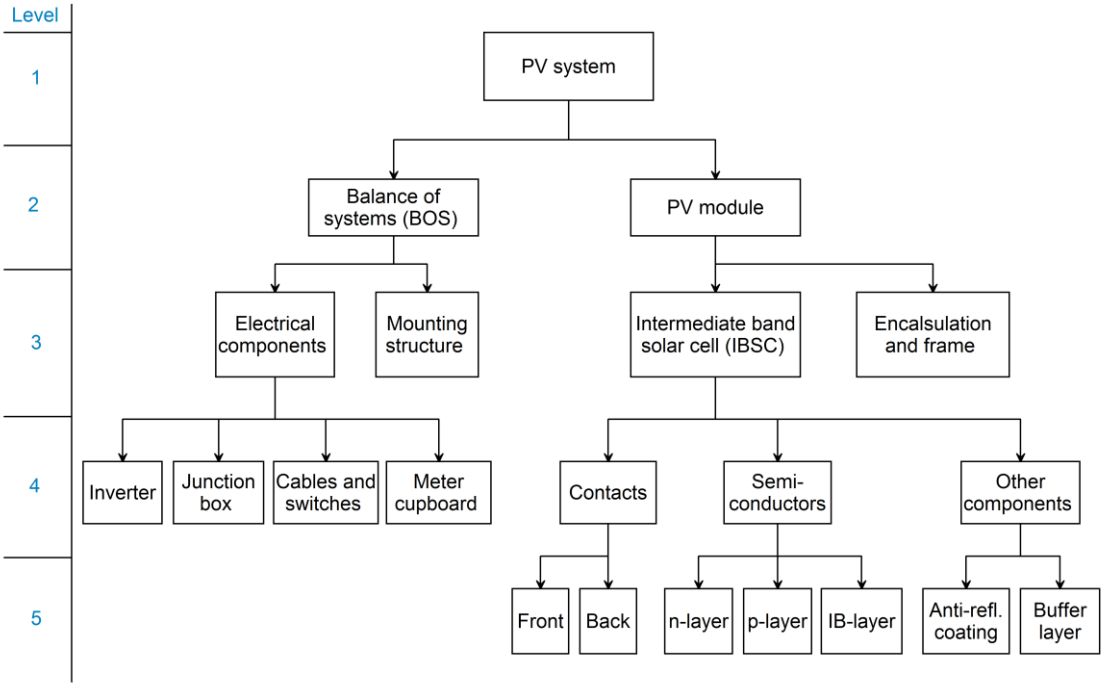

Figure 6.2: The intermediate band solar cell system with subsystems and system elements, divided into system levels.

6.2.1 The BOS subsystem

As mentioned earlier, the IBSC system in question is supposed to be a high efficiency, sustainable grid-connected PV system. At level 2 of the system structure in Figure 6.2, there are two subsystems; balance of systems (BOS) and PV module. The needs for the electrical components and mounting structure of the BOS subsystem are summarized in Table 6.4. For a description of the BOS components, see section 2.5.

Table 6.4: The identified needs for the BOS subsystem at level 2.

What is needed?	- Low resistance, high quality and sustainable electrical components for the junction box, DC main disconnecter, inverter, DC and AC cabling and meter cupboard. - Sustainable mounting structure for a PV system.
Why is it needed?	- To assure sustainability *and* the highest possible output from the IBSC system. - To secure the PV modules in an array on the desired surface.
How may the needs be satisfied?	- Find electrical components suitable for a high efficiency, sustainable IBSC system. - Choose an appropriate mounting structure for the desired mounting method.

6.2.2 The PV module subsystem

As mentioned earlier, the focus in this thesis will be on the materials needed in the IBSCs, and thus the PV module, see section 2.4. The intermediate band solar cells are the most important component of the modules. When the cells are fabricated, they are encapsulated in e.g. EVA and protected with a glass in front and a back sheet, e.g. Tedlar, see section 2.4.1 and 2.4.2. Standard modules are also equipped with a frame to protect the fragile glass edges. The frame facilitates the mounting, improves the modules' rigidity and is used for fastening the mounting system.

The needs for the PV module in Table 6.5 are stated for the total module and the module parts; cells, frame, protection and encapsulation.

Table 6.5: Needs for the PV module at level 2 including the IBSCs, cell encapsulation and module frame.

What is needed?	- A high quality module with; …well-functioning, high efficiency IBSCs based on sustainable materials of high quality. …encapsulated and stringed IBSCs in a sustainable module frame with front and back protection.
Why is it needed?	- To minimize losses, and achieve highest possible efficiency of the module. - The cells need to be stringed together to achieve higher power output than the individual cells, and in order to be used as a unit (module). - The cells need to be protected from weather and other stressing factors.
How may the needs be satisfied?	- High quality production route with high quality materials, with the possibility to upscale to industry production. - Surface treatment and buffer layer between materials to reduce recombination and other interfacial problems. - With well-functioning cell contacts and a suitable anti-reflective coating. - Choose appropriate number of cells, and string them together. - Choose a desired cell encapsulation method and module frame with both high quality and environmental performance.

7 Step 2: System requirements

Step two in the systems engineering process deals with the requirements of the total system, subsystems and system elements; see the system diagram in Figure 6.2. There are many parameters that should be within certain ranges or preferably a specific value when designing a solar cell system. Since the focus of this assignment is on the field of material science, the operational area, meaning the technology discipline will be regarded here, see section 5.1.2 and Figure 5.4. The system requirements are therefore only defined within the system boundaries as illustrated in Figure 7.1, modified after Fet [21].

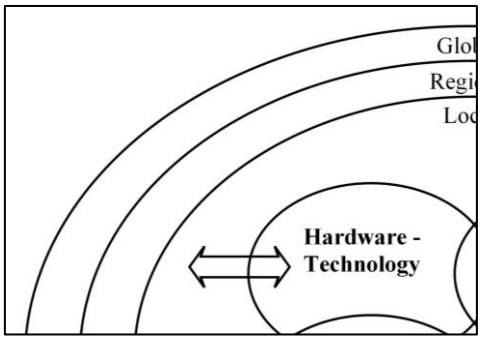

Figure 7.1: Technology is the only discipline regarded in this study. The figure is modified after Fet [21].

The overall requirements for the PV system, its surroundings and its two subsystems are found in section 7.1. The system units and components further down in the system diagram (see Figure 6.2) are presented in sections 7.2 and 7.3. The requirements of the PV module units in section 7.3 are given in detail to translate the needs for the IBSC, encapsulation and framing, which were stated in section 6.2.2.

All requirements are divided into three performance perspectives; operational, functional and physical, as described for step 2 of the SEP 6-steps approach in section 5.1.2.

7.1 Main requirements

First, the requirements for the whole system, surroundings and the main requirements for the two subsystems; BOS and PV module, are identified. See Figure 6.2 for system overview.

After consultation with the main stakeholder, T. W. Reenaas, the location of the PV system was set to Oslo, Norway. PV systems on open areas are not much used in Norway [162]. Oslo is quite crowded with buildings and the open areas are mostly protected land. Based on the results from an interview with Multiconsult [162], the installation method for the system is chosen to be rooftop mounting (see section 2.5.2).

The areas around Oslo could also be considered when planning a PV system based on the findings in this thesis. This is because the system performance parameters of a system under first-phase planning are uncertain and can therefore be varied to fit different locations.

The main hardware requirements for the PV system and its surroundings are listed in Table 7.1. The surroundings are thought of as the environment surrounding the PV system on a rooftop, and are thus found outside the PV system boundaries in the diagram in Figure 6.2 and 6.2.

Table 7.1: Overall requirements for the PV system and the surroundings.

Performance requirements	Surroundings (-)	PV system (1)
Operational	- The underlying material must withstand the stresses from the PV system during its entire lifetime	- Effective electricity generation - All parts should function satisfactory during the whole lifetime - Most of the modules should operate at MPP
Functional	- No shadowing effects by nearby buildings, trees, etc. or the site itself (chimneys etc.) - Possibility to connect to the grid	- The electronic components should be compatible with the I-V characteristics of the PV modules
Physical	- A roof suitable for a PV system in Oslo, Norway - The surroundings should not include any tall objects blocking the sunlight irradiating on the PV array	- Orientation and tilt of the PV array to ensure maximized incoming sunlight and minimize module shading - Sustainable materials in all parts of the PV system

Based on the requirements above, the requirements for the two subsystems; BOS and PV module, are found through an iterative loop of needs, requirements and performance specifications as described in section 5.1.3. The performance specifications are first addressed in Chapter 7.

With limited knowledge of the parts of PV systems other than the IBSCs, most attention is given to the subsystem requirements with the largest impact on the IBSC performance. The overall requirements for the two subsystems, BOS and PV module, are summarized in Table 7.2. Both requirements for the individual subsystems and interactions across the subsystem boundaries are given.

Table 7.2: The requirements for the BOS and PV module subsystems at level 2.

Performance requirements	BOS (2)	PV module (2)
Operational	- Lifetime as long as the PV modules - Minimum maintenance - Resistant to harsh weather conditions	- Long lifetime; 30 years - High efficiency; approx. 50 % higher than Si-modules - Tolerate the weather and temperature at the chosen location
Functional	- The structure should hold the PV modules steady at the desired tilt - Carrying the generated current from the modules to the grid	- Maximum sunlight should enter the cells - The modules must generate electricity - The modules should be connected for optimal electricity transfer to the electrical components
Physical	- Mounting structure and electric equipment fit for rooftop installation - Must be compatible with the module dimensions and performance	- Size of the rooftop modules for: 1x1.6 m - The modules should consist of 60 stringed, encapsulated and framed cells

7.2 Requirements for the balance of systems units

The most important requirements for the mounting structure and electrical components are addressed in this subchapter. This subsystem is generally not included in materials science studies, and some reasoning is therefore needed to justify the chosen requirements.

The mounting method

The mounting structure is supposed to fit a rooftop and be grid-connected. On a rooftop there are four main possibilities for mounting; on a flat roof, in a flat roof, on an inclined roof and in an inclined roof, see section 2.5.2. The alternative which involves building-integrated photovoltaics (BIPV) on a flat roof is not suited in Norway, because of the high latitude that will lead to low amounts of solar radiation perpendicular to a flat surface.

The other three alternatives can be considered when choosing a mounting structure for installing a PV system on a rooftop in Norway. Many of the existing buildings in the Oslo area are possible sites for a PV system. Considering the varying weather conditions in Oslo, an on-roof method may be most suited. During summer time, an on-roof system will have better natural ventilation than in-roof systems, and during the other seasons, the rain and snow will not be as big a threat. In-roof systems may have problems with waterproofing at the roof – module interface, see section 2.5.2.

The inverter

The inverter requirements are evaluated separate from the other electrical components, because choices regarding the inverter influence the system's performance in a much higher degree than the other electrical components. As seen from Table 7.1, most of the modules should be operated at MPP. This implies that either an inverter concept with many inverters, or inverters with multiple MPP inputs should be chosen, see section 2.5.1.

The other electrical components

The junction box should be in close proximity to the PV array, to minimize losses. The cabling, both DC cabling before the inverter and AC cabling after the inverter, should have low resistance to minimize losses during operation, and be of suitable size and capacity for the PV system. The DC main disconnector should be able to isolate the inverter from the PV generator in case of faults, maintenance or repair. The meter cupboard is needed for grid-connected solutions to measure the electricity generated from the PV array.

The most important requirements for the mounting structure, inverter and the other electrical components are summarized in Table 7.3.

Table 7.3: Performance requirements for the units of the BOS subsystem in level 3.

Performance requirements	Mounting structure (3)	Electrical components (3)
Operational	- Should hold the PV array steady during its entire lifetime - Minimum or none maintenance required for the structure during the system's life time	- Function as long as the lifetime of the PV array - As little maintenance as possible - Low resistance through all components to assure minimum electricity losses - Inverter: As high efficiency as possible, and appropriate amount of MPPTs
Functional	- The tilt angle should give maximum average incoming sunlight. - The module structure should not cover/shade other modules - Withstanding cold and harsh Norwegian weather	- Must withstand the high voltage load from the cell - If some of the electrical components are exposed to weather, they should tolerate cold temperatures down to -25ºC - Inverter: Must convert DC current into AC
Physical	- Mounted on an inclined roof or tilted modules on a flat roof - Light weight, minimized material use - Sustainable materials	- Should be as small as possible, to fit into (or onto) the building's construction - Should be as close to the PV array as possible to minimize losses - Inverter: As small as possible, and as many needed for the chosen inverter concept - Sustainable materials to obtain the requirements

7.3 Requirements for the PV module units

The requirements analysis for the module is done at a deeper level than the rest of the system, since both of the goals for this thesis (see Chapter 1) are strongly related to the PV module. The module is also the most important component of a PV system from a materials science perspective, being the PV system unit with probably the highest degree of possible performance improvements through materials technology.

At this point in the SEP, a system feasibility analysis is proposed by Blanchard [163], to evaluate different technological approaches. The various possible design approaches should be identified, the most likely candidates regarding performance, effectiveness, etc. should be considered and a preferred approach should be recommended.

The IBSC

Different technological approaches for production of solar cell materials were mentioned in section 2.3, and IBSC synthesis was briefly described in section 4.6 of the literary review. As mentioned in the introduction, most work has been done on quantum dot IBSCs with poor performance results. The object of this thesis is to design an IBSC system based on bulk IBSCs where the intermediate band (IB) may be formed by ion implantation. This technology has several advantages regarding material quality, but the environmental performance should also be high. The rest of the materials in the IBSC should be produced by high quality and environmentally friendly methods. Toxic and non-abundant materials should be disregarded when selecting cell materials, see Appendix E.

Based on discussions with the stakeholder, Turid Worren Reenaas, the module size was chosen to be 1 x 1.6 meters, and the common cell size of 156 x 156 mm results in modules of 60 cells.

Encapsulation and frame

The most common methods for cell encapsulation and framing of crystalline cells were listed in section 2.4. The modules are supposed to be "standard size" so they easily can compete with other PV technology on the market. Common encapsulation and framing procedures can thus be chosen. However, the environmental aspect should still be taken into account. The encapsulation materials can be toxic, and available framing material is mostly metals. For a future LCA, the raw material data of these materials will contribute to the environmental impact results, therefore care should be taken when choosing materials and technology of these system elements. Solar glass will be used as a top sheet to protect the encapsulated cells, as this is used in almost all existing modules [44]. Anti-reflective coating on the glass can be considered to reduce loss of incoming light at the module surface. However, this solution is not particularly common today.

The overall requirements for the IBSC and encapsulation and frame at level 3 of the system, see Figure 6.2, are listed in Table 7.4.

Table 7.4: Performance requirements for the two units of the PV module subsystem in level 3.

Performance requirements	The IBSC (3)	Encapsulation and frame (3)
Operational	- High quality for growth of the desired layered IBSC-structure during production - Long lifetime - High conversion efficiency through the whole cell lifetime - Stabile, strong cells requiring minimal or no maintenance - IBSC materials should not fracture - Satisfying carrier transport across interfaces should be maintained	- Minimize emissions and material loss during encapsulation and framing - Easy or no maintenance needed - Encapsulating material that do not degrade during the system's lifetime
Functional	- Generation of current from photon absorption - Prevent or minimize reflection of incoming sunlight	- The encapsulation should keep the cells at correct place - Stabile and robust components through all kinds of weather
Physical	- Bulk IBSC with high doping content - Sustainable production route (incl. non-toxic precursors) - Designed for 1 sun and single cell optimum band gap. - The dimensions of cells should be square 156 x 156 mm.	- 60 cells encapsulated for each module framing - Light metal framing for easy handling - Sustainable encapsulation materials and method - Frame that fits into a rooftop mounting structure - High strength frame that shields the fragile glass edges

Requirements of the IBSC components are addressed in more detail below, to elaborate on the specific requirements for the IBSC with emphasis on structure and materials.

7.3.1 Requirements for the components of the IBSC device

As mentioned in the introduction, the main stakeholder, Turid Worren Reenaas, wants to evaluate the performance of a Cu_2O/IB-Cu_2O/ ZnO heterostruction IBSC for possible further work in the SoRoSol-project. The host materials for the IBSC was chosen to be Cu_2O and ZnO from the material screening in the previously mentioned specialization project [17]. However, there are many uncertainties regarding these materials for solar cell purposes, as they are both too immature for industrial purposes. A literary search was conducted on heterostructures with these two materials, see Chapter 4, and several material challenges were discovered. As mentioned in the introduction, these materials were chosen as case materials for initiating the planning of an IBSC system. Other materials could have been chosen. See Appendix C for the top five host material candidates identified in the specialization project mentioned above.

The specific material requirements for each material in the cell (see Figure 7.2) are dealt with in the section below. First, the criteria for the heterojunction materials; p-Cu_2O, IB-Cu_2O and n-ZnO are found, followed by specifications of performance requirements for electrodes, anti-reflective coating and a bufferlayer for the IB-Cu_2O/n-ZnO interface.

7.3.1.1 Cell structure

Of the five materials identified in the specialization project [17, 164], only cuprous oxide has a perfect band gap for the IB-layer, see Appendix C. However, this material turned out to be very hard or impossible to n-dope after further literary search, since Cu_2O is native p-type. Therefore, the resulting structure of the IBSC was a heterostructure, as explained in section 2.2.1.

In most heterostructure cells based on Cu_2O and ZnO found in literature, epitaxial Cu_2O layers were grown on top of a ZnO layer [105, 114]. Having the Cu_2O p-emitter as an active substrate for growth of ZnO is also a logical structure, since ZnO has a larger band gap than Cu_2O. Furthermore, Cu_2O has the most challenging material properties and should be grown with highest quality. The two highest efficiency cells based on Cu_2O and ZnO had in fact a structure where ZnO was grown on high quality Cu_2O sheets [115, 116].

The structure for the IBSC is therefore chosen to be; Cu_2O p-emitter at the bottom, the Cu_2O IB-layer above, and deposited ZnO layer on top. This structure is shown in Figure 7.2.

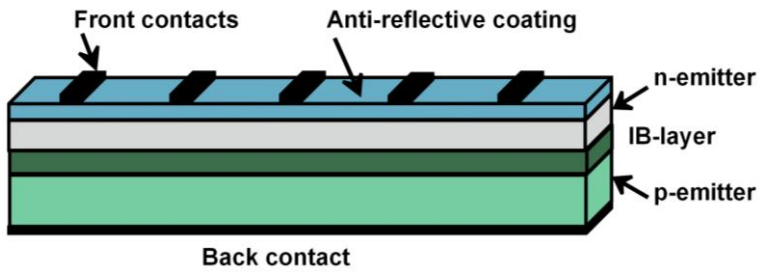

Figure 7.2: An intermediate band solar cell. Not to scale.

See Figure 6.2 for level navigation during the following requirement analysis for the components of the IBSC.

7.3.1.2 The layers of the cell

The p-emitter and IB material will consist of Cu_2O, as mentioned above, and the n-emitter will be ZnO. These materials should be very pure and of high crystallinity, and also exhibit transport properties within certain ranges that will be identified from literature. The environmental requirements regarding abundance and non-toxicity were already considered when these materials were identified in the specialization project [17].

N-emitter

The electronic properties are most important for the n-emitter, as described in Appendix B. High electron mobility, very low resistivity and low electron effective mass are important properties. ZnO was identified to have these properties, see Appendix C. The high value of the band gap can be challenging, because of the resulting band bending at the junction, see Figure 4.2. The ZnO-layer could be doped to improve semiconducting properties, and also to decrease the band gap.

P-emitter
The electronic properties are most important for the p-emitter, see Appendix B. High hole mobility, very low resistivity and low hole effective mass are important properties. Cu_2O was identified to have these properties, but the resistivity is above the desired value, see Appendix C. The resistivity issue can be a problem regarding the performance of the p-emitter. Careful doping of the host material could minimize this issue.

To obtain lowest possible resistivity, the Cu_2O active substrate should be single crystal. The high quality of a single crystal will also ensure good transport properties through a suitable production method where the conditions are controlled.

IB-layer
The optical properties are most important for the IB host material, see Appendix B. These are mainly the band gap and absorption coefficient. Cu_2O has suitable properties for being the IB host material, see Appendix C. The host material of the IB-layer needs to form the intermediate band at an appropriate place in the band gap through heavy doping.

Electrodes
The front electrode should either be transparent or fingered/grid-structured, and the back electrode could be solid, as no light needs to pass through it. To find suitable electrode materials, the work function for possible electrode materials should be compared to the work function of the p- and n-emitter, see section 2.3.3. The electrodes should form ohmic contacts with the p-emitter and n-emitter.

Anti-reflective coating
An anti-reflective coating (ARC) can be deposited on or under the front contact. This coating should exist of non-toxic and abundant materials, and have properties that ensure as much sunlight to pass through the cell surface as possible. Here, the refractive indices of the surrounding and underlying material of the ARC, as well as the wavelength of desired incoming light, will play a role in determining optimal ARC material and thickness.

Buffer layer
To obtain a high performance heterojunction, a buffer layer and/or other aids to minimize losses at the ZnO/IB-Cu_2O interface should be evaluated.

7.3.1.3 Cell material requirements summarized

The operational requirements for the IBSC were summarized in Table 7.4, and they apply to the different materials as well as the assembled cell. The functional and physical performance requirements however, are summarized at the IBSC assembly level divided into contacts, semiconductors and the two remaining layers; ARC and buffer layer, see Table 7.5 below.

Table 7.5: Performance requirements for the materials of the IBSC in level 4 of the system.

Performance requirements	Contacts (4)	Semiconductors (4)	ARC and buffer layer (4)
Functional	- Ohmic contacts - Able to transport the generated current from the cell to the electrical circuit - The front electrode should not shield the incoming light - The back electrode should stop the light from leaving the cell - Carry current from the cell to the DC cabling.	- Absorb photons that excite electrons with as little recombination as possible - Formation of an intermediate band - High mobility of charge carriers - Generally good transport properties - Good optical properties	- ARC: Antireflection of sunlight at the cell surface - Buffer: Surface passivation and reduce defects, interdiffusion and recombination at the p-ZnO/IB-Cu_2O interface - Minimize losses due to interface defects, band bending at the junction and reflection of light
Physical	- High quality materials - Abundant, non-toxic materials - Metals or other conductive materials	- High quality materials - Abundant, non-toxic materials: Cu_2O and ZnO and non-toxic precursors - Single crystal of Cu_2O	- High quality materials - Abundant, non-toxic materials - Transparent ARC with suitable refractive index

The performance of the IBSCs is most dependent on the semiconductor materials of the n- and p-emitter and IB-layer. Table 7.6 summarizes the required material properties of these important components of the cell. See Appendix C for reference values for the material properties, and some actual values for Cu_2O and ZnO. However, these are experimental values, and care should be taken when comparing theoretical reference values with experimental values that depend on the experimental conditions.

Table 7.6: Material requirements for the three most important components of the IBSC at system level 5.

	n-emitter	IB material	p-emitter
Material properties requirements	Most important properties: - Low resistivity (< 1 Ω) - High mobility (> 150-200 cm^2/Vs) - High effective electron density/low effective electron mass → Good charge carrier transport - Very high purity - Quality: polycrystal with large grains	Most important properties: - High absorption coefficient (>10^4 cm^{-1}) - Right band gap; 1.7-3.2 eV (1 sun) → Good photon absorption - High dopant concentration - Intermediate band formation	Most important properties: - Low resistivity (< 1 Ω) - High mobility (> 150-200 cm^2/Vs) - High effective hole density/low effective hole mass → Good charge carrier transport - Very high purity - Quality: Single crystal

7.4 Discussion of the requirements

The most influencing system choices made in this Chapter are discussed in the three following sections. They are evaluated to show how altering some of these system choices could influence the rest of the SEP and the final results.

7.4.1 Mounting structure

The choice of mounting structure was based on the location with respect to the existing building structures in Oslo, the weather conditions and the high latitudes resulting in optimal steep tilt angle.

Building integrated photovoltaics

Based on another project within the SoRoSol-group [165], the future photovoltaic trends seem to turn to building integrated photovoltaics (BIPV). Even though BIPV on flat roofs might be unfavorable with the low sunlight at high latitudes like in Norway, both tilted roofs and façade structures could also have been considered in this thesis. Especially when the location is set to Oslo, Norway, façade integration could be a good mounting method alternative. The "flat" sunlight in Oslo latitudes will irradiate on a vertical solar array large parts of the day, both summer and winter.

Stand-alone systems

Norway in general is a suitable country to use PV systems. Cabin owners in Norway have used stand-alone PV systems for a long time. Usually cabins are located far up in the mountains, and will thus have slightly increased irradiance because of the high altitude.

7.4.2 Electrical components

The choices made related to the electronic component throughout this systems engineering process (SEP) were based on private communication [162] and mainly the book "Planning and installing photovoltaic systems; a guide for installers, architects and engineers" as the literary source [44]. The requirements for these components were kept quite general not to limit the design choices too early in the process. However, the location was decided in the beginning of this process, leading to the main limitation for the electrical components that are highly dependent on the local climate, as well as the possibility to use available research as an example PV system. Since the electrical components were not part of the main focus in this thesis, they were not evaluated in a detailed manner.

7.4.3 PV module

The dimensions of the module were chosen because 1 x 1.6 m is the predominantly used module size today. To be able to compete with other PV techniques, the manufacturing and installation of the IBSC system should be as simple and conventional as possible. To be able to use the methods of other PV techniques for encapsulation, framing and mounting of the modules may be necessary for the new IBSC technology to make an introduction to the PV market.

However, in the future, it might be possible to produce smaller IBSC modules as a result of the increased efficiency. Smaller modules and arrays might be preferred, with the same output

as standard sized Si-modules. The smaller IBSC arrays could fit better on roofs and other installation sites because of the more flexible array design with smaller modules.

7.4.4 The cell structure

The chosen cell structure was based on the literary study of the material challenges of Cu_2O and ZnO. It turned out that Cu_2O had the poorest material properties that might be the source of the poor cell performance of Cu_2O/ZnO heterostructures, see section 4.3. The cell structure alternative with Cu_2O as the bottom layer seemed favorable with respect to optimizing the Cu_2O properties through single crystal production. The resulting wafer could be used as an active substrate. In addition, this choice opened the possibility of ion implementation of nitrogen into the top layer of the wafer to form the IB-layer.

However, the lattice mismatch has been reported as a more prominent challenge with ZnO grown on top of Cu_2O than the opposite structure, see section 4.4.1. The cubic structure of Cu_2O seems easier to control epitaxially when grown on a layer of ZnO. Nevertheless, as mentioned in Chapter 4, the condition based experimental results found for Cu_2O/ZnO heterostructures should not limit further research, as these materials are currently hot topics for further improvements.

The cell dimensions of 156 x 156 mm are the standard size of silicon solar cells, and were chosen with the same reasoning as for the module dimension above. The chosen production method must be suited for this cell size. Production methods suited for smaller sized cells, possibly with higher quality, might be of interest if the cell dimensions are decreased in the future due to higher efficiencies.

8 Step 3: System performance

In the third step of systems engineering, the requirements defined in Chapter 7 are translated into performance criteria for the total system and subsystems. In section 8.1 the performance parameters of the PV system are specified. A system activity flow chart is given in section 8.2 to get an overview of possible processes and flows for an IBSC system from a life cycle perspective. Through the functional analysis in section 8.3 the performance of materials and production of the intermediate band solar cell is specified. In section 8.4 some performance choices are discussed.

8.1 Performance specifications for the PV system

First, the location based performance is outlined in section 8.1.1, and next the desired operational performance of the PV system is selected in section 8.1.2. The whole system showed in Figure 6.2 is in focus.

8.1.1 Location based performance

To predict the performance of a PV system, the exact location of the installation site is important to know. The amount of solar radiation, average angle of incoming sunlight and weather conditions with emphasis on the temperature, are all important parameters of the specified location. From an environmental perspective, the energy-mix of the location is also important to take into account.

Amount of solar radiation

As described in section 2.6.3, the latitude of the location for the PV system affects the performance. The location is set to Oslo, Norway, as the stakeholder requested. Oslo has an average annual irradiance of 967 kWh/m^2 at latitude 59º56' North [5]. To maximize the power output of the PV system, as much of this sunlight as possible should be absorbed by the solar panels throughout the year. To achieve this, the tilt and orientation of the modules must be optimized with respect to the angle of the sun, which varies greatly through the year. For additive flat roof installations, the tilt angle should also be optimized with respect to neighboring module racks to avoid shadowing. Inclined roofs have a fixed angle and orientation that may not be suited for PV installation at the specific location. Optimal tilt of PV panels is approximately 10-15º less than the local latitude [58]. This implies that the optimal tilt angle for installations in Oslo is around 45-50º.

Temperature and voltage relationship

The temperature of the location will influence the performance of the PV system. Generally, colder temperatures give higher efficiency because of the increased voltage [25]. The temperatures of the modules influence the I-V characteristics of the cells. Nominal operating cell temperature (NOCT) is usually in the range of 42 – 46 ºC [33, 166]. The highest and lowest ambient temperatures in Norway are 33 ºC and -20 ºC [167]. For Oslo, the site-dependent module temperatures based on some assumptions [167] are listed in Table 8.1.

Table 8.1: Module temperatures during Norwegian summer and winter.

NOCT [ºC]	T_m, summer [ºC]	T_m, winter [ºC]
42.0	60.5	7.50
45.0	64.3	11.3
49.9	70.4	17.4

Depending on the NOCT, the module temperatures can vary greatly in Norwegian weather as seen from the table above. The voltage increases with low temperatures during winter, and the varying seasonal temperatures in Norway must be taken into account when choosing the electrical components. The voltage deviation of a ventilated 50 W module at standard conditions (STC) can be + 10 V in winter [25]. When several modules are connected in series, the increase in voltage at low temperatures can amount to more than 100 V, and may even exceed the voltage limit of downstream devices, as mentioned in section 2.6.3. Large PV systems in Norway should therefore be designed to make sure that the system voltage does not exceed the voltage limit of downstream devices.

However, increased voltage results in increased power output, see I-V characteristics in section 2.6.1, and a PV installation in colder weather can therefore be beneficial for the power output.

Environmental performance

The local energy mix of the production of the PV system is probably the factor with the highest potential to influence the environmental performance of the PV system. As already discussed in section 3.3, the production phase of PV systems is the most material and energy intensive phase of the system lifetime.

The electricity mix of 26 countries in four different continents, and concluded that Norway has the cleanest energy mix of all, consisting almost only of hydropower [5]. However, Norway also has the lowest potential for CO_2 mitigation (PCM), based on the already clean energy. This means that the potential to decrease GWP by optimizing the PV system with regard to material and energy use during the production phase will not have a large positive environmental impact if the PV system is fabricated in Norway.

8.1.2 Desired operational performance

Based on the literary review of LCAs of PV systems, and the fact that this thesis should be a stepping stone for a future LCA study, the three most important PV system performance parameters are chosen; the conversion efficiency, lifetime and performance ratio.

Conversion efficiency

The conversion efficiency of the IBSC system is impossible to predict since the intermediate band heterojunction Cu_2O/IB-Cu_2O/ZnO does not exist. However, based on theoretical values for IBSC efficiency, actual efficiency of Cu_2O/ZnO heterojunctions and efficiencies of existing high performance cells of other PV technology, an intelligent guess can be made.

The black body radiation theoretical efficiency of an IBSC is 63.1 % [11] with optimal band gap and placing of the intermediate band, see section 2.2.1. The optimal band gap of a single

junction IBSC at one sun, meaning non-concentrated sunlight, is 2.4 eV, which gives a theoretical maximum efficiency of 49.3 % [164, 168]. The heterostructure IBSC investigated in this thesis has a limiting band gap of 2.2 eV, which is the most cited band gap of Cu_2O, see Appendix C. From the IBSC simulations by Linge [164], this band gap gives a theoretical max of approximately 48 % at one sun.

The relation between theoretical maximum at one sun and the highest achieved efficiency of a sc-Si cell can be used to get an idea of expectations for best efficiencies of IBSCs with IB material of band gap 2.2 eV. As mentioned in section 2.6.1, the theoretical limit for cells with band gap of 1.1 eV at 1 sun is 30 % [49]. The best experimental sc-Si cell today has an efficiency of 24.7 % [169, 170], and the highest value for a sc-Si module is reported as 22.4 % [170, 171]. The ratio of the highest efficiency values and theoretical max at one sun is found to be 0.823 for the cell and 0.747 for the module.

If the same ratio between theoretical maximum efficiency and actual conversion efficiency is possible to obtain for IBSC with 2.2 eV IB band gap, the cell and module efficiencies could be as high as 39.5 % and 35.8 %, respectively. This means that in the optimized case with an almost perfect Cu_2O/IB- Cu_2O/ZnO cell, the cell and module efficiencies could be 62.5 % and 62.6 % higher than the best Si-cell and Si-module described above. The rule of thumb for the IB-layer is around 50 % increased efficiency [172], so these are very high and maybe unrealistic values.

Theoretic max efficiency for Cu_2O is 20 % and for ZnO 18 %. The best experimental cell efficiency for this heterojunction is 4.12 % [116]. The obtained efficiency is 20.6 % of the theoretical max limited by the maximum absorbing Cu_2O layer efficiency of 20 %.

If the experimental progress of the heterostructure Cu_2O/ZnO cell continue to in the same rate; from 0.12 to 4.12 % in 9 years (see section 4.3), it can be safe to say that the efficiency will increase further through continued research. A reasonable assumption might be that optimization of material properties and cell manufacturing process in the future can lead to an efficiency of 60 % of the theoretical limit; a 12 % conversion efficiency. If the efficiency of the Cu_2O/ZnO-based IBSC reaches the well-established rule of thumb "50 % higher efficiency than single junction cells", an estimate for the IBSC conversion efficiency could be about 18 %.

The one-sun theoretical and experimental maximum efficiencies for Si-cells and Cu_2O/ZnO heterostructure cells, as well as the theoretical limit of 2.2 eV band gap IBSCs are listed in Table 8.2 together with the efficiency values for the IBSC estimated above.

Table 8.2: One-sun efficiencies for high efficiency Si cell and module, Cu_2O/ZnO cell and wanted IBSC.

		Theoretical limit [%]	Cell efficiency [%]	Module efficiency [%]	Reference
Best	**sc-Si**	30	24.7	22.4	[49, 169, 171]
	Cu_2O/ZnO	20	4.12	n.a.	[103, 116]
Optimistic	**Cu_2O/IB- Cu_2O/ZnO**	48	39.5	35.8	Theor. limit [164]
Realistic	**Cu_2O/IB- Cu_2O/ZnO**	48	18	n.a.	Theor. limit [164]

The optimistic case based on the highest efficiency Si-cell and module, and the more realistic case based on Cu_2O/ZnO-cells are both considered further in this thesis.

Lifetime

The lifetime of a PV system is important for the users, but especially for those performing economic and environmental calculations. For instance, when the EPBT is calculated, the exact number of years set as the lifetime of the system will affect the answer significantly.

As seen from Table 3.1 in section 3.2, the lifetime of PV systems used in LCA studies of PV systems the last five years usually promise a 30 years lifetime. Because one of the goals with this PV system design is to prepare for a LCA, a lifetime of 30 years will be used for this system as well.

Performance ratio

The performance ratio is a factor to measure the losses in a PV system, as explained in section 2.6.2. In the master's thesis by Siv Helene Nordahl [167], a base case of 100 modules on a rooftop in Oslo was used to illustrate the performance ratio varying throughout the year. This base case gave the performance ratio results illustrated in Figure 8.1 [167]. From this figure and the results from the LCA review in section 3.2, it seems safe to propose a performance ratio of 0.77 for the Oslo-located IBSC system studied in this thesis.

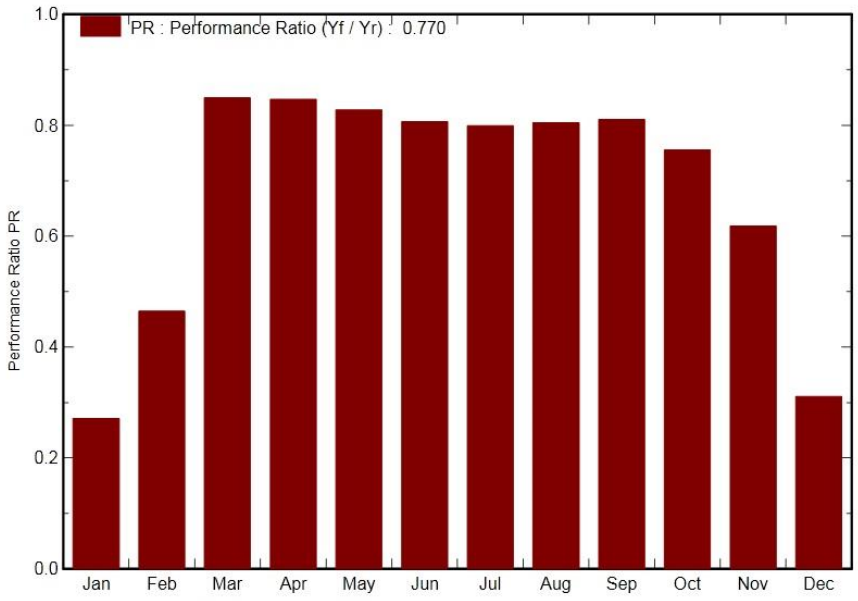

Figure 8.1: The performance ratio of each moth and the average value for the base case of 100 modules located in Oslo [167].

8.2 System activity flow chart

To create an overview of the system from a life cycle perspective, a process flow-chart can be made. The processes linked together by material flows and transportation of materials forms a qualitative graphical representation of the system. The flow chart given in Figure 8.2 [78] includes the processes for a conventional Si-based PV system, but the processes involving the fabrication of the Si-cells can be swapped with processes for other PV technologies with otherwise same or similar system components of the same materials.

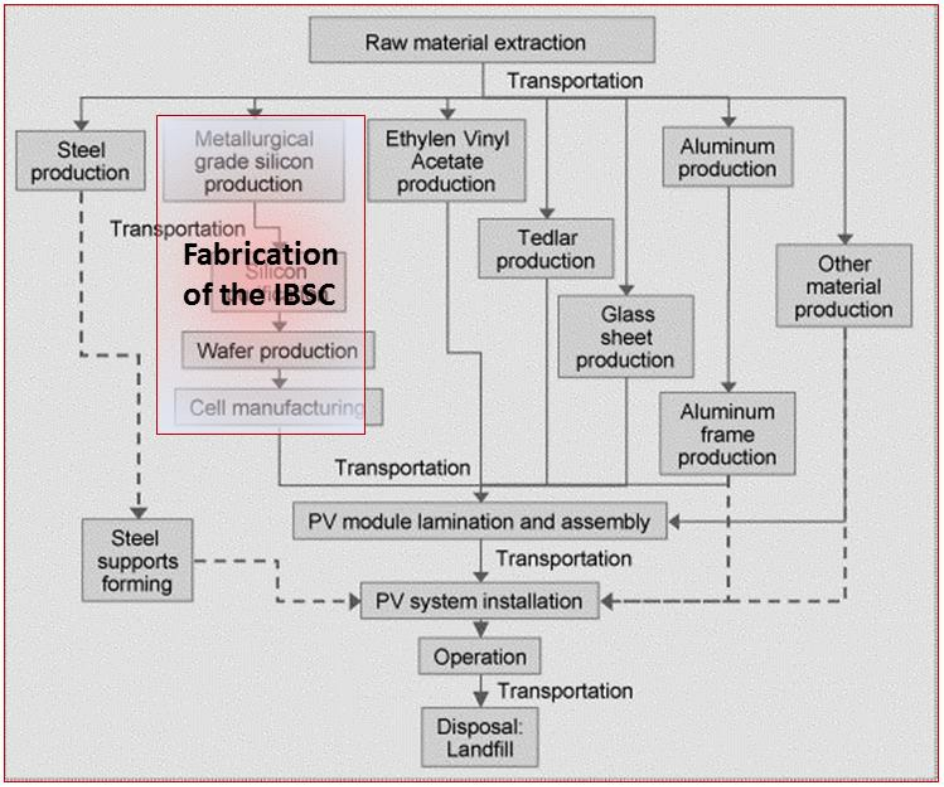

Figure 8.2: The most important processes of the life cycle of a conventional Si solar cell system [78], where the inner red frame indicates the IBSC fabrication processes instead of the processes for Si-cell production.

The flow chart describes the material flows throughout the PV system's life cycle from raw material extraction to landfill disposal. A recycling loop could be included here, from the "Disposal: Landfill" process to "Raw material extraction". If the recycling process was more material and energy efficient than extraction of raw materials, this would decrease the environmental impact.

The solar cell system in this thesis could also be described from a life cycle perspective like the one in Figure 8.2. The IBSCs would in this case be encapsulated in Ethylene Vinyl Acetate (EVA), protected with glass in front and Tedlar as a back sheet frames and framed in aluminum module frames, see section 2.4. The system could also be installed with a steel mounting structure as the original Si-system flow chart suggests. Only the processes from "Metallurgical grade silicon production" to "Cell manufacturing" need to be changed (see the inner red frame in the figure). Instead, the processes "Single crystal Cu_2O wafer production", "IB formation" and "Cell manufacturing", where the remaining layers are deposited and electrodes attached, could be appropriate processes for the fabrication of IBSCs.

8.3 Functional analysis of the IBSC device

The rest of this chapter will deal with the intermediate band solar cell, as indicated in Figure 8.3 below.

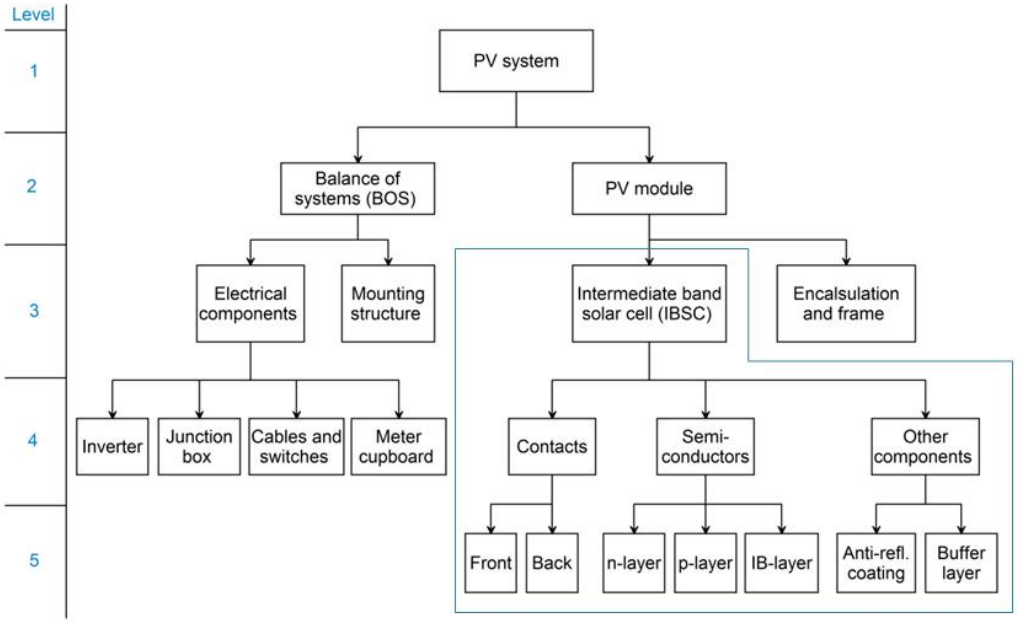

Figure 8.3: The focus from this point on is the intermediate band solar cell.

8.3.1 Functional and physical architecture of the IBSC

The functions an IBSC must carry out to obtain high performance are related to different parts of the cell. The functional relationships between physical parts of the cell are shown in Figure 8.4. The layers of the IBSC are placed in correct order from top to bottom of the cell in the physical architecture IBSC diagram.

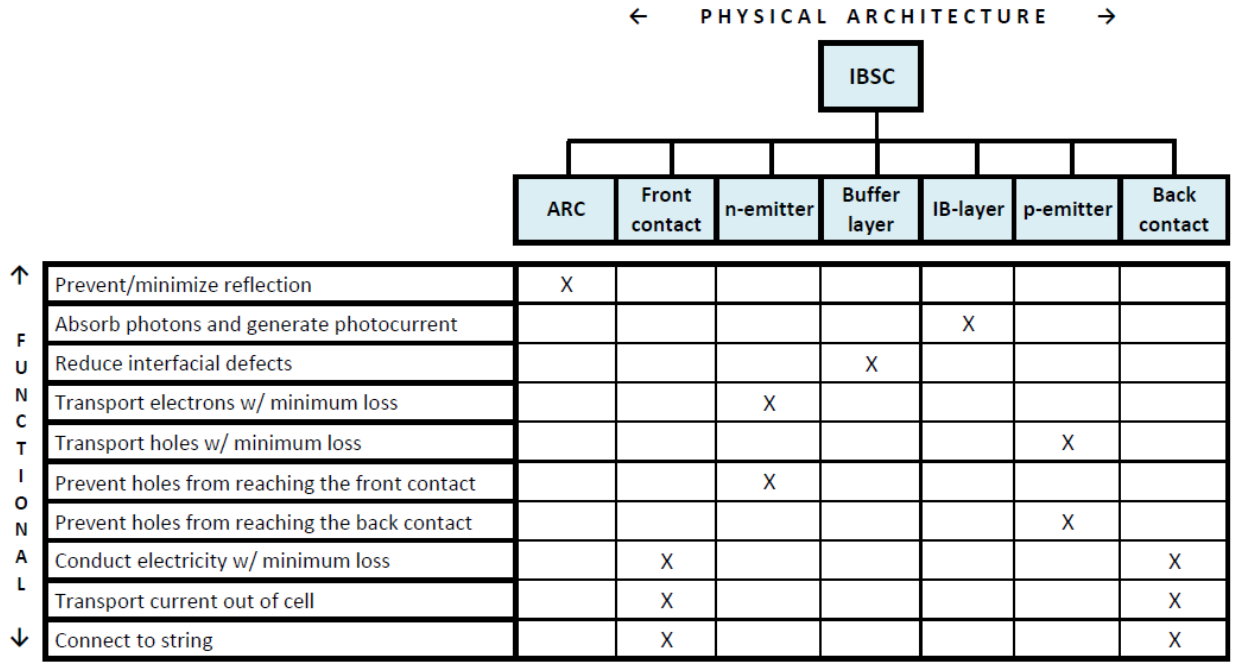

Figure 8.4: The functional/physical matrix for the IBSC system elements.

All the functional and physical relationships of the IBSC described in the figure above should be kept in mind when proposing materials and a suitable production method.

8.3.2 Production of the IBSC

Production of the desired IBSC starts with the single crystal production of Cu_2O followed by the IB-formation and deposition of the buffer layer, ZnO layer and remaining components. Figure 8.5 shows a simplified production route with the three main production processes. The production route should lead to the material properties required, see section 7.3.1.

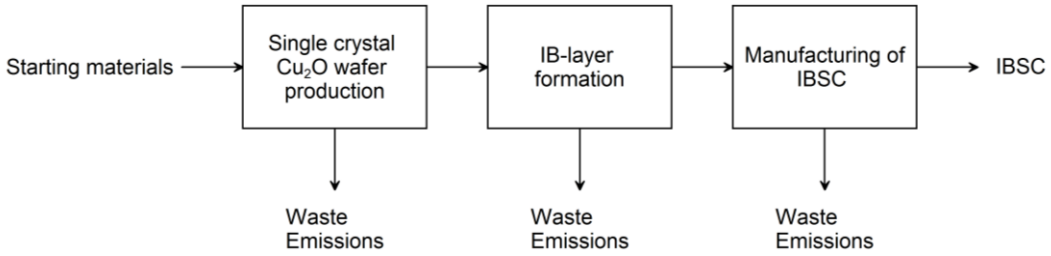

Figure 8.5: A simplified process diagram of the activities and flows involved in fabrication of the IBSC. Included in this simple diagram could also be material and energy flows in to every process.

In addition to being abundant and non-toxic, the starting materials and added materials during the production route should be of simple configuration. Complex precursors can lead to challenges during production in terms of quality and purity. The desired performance of the processes and activities included in the fabrication of IBSCs is specified in Table 8.3, divided into the three processes indicated in Figure 8.2.

Table 8.3: Performance specification of production route of the intermediate band solar cell.

Performance requirements	Single crystal production of Cu_2O	IB-layer formation	Cell manufacturing
Functional criteria	- Easy to control stoichiometry and amount during production - Single crystal production with focus on the desired material properties	- Formation of deep levels at appropriate energy level in the band gap	- Reducing interface problems like lattice mismatch and recombination by surface treatment - The buffer layer, n-emitter, ARC should be deposited at high precision to achieve desired material properties - Form ohmic contacts to n- and p-emitter
Physical criteria	- Possible to produce 156 x 156 mm wafers of larger ingots - High quality single crystal - High purity of materials	- High doping content - The top layer of the Cu_2O wafer - Under the buffer layer in the cell structure	- Deposit layers on the 156 x 156 mm wafers - High quality vapor deposition - Possible to upscale from laboratory to industry - Contacts formed by existing, sustainable technology

8.4 Discussion of the performance

During the performance specification in this chapter, many of the decisions made were accounted for right away, but two of them could be discussed even further; the desired efficiency and the environmental performance of the chosen location.

8.4.1 Efficiency

The estimated values are so uncertain that it is almost impossible to say anything about their trustworthiness. The optimistic case with above 60 % better efficiencies than the best Si-cells and modules, are not very realistic with respect to the material challenges explored for the Cu_2O/ZnO heterojunction cells in Chapter 3.

However, the more realistic case where the efficiency Cu_2O/ZnO heterojunction cells would reach 60 % of the theoretical limit, meaning 12 % efficiency, would with the IBSC rule of thumb (50 % higher efficiency) lead to 18 % conversion efficiency for the low-cost, environmentally friendly Cu_2O/ZnO-based IBSCs.

As mentioned in section 8.1.2, previous research of Cu_2O/ZnO heterojunction cells led to an increase in efficiency from 0.12 to 4.12 % in nine years. Although 4.12 % is still low conversion efficiency considering the theoretical limit of 20 % for Cu_2O, the efficiency will probably increase further as the material challenges regarding these cells are still a hot research topic. Both ZnO and Cu_2O are very immature materials in the science world, and much focus will probably be given these abundant, non-toxic and cheap materials in the future. These future experiences and solutions may be implemented in the Cu_2O/ZnO-based IBSC research.

Regarding the competing high-efficiency PV technologies, other 3rd generation cells, such as three-junction non-concentrator cells have reached 37-38 % conversion efficiency [170]. The optimistic case for the IBSC have efficiencies in the same range as the best multi-junction cells today.

8.4.2 Location based performance

The location is set to Oslo, Norway for this PV system. There are many advantages with PV system operation in Norway; low temperature and clean air both contribute to increased efficiency as mentioned earlier in this chapter. Also, the annual solar radiation is not significantly lower than the average value for middle Europe; 1000 W/m^2 [57], see Appendix D.

Environmental performance

Regarding the environmental performance, production of solar cell systems in Norway probably has the lowest impact in the world regarding energy use. With the green energy of this country, the average emissions in Norway from electricity production were as low as 0.000 $kgCO_2/kWh$ from a study by Stoppato [5]. As mentioned in section 8.1.1, this also implies that installing PV systems would not affect the already clean electric mix of Norway.

On the other hand, increasing the green energy production in Norway will lead to increased exportation of clean energy to other countries. With underwater cables to England and Germany [173], the transportation emissions will also be reduced. From a global perspective,

both PV production and installation in Norway can thus be environmentally beneficial when the generated electricity is accessible.

In addition, the currently increasing number of electrical cars in Norway and surrounding countries will need large amount of electricity. Norway is one of the leading countries with respect to number of electric vehicles per capita, and electricity generation from PV systems might be needed to complement the clean hydro-generated electricity to maintain the Norwegian green energy profile.

9 Step 4: Analyze and optimize

The fourth step in the systems engineering process is the "Analyze and optimize" step. Here, different system alternatives are evaluated based on conflicting needs. In this thesis, this step is focused only on the IBSC unit to give a more detailed design of the cells, see Figure 9.1 below. Based on the specified system and cell performance found in Chapter 7.4, suitable materials for the IBSC are evaluated in section 9.1, and two material scenarios with conflicting needs are discussed in section 9.2 to attempt to find an optimized IBSC. In section 9.3, the two identified cells based on different needs are discussed.

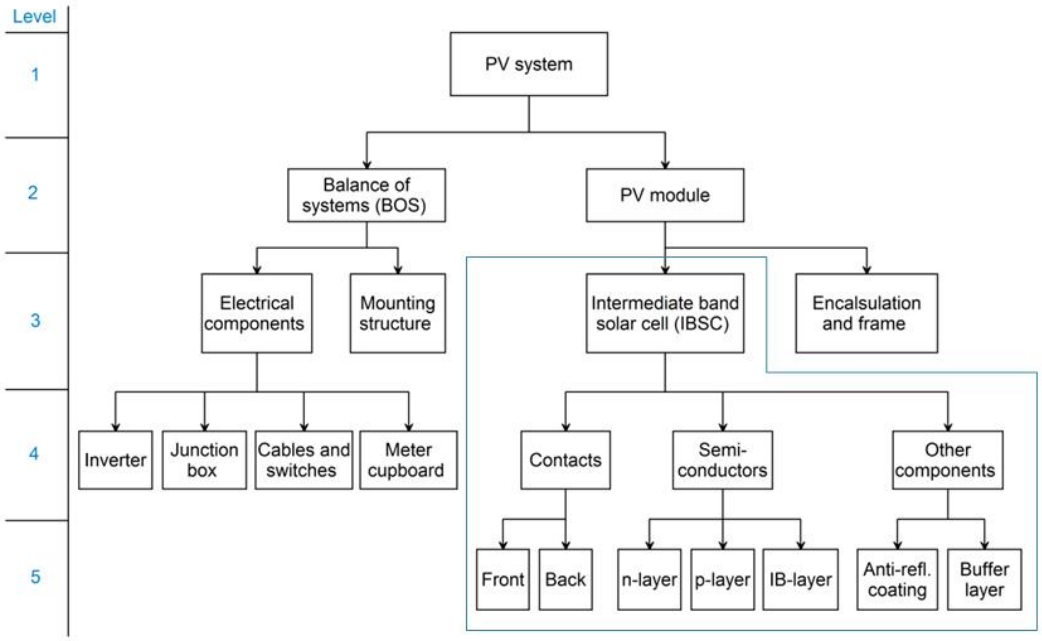

Figure 9.1: Only the IBSC subsystem is investigated in this chapter, based on the cell performance specified in the previous chapter.

9.1 Material analysis

Based on the material requirements in section 7.3.1 and the system performance specified in Chapter 7.4, the materials of the IBSC are further investigated. Possible materials for electrodes, anti-reflective coating and buffer layer are evaluated in more detail.

Nanostructures for improved interfacial properties that were discussed in section 4.5.1 are not considered because of the requirement conflicts with large scale and sustainable production industry method. The nano-scale techniques for improving Cu_2O/ZnO found in literature are not ready for commercialized cells, and may be consider in the future if the techniques are further explored for up-scaling from laboratory conditions.

9.1.1 Emitters and IB material

The emitters and IB material are briefly discussed in terms of material properties for solar cells and possible dopants to enhance these properties. The choices are based on the literary review in Chapter 4.

N-emitter
As already stated, ZnO was one of the identified semiconductors with suitable band gap, high mobility, high absorption coefficient and extremely low resistivity, see Appendix C. ZnO can be doped with Al or Ga to increase n-type properties [108], and according to the review article on Cu_2O by Meyer *et al.* [149]; is ZnO a suitable window layer for a Cu_2O absorbance layer. ZnO is (1) transparent to visible and IR spectral range, has (2) a large band gap, (3) excellent electronic transport properties, and (4) can easily form a metal-contact.

The n-emitter is chosen to be Al-doped ZnO (AZO) based on the promising findings for heterojunction AZO/un-doped ZnO (ZO)/Cu_2O cells ny Minami *et al.* and Nishi *et al.* [115, 116].

P-emitter
Cu_2O has a perfect band gap for intermediate band solar cell applications [17, 164]. Cuprous oxide also has high mobility [124], low effective hole mass [174] and a reasonable minority carrier diffusion length for solar cell applications [109].

The p-emitter will initially be intrinsic Cu_2O, but through a controlled production, the single crystals can be prepared with large amount of Cu^+-vacancies that lead to conduction [175]. The cation deficiency can be controlled by the oxygen flow during growth, and the resistivity decreased by two orders of magnitude during such an experiment [149]. At the same time, the carrier concentration increased from 10^{15} cm^{-3} to 10^{19} cm^{-3}, which resulted in the desired carrier concentration for IBSC host materials [126], see Appendix B. However, because of the widely reported problems with high resistivity of Cu_2O, possible dopants for the p-emitter should be investigated. The most promising dopant to increase the p-type behavior of Cu_2O is nitrogen [149]. The potential dopants must not interfere with the formation and properties of the IB-layer.

IB-layer
With optimized nitrogen doping, Cu_2O is a highly promising intermediate band material [156], and the IB material is therefore chosen to be Cu_2O with ultra-high doping of nitrogen.

9.1.2 Electrodes
The front electrode will be connected to the ZnO n-emitter, and the back electrode will be formed with the cuprous oxide p-emitter. To find suitable electrode materials, the work function of possible electrodes should be compared to the work function of Cu_2O and ZnO.

The front electrode should form an ohmic contact with the n-emitter, and the back electrode should form an ohmic contact on the p-emitter (see section 2.3.3). The work function of the back contact should thus be higher than that of cuprous oxide; 4.84 eV [176], and the front contact should have lower value than the work function of zinc oxide; 4.7 eV [177]. From Figure 9.2 [178] it can be seen that many elements have work functions in ranges potentially suitable for both the front and back electrode. Some elements with suitable work functions for ohmic contact formation with Cu_2O and ZnO are:

- Cu_2O ($\Phi_m > \Phi_p$): Be, C, Co, Ni, Se, Rh, Te, Re, Ir, Pt and Au
- ZnO ($\Phi_m < \Phi_n$): B, Al, Ti, V, Cr, Fe, Cu, Zn, Nb, Mo, Ru, Ag, Sn, Sb, Ta, W, Hg, Pb and Bi

Considering availability and toxicity of elements, see Appendix E, many of the above materials are not suitable. Boron is a poor room-temperature conductor with resistance higher than 300 MΩ [179], and is therefore disregarded as electrode material.

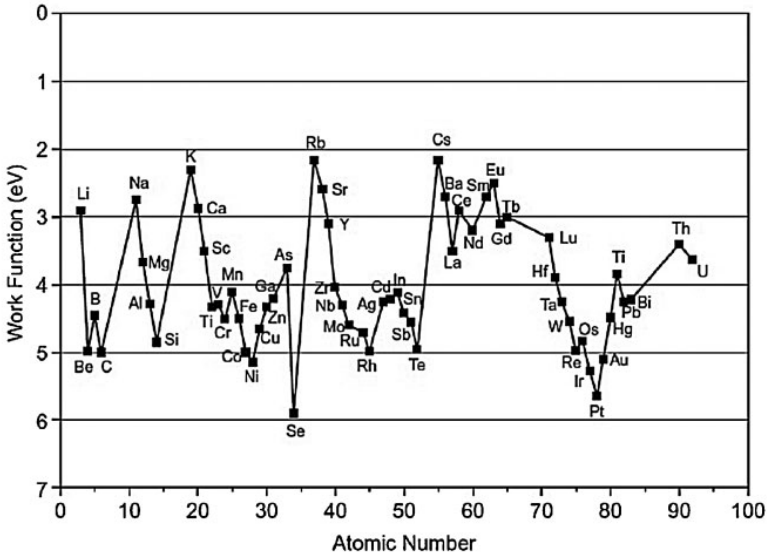

Figure 9.2: The work functions of different metals [178].

Michaelson [180] listed several experimental values for the work functions of the elements mentioned above were found. Cu_2S and ITO + Cu are also good candidates because they have shown great performance in Cu_2O/ZnO heterostructures [108, 115]. The final list of suitable contact materials based on work function, availability and non-toxicity is given in Table 9.1.

Table 9.1: The work functions of possible contact materials for the p- and n-emitter.

Contact for Cu_2O (ϕ = 4.84 eV)		
Element	**Φ [eV]**	**References**
Au	5.1	See Michaelson [180] for references
C*	5.0	
Cu_2S	n.a.	Used by Minami *et al.* [115]
Re	4.96	[181]

*Graphite

Contact for ZnO (ϕ = 4.7 eV)		
Material	**Φ [eV]**	**References**
Ag	4.26	See Michaelson [180] for references
Al	4.28	
Cu	4.65	
Fe	4.5	
ITO*	4.4–4.5	[182]
Mo	4.6	See Michaelson [180] for references
Sn	4.42	
Ti	4.33	
V	4.3	
Zn	4.33	

* Indium tin oxide

Back electrode
Forming low-resistivity contacts on cuprous oxide is an essential step toward demonstrating its suitability as a candidate solar cell material [183]. Au is much used as the electrode for Cu_2O in Cu_2O/ZnO cells, as mentioned in section 4.5.3. However, the economic aspect that should be considered for a sustainable design, this may not be the best choice. Another electrode for Cu_2O that has proved efficient is Cu_2S, that was used in the highest efficiency Cu_2O/ZnO cells [115].

Also worth considering is graphite paste (C-paste) electrodes. The high availability and low cost of graphite, makes it a suitable electrode material for cuprous oxide [106, 184]. The graphite paste will block the light, but since this is the back electrode that will not be an issue. On the contrary, this could be an advantage, since a solid back electrode may decrease the amount of light escaping the rear of the cell.

The performance of graphite pastes with various dopants as back contact for CdS/CdTe solar cells was investigated by Hanafusa *et al.* [185]. The dopants that resulted in highest conversion efficiencies were Ag_2Te, NiTe and Zn_3P_2. After toxicity was considered, see Appendix E, graphite paste with 2.5 wt% Zn_3P_2 seems to be a good candidate for the back electrode connected to the Cu_2O p-emitter.

No literature was found on Re as electrode material, and the alternatives for the back electrode are thus chosen to be Au, C-paste and Cu_2S.

Front electrode
As the front electrode, indium tin oxide (ITO) is a much studied material for solar cell and other applications. The fact that this material is already experimentally tried out as a Cu_2O/ZnO heterojunction solar cell front electrode [102], makes it promising for IBSC production also. Mittiga *et al.* [102] used a Cu-grid with ITO to increase the conductivity of the front electrode. As seen from Table 9.1, both ITO and Cu have suitable work functions for use as the ZnO-electrode.

However, indium is listed as a critical element by the European Commission, see Appendix E. The functional requirements for the electrode, however, are fulfilled with the ITO and Cu-grid alternative, see Table 7.5.

Aluminum is also used as a front electrode choice in Cu_2O/ZnO heterojunction solar cells [128], and this metal electrode fulfills all electrode requirements.

As seen from Table 9.1, Ti is also a suitable electrode candidate. From the review of ZnO contacts by Brillson and Lu [41], an Ti-Al alloy contact was the most promising ohmic contact for ZnO regarding toxicity (see Appendix E), abundance and contact performance. As a ZnO ohmic contact, Ti-Al has been reported to a produce a number of oxygen vacancies, acting as donors for electrons, below the contact [186]. This leads to the increase of electron concentration via the reduction of contact resistivity.

Other than the ones mentioned here, none of the suggested front electrode materials in Table 9.1 were found in literature as ZnO ohmic contacts. The alternatives evaluated further are therefore the combination of ITO and Cu-grid, Al and a Ti-Al alloy with the composition reported by Young Kim *et al.* [186].

9.1.3 Anti-reflective coating

The top layer of the solar cell is ZnO, and alternatively ITO if the combination of ITO and Cu-grid is chosen as the front electrode. As mentioned in section 2.3.3, the refractive index of the anti-reflective coating (ARC) should be between the refractive indices of the surroundings and underlying material. The refractive index of ZnO is 2.00-2.05 at wavelengths 5-600 nm at room temperature [187], and most glass have a refractive index around 1.5 [33]. According to Equation (2.1), the appropriate refractive index for an ARC placed between ZnO and glass is about 1.75-1.76. The optimal thickness of the ARC was also calculated at desired wavelength of incoming light and a refractive index of 1.76 for the ARC. From Equation (2.2), the optimal ARC thickness is around 85 nm.

Previously, MgF_2 have been used as ARC on both ITO and ZnO in solar cells with thickness 80 nm and 100 nm [102, 188]. However, the properties of these cells were probably investigated in air with a refractive index around 1.0. The refractive index of MgF_2 is 1.38 at $\lambda \approx$ 5-600 nm [189], and is therefore suitable for experiments in air, but may not be suitable for solar cells framed with a top glass layer as in most modules.

ARC with refractive index around 1.75-1.76 should be suitable for the IBSC cells covered with glass. The requirements of transparency, non-toxicity and abundance are also important to keep in mind when choosing an ARC. Of possible ARC materials that exhibit these three required properties, especially simple oxides, nitrides and fluorides are of interest for solar cell applications; e.g. TiO_2 [190], SiN [191] and MgF_2 [102]. However, none of these example materials have the optimal refractive index for the IBSC studied here.

To narrow down the search for suitable ARCs for the IBSC, only simple oxides are evaluated because they are much studied and possible to produce by conventional deposition techniques. Shannon *et al.* [192] listed 509 oxides and their refractive indices. Of them, the only simple, abundant and non-toxic oxides with suitable refractive index at λ=589 nm were MgO and Al_2O_3 with n=1.74 and n=1.77, respectively. Since Al_2O_3 has been used as ARC for other applications [193], this material is chosen as the ARC for the IBSC.

9.1.4 Buffer layer

A buffer layer between the Al-doped ZnO (AZO) and IB-Cu_2O may minimize defects and band bending in a similar manner as for ZnO/Cu_2O heterostructure cells as discussed in section 4.5.1. According to Jeong et al. [105], a thin TiO_2 buffer layer can reduce the unwanted tunneling across an interfacial barrier in Cu_2O-ZnO heterojunctions, as mentioned in section 4.4.2. However, lattice mismatch between Cu_2O and TiO_2 has been reported to lead to unwanted band bending and also inevitable interfacial vacancies and defects at the interface between Cu_2O and TiO_2 [194].

The investigation of ZnO-In_2O_3 with varying Zn/(In+Zn) atomic ratio and $Zn_{1-x}Mg_xO$ buffer layers by Miyata *et al.* [120] concluded that the ZnO buffer layers gave the best results for AZO/Cu_2O devices.

An un-doped ZnO buffer layer deposited by PLD on Cu_2O sheets resulted in the two best conversion efficiencies reported for Cu_2O-ZnO based heterostructures; 3.83 % [115] and 4.12 % [116]. The improved band alignment of these cells is shown in Figure 9.3 [115]. ZO seems to be a suitable buffer layer for the AZO/IB- Cu_2O/Cu_2O IBSC.

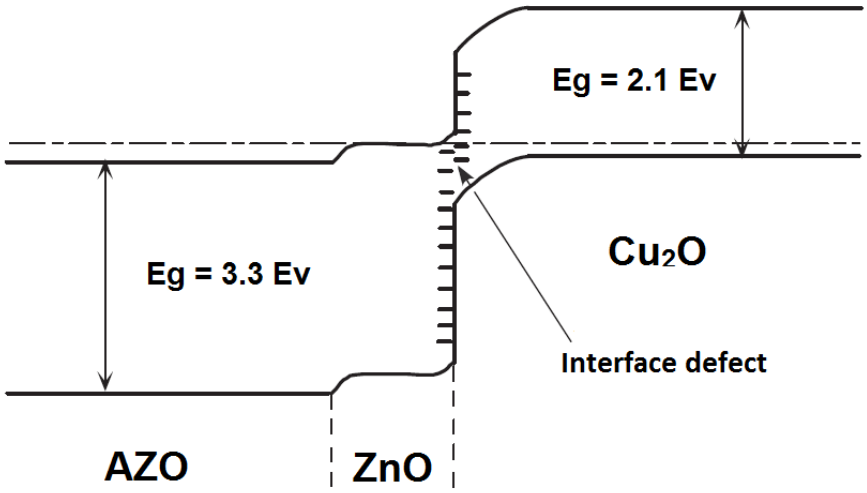

Figure 9.3: Un-doped ZnO serves as a buffer layer in an AZO/Cu_2O heterojunction cell [115].

Another material to evaluate is the ALD deposited amorphous zinc tin oxide (a-ZTO) that successfully reduced interfacial recombination and mitigated non-ideal band alignment in the AZO/Cu_2O cell reported by Lee [128].

9.2 Optimization of the IBSC device materials

In this simplified systems engineering process (SEP), this optimization part of the fourth step will not be conducted in detail. Different scenarios and alternatives will be found, but only speculations can be done for the IBSCs since they do not exist and cannot be tested during this work. However, assumptions and arguments have been given, and some promising alternatives are found.

Further investigation of the IBSCs is needed to test different material and production alternatives, and optimize the cells in practice based on conflicting needs and requirements, see Chapter 6. Nevertheless, some of the design alternatives and material choices found above can be evaluated through theoretic reasoning and assumptions. First, some conflicting needs are outlined and evaluated for two material scenarios in section 9.2.1. In section 9.2.2, two cell cases are evaluated based on different needs.

9.2.1 Conflicting needs for the IBSC materials

The most obvious conflict of needs is identified already in Table 6.3; "a sustainable IBSC system with about 50 % higher efficiency than conventional solar cells". Such a system must have sustainable cells of high quality, but unfortunately sustainability and high quality might not always go hand in hand. To find the needed "environmentally friendly (non-toxic, abundant) and high quality materials", see Table 6.3, a trade-off analysis might be needed.

Two scenarios are evaluated to show how the material sustainability and quality needs can interfere with each other. Based on the material analysis in section 9.1.2 and 9.1.4, two scenarios are addressed. In the electrode material scenario different electrode pairs are assessed, and the buffer layer scenario deals with the optimization of different buffer layer parameters.

9.2.1.1 Electrode material scenario

Choosing electrodes for the IBSC is an important step in the planning that can influence the performance significantly. Electrode pairs found in literature and one proposed pair based on the electrode material analysis given in section 9.1.2 are listed in Table 9.2.

Table 9.2: Possible front and back electrodes for high performance Cu_2O-ZnO based IBSC.

	FRONT AND BACK ELECTRODE PAIRS			
	From literature			**Proposed**
Front	ITO + Cu-grid	AZO	Al	Ti/Al alloy
Back	Au	Au or Cu_2S	Au	Doped C-paste
Reference	[102]	[115, 116]	[128]	[185, 186]

As an example, a high quality IBSC could optimize the electrodes with expensive and non-abundant materials like the much used Au-electrode for Cu_2O and ITO combined with a Cu-grid for ZnO. These electrodes were used in a ZnO/Cu_2O cell with good performance [102]. If looked at from a sustainable perspective, taken into account the environment and economy aspects, the gold contact would be expensive and the indium in ITO is considered a critical element [17]. These electrodes will therefore not only fail to fulfil the requirements of

abundant and sustainable materials, but they would have a negative effect on the overall need for the whole IBSC system.

The second alternative for electrode pair is the electrodes used in the two highest efficiency ZnO/Cu_2O cells [115, 116]. Here, the AZO n-emitter is used as the front electrode. This would result in less material needed, as no other material is needed for the front electrode. The cells reported with this electrode solution may only be suited for laboratory purposes. There might be problems with stringing of the cells, since this is normally done by connecting the metal electrodes of neighboring cells [44]. AZO is disregarded as electrode material because of the uncertainties around up-scaling of this electrode alternative. However, the Cu_2S back electrode used in some of the cells grown by Minami *et al*. [115] could be considered. Such electrodes have shown potential for large scale screen printing contact formation [195], the same electrode formation process frequently used in conventional Si-cells.

Aluminum front electrodes might be a good choice, but this solution will block some of the incoming light. The AZO and ITO/Cu-grid solutions described above would have minimized loss of incoming light because of their transparency. However, together with an Au back electrode, the Al and Au electrode pair led to the best performing thin film ZnO/Cu_2O cell [128].

On the other hand, the possible back electrode with doped graphite paste will be a low cost sustainable solution, but no guarantee can be given for high performance of the electrode-semiconductor contact since no literature were found on this material as contact for Cu_2O. Ti/Al-alloy and graphite paste electrodes will probably be a more sustainable solution than the alternatives with an Au-back contact. No toxic or critical elements are found in the "Ti/Al and C-paste" alternative, and their performance seems satisfactory from the reported use of these electrodes [185, 186].

However, this alternative may not lead to a sustainable production route. The Ti/Al electrode was deposited by electron-beam evaporator in the sequence; Ti (300 Å)/Al (3,000 Å) [186]. This electrode was, as mentioned earlier, one of the best performing electrodes for ZnO from the electrode review by Brillson and Lu [41], so it should not be disregarded because of the complicated production. Further investigation could lead to an easier contact formation process with the same high quality.

The two final alternatives are: Al or Ti/Al-alloy for the front contact, and Cu_2S or C-paste for the back contact. These alternatives are further evaluated for different production needs in section 9.2.2.

9.2.1.2 Buffer layer scenario

A suitable buffer layer in the AZO/IB-Cu_2O junction has the possibility of optimizing the interface transport, and thus leads to the higher performance of the cell. Possible buffer layer parameters to evaluate can be:

- Buffer layer material
- Buffer layer deposition technique and conditions
- Thickness of buffer layer
- Crystallinity of buffer layer

The materials showing the best results as buffer layers in the analysis in section 9.1.4, are un-doped ZnO (ZO) and amorphous zinc tin oxide (a-ZTO). The optimal layer thickness of ZO was found to be 50 nm and for a-ZTO 5 nm. This suggests that less material will be used for a-ZTO than ZO, but obtaining the optimal ratio of Zn and Sn in a-ZTO demands a deposition method with extreme precision. The ZO can be deposited by PLD, but the a-ZTO buffer layer requires atomic layer deposition (ALD).

The subsequent layer to be deposited is the Al-doped ZnO (AZO) n-emitter. This layer has been deposited by PLD in the two highest efficiency ZnO/Cu_2O cells [115, 116]. However, ALD is a vapor-phase deposition technique capable of depositing high quality, uniform and conformal thin films at relatively low temperatures, and is predicted to overcome challenges of next-generation solar cells [196].

Another parameter to consider is the band gap. ZO is the un-doped ZnO with a band gap of around 3.3 eV, see Appendix C, that is the same as AZO (see Figure 9.3), and will give nothing but a little shift in the band alignment. The desired band configuration should minimize band bending for Cu_2O, see Figure 4.2. A-ZTO with Zn:Sn ratio of 1:0.27 has a band gap of 3.12 eV, and will probably decrease the band bending slightly.

A-ZTO has the possibility of reducing interface problems in a ZnO/IB-Cu_2O interface with a high quality deposition technique; ALD, as reported for the highest efficiency thin film ZnO/Cu_2O cell [128]. Since the wafer-like cell with the highest conversion efficiency is fabricated with a similar structure to the IBSC, except the IB-layer of course, the un-doped ZnO buffer layer technique [116] should also be a good choice for the IBSC buffer layer.

The two buffer layer alternatives are further evaluated for different production needs in section 9.2.2.

9.2.2 The simple case and advanced case

The need for "a high quality, sustainable production route that preferably is available at NTNU; both equipment and the competence, and more importantly ready for large scale production" stated in Table 6.3, can be evaluated for optimal solution(s). Here, this is done with the alternatives found in the two material scenarios above as a starting point.

A sustainable production route can in some cases need simple materials that can be produced by conventional methods, and on the other hand, high quality solar cell production might be reached by complex and accurate production methods with carefully tailored materials. Without any validation for this statement, it is used here to illustrate two alternatives for the production of two IBSCs where one uses "simple" and the other "complex" materials. These two cases can indicate how simple materials can lead to a sustainable production route, while more complex materials might need a more advanced production method.

From the two material scenarios above that addressed the electrode and buffer layer cases, one "simple" IBSC case with socially robust materials in focus and one "advanced" IBSC case with the highest possible quality are evaluated. The simple case is evaluated from an environment and economic perspective, while the advanced case has technology in focus.

The simple IBSC case

As mentioned above, this simple cell case has sustainability; environment and economy, in focus. From the electrode scenario, the front electrode is therefore chosen to be Al, as it is a simple metal element with long experience as an electrode material for other solar cells. Conventional screen printing used for Si-cells can be used to form an ohmic contact with aluminum [197]. For the back contact, both C-paste and Cu_2S can be good alternatives since it is difficult to compare these electrodes from a sustainable perspective at this point. They are both non-toxic and cheap materials, but Cu_2S is a binary material while C is elementary and thus of simpler configuration. The graphite paste may need careful doping, however, so its simplicity may not be valid if the doping technique needed is complex after all. Also, the sulfur in Cu_2S may not be desired during production. Thus, both the back contact alternatives should be evaluated further for use in the IBSC device. When it comes to the production technique, the C-paste contact is known to be formed by conventional screen printing [185].

From the buffer scenario, un-doped ZnO can be a suitable buffer layer for the simple IBSC case. A conventional, good quality deposition technique can be used to deposit this layer, and the subsequent AZO and ARC layers. PECVD can be a good choice here, since this method already is used for fabrication of conventional Si-cells.

These material solutions are sustainable and cheap compared to the Ti/Al-alloy for front electrode and a-ZTO buffer layer described in the respective material scenarios above. With Al front electrode and ZO buffer layer, the simple cell evaluated here can probably be fabricated by conventional techniques mentioned above, and thus be competitive on the solar cell market today. These production methods are also simpler than the advanced techniques that may be needed in a more complex cell. Less energy and materials are needed from an environmental perspective, and regarding the economy; money can be saved when complex, low-scale production methods do not have to be industrialized.

The advanced IBSC case

In contrast to the cell case described above, the advanced cell optimization conducted here has technology and especially high quality in focus. The maybe most important need for high efficiency IBSCs, see e.g. Table 6.3, can best be achieved by obtaining the improved material properties described in section 4.5 of the literary review on Cu_2O/ZnO heterostructures. High quality materials are needed in this case, and except for the single crystal Cu_2O wafer that will be used in both cell cases; the advanced described here and the simple case above, the remaining layers and electrodes should also be produced by high quality techniques for this cell. The highest quality deposition techniques described in section 2.3.2 can be evaluated.

The Ti/Al alloy evaluated as the high quality front electrode choice in the material scenario above, has been formed by electron-beam evaporator, as mentioned. Other high technology techniques to form this ohmic contact can be explored, but chances are that the simple, conventional screen printing might not be suitable. The reasoning for the back electrodes alternatives; C-paste and Cu_2S, as evaluated for the above simple case is valid for this advanced case as well.

The best performing buffer layer for thin film Cu_2O/ZnO heterostructures described in the buffer scenario above; a-ZTO, can be a suitable buffer layer in this advanced cell case. This material decreased the band bending of the heterojunction interface, and can thus contribute to the desired high cell efficiency. The a-ZTO buffer layer was deposited by ALD in a complex

sequence to obtain the needed Zn:Sn ratio of 1:0.27. ALD is an extremely accurate and high quality deposition technique, and can result in very high performance layers of AZO and ARC that will be deposited on top of the buffer layer.

This advanced cell case implies that the highest quality production methods can result in higher performance cells, and can be the best alternative from a purely technological focus. However, the layers of the IBSC will in this case be deposited by the more energy-consuming and expensive ALD method that is not ready for industrialization, in contrast to the conventionally used PECVD that was portrayed in the simple cell case.

9.3 Discussion of the simple and advanced IBSCs

The simple cell case can compete on the market today if the material properties can be optimized to achieve high cell efficiency. The production routes are already implemented in the industry, except for the FZ method that needs up-scaling for single crystal Cu_2O.

The advanced cell case with the most complex materials and production route will have development costs for up-scaling of the ALD technique and possibly the electrode formation process. However, it can be realistic to develop more advanced cells even if the cost is higher. An analogy can be drawn to the crystalline first generation cells versus second generation thin film cells. The simple thin film (TF) deposition techniques were developed to decrease the cost of photovoltaics. Still, the crystalline cells with more complex production routes and higher efficiency are still in demand. The high demand has decreased the production cost of crystalline Si-cells, and now they are usually preferred with higher efficiency at about the same cost as TF cells.

10 Step 5: Design and solve

The compositions of the final two cells described in section 9.2.2 are outlined in section 10.1. From the material analysis and production optimization in Chapter 9, a production route with emphasis on possible industrialized methods will be outlined in section 10.2. In section 10.3 an example of a complete IBSC system with the final IBSC devices are stringed together in modules in a rooftop array in Oslo.

10.1 Final cell materials

The components of the intermediate band solar cell are shown in Figure 10.1.

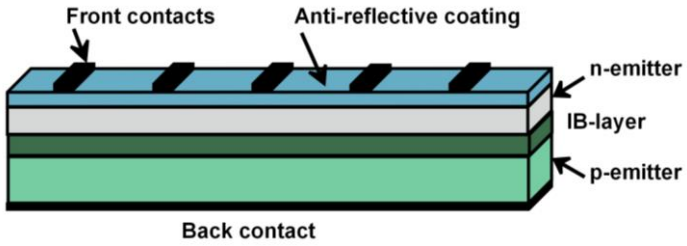

Figure 10.1: The components of the intermediate band solar cell. Not to scale.

The materials chosen for every component of the IBSC in the figure above are listed from top to bottom of the cell structure:

1. Front electrode/contact: Finger electrodes of **Al or Ti-Al alloy**
2. Anti-reflective coating: Al_2O_3
3. N-emitter: Al-doped ZnO
4. Buffer layer: **ZO or a-ZTO**
5. IB-layer: N-implanted Cu_2O
6. P-emitter: Cu_2O single crystal, grown with Cu-vacancies
7. Back electrode/contact: **C-paste or Cu_2S**

10.2 Production route

Single crystal of Cu_2O will function as both the substrate and p-emitter. The ZnO layer will then be deposited on top of the IB-layer (N:Cu_2O), after a buffer layer is added. The antireflection coating is then deposited on the structure of n-emitter, IB-layer and p-emitter. Lastly, the front and back contacts are evaporated on or sputtered on the respective sides.

To choose the final production route, the starting point will be the production criteria stated in section 8.3.2. The two possible production alternatives discussed in section 9.2.2 can be kept in mind, but these production choices were strongly biased by the electrode and buffer layer scenarios. All the high quality deposition methods should be evaluated for this final choice of production route.

Figure 10.2 shows a simple process diagram of the main phases in the production of an IBSC device.

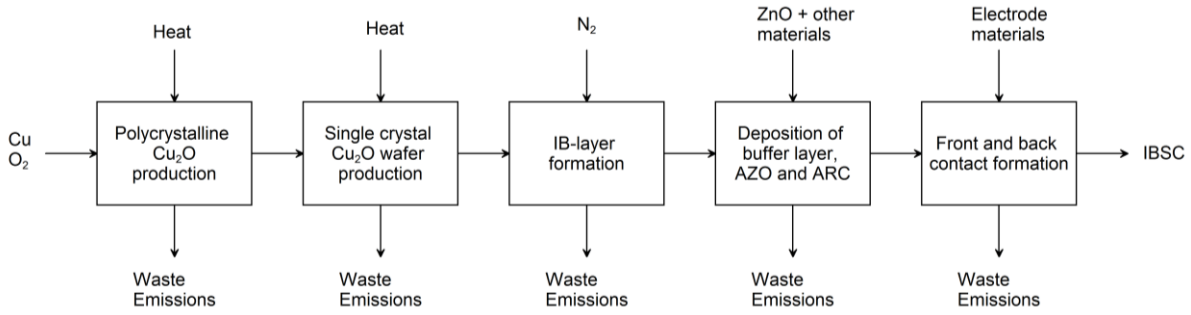

Figure 10.2: The processes included in the intermediate band solar cell production.

The inflows from the top of each process indicate that energy and materials are added to each step of the production route. However, these flows only account for the main ingredient(s) in addition to the inflow from the preceding process. These five processes are discussed in the five sections below.

10.2.1 Cu_2O single crystal

Since the resistivity of Cu_2O is one of the greatest issues regarding the performance of Cu_2O-based heterojunctions [131], the single crystal growth should be tailored to minimize the resistivity. High-quality single crystals of Cu_2O can be prepared by the floating zone melting method in air [32], see section 4.5.2. Polycrystalline Cu_2O rods resulting from oxidizing high purity copper are used as feed rods in a thermal treatment to obtain FZ sc-Cu_2O. The up-scaling of this technique is still in progress, but similar rods to the high quality FZ-grown sc-Si with a diameter of 15 cm and length 1 m [33] may be obtained in the future.

The single crystal can then be placed into the deposition chamber where the IB-layer is formed before the rest of the layers are deposited.

10.2.2 IB formation

The active single crystal Cu_2O wafer should be doped to form the IB in the top layer of the wafer. The ion implantation method similar to that used for IB-formation in Si, see section 4.6.1, will be tried out for the Cu_2O:N IB material. The goal is to form deep levels in the single crystal Cu_2O through ultra-high doping of N.

10.2.3 Deposition

Three layers should be deposited on top of the Cu_2O single crystal in this order:

1. Bufferlayer: un-doped ZnO or a-ZTO
2. N-emitter: Al-doped ZnO
3. Anti-reflective coating: Al_2O_3

Between the deposition steps, surface treatment might be necessary.

10.2.3.1 Surface treatment

Surface treatment before a different material is deposited might be necessary to remove unwanted substances that might have formed on the surface. For example, a wet chemical etching procedure with HNO_3 solution has been used to remove any trace of CuO from the top face of a Cu_2O substrate before depositing the ZnO layer in a Cu_2O/ZnO heterostructure [102, 115]. Hydrogen passivation can also be evaluated for the layers. For ohmic electrode formation on the Cu_2O wafer, surface treatments using sulfur and selenium may be useful [120].

10.2.3.2 Choosing deposition technique

When choosing a high deposition technique, the needs and requirements in Table 6.3 and Table 7.4 should be kept in mind, as well as the production criteria in Table 8.3. The best alternatives of the epitaxial deposition methods mentioned in section 2.3.2 might be; Plasma-Enhanced Chemical Vapor Deposition (PECVD), Metal-organic Chemical Vapor Deposition (MOCVD), Pulsed Laser Deposition (PLD), Atomic Layer Deposition (ALD) or Molecular Beam Epitaxy (MBE).

Selection of deposition technique should be based on the cell requirements and the results from the literary review of cells where ZnO is successfully deposited on Cu_2O. The cell size should be 156 x 156 mm, and the deposition chamber should thus fit this size of cells. In addition, the deposition method should be ready for large scale production at high quality and low cost. With these requirements in mind, the four high quality deposition techniques are evaluated for IBSC production.

PECVD

PECVD is a CVD process that uses cold plasma that leads to the possibility of keeping wafers at low temperatures and thus enhances the properties of deposited layers. Typically PECVD is used in formation of the SiN_x ARC layer of crystalline Si-cells, and recently a high-power-plasma (HPP) vertical PECVD system was developed for hydrogenated passivating amorphous SiN_x and Al_2O_3 films [198]. The throughput was about 1200 wafers/h for one deposited film at a small footprint. With the deposition step of the IBSC production by this technique, fabrication of the cell would be one step closer to be comparable with excising industrial solar cell fabrication. However, the quality of the films needs further evaluation for production of high efficiency IBSCs.

MOCVD

In the literary review, several deposition methods of Cu_2O-ZnO heterostructures were mentioned. Many of the Cu_2O/ZnO cells studied in section 4.3 were produced by depositing

ZnO on Cu_2O. MOCVD seemed to be suitable for Cu_2O deposition on ZnO, but the precursors are often toxic metal-organic substances [113]. This excludes MOCVD as a suitable deposition method because of the environmental requirements regarding non-toxic precursors. Deposition of ZnO on Cu_2O, as will be the case here, seems less complicated because of the stability of ZnO compared to the easily oxidized Cu_2O.

PLD
The two reviewed cells with the highest conversion efficiency of 3.83 % and 4.12 % [115, 116] had the desired stacking sequence of ZnO deposited on Cu_2O. The layers grown on the Cu_2O active substrate in this experimental work were deposited by PLD.

For up-scaling purposes, PLD could be a good high quality choice; Robert Eason [36] claimed that PLD will be established as an industrial process by 2017.

ALD
ALD should also be evaluated, and based on ALD deposition of a high performance Cu_2O/ZnO cell [128], this technique could be suited for high efficiency IBSCs. As mentioned in section 2.3.2, no other technique can approach the conformity on high aspect structures, and in addition ALD extendible to very large substrates and even for parallel processing of multiple substrates. This deposition technique is more advanced than PLD, and would probably give higher quality. However, the extreme level of accuracy might come at a too high cost compared to the high enough quality of PLD.

MBE
ZnO layers deposited by MBE are investigated in detail by Mohamed Henini [199], with the possibility of upscale MBE deposition from research to mass production. However, during the literature search of Cu_2O-ZnO heterostructures, no reported research of MBE deposition of ZnO on Cu_2O substrates was found.

Compared to PLD, both techniques give very high material quality, but MBE is a slower and more complex technique. In PLD, it is possible to grow films at instantaneous rates as high as one monolayer per microsecond, six orders of magnitude faster than with MBE, and the average growth speed is limited only by the repetition rate of the laser [200].

Final alternatives
PLD and ALD are the best choices for the high quality deposition. PLD is assumed to give high enough quality for the advanced cell case described in section 9.2.2. PLD can be used in experimental studies of the IBSC in the laboratory, before industrialized process is developed. PECVD is the highest quality deposition technique of the already industrialized deposition methods, and might be used for large scale production of the IBSC in the near future if the material challenges are overcome.

10.2.4 Electrodes

Al has previously been vacuum depositited in a thermal evaporator as back electrode in heterostructure cells where the ZnO layer lies beneath the p-emitter [201]. Conventional

methods used to form the semiconductor-metal contact in Si-cells can also be considered here. Al is already used as a contact material in high performance Si-cells [197], and by using this existing method, the IBSC cells will easier slide into the PV market. Being able to use existing technology methods on an industrial level is crucial for the implementation of IBSC.

Ti-Al alloy electrode is known to have been electron-beam evaporated onto ZnO films [186], and the graphite paste electrodes for the Cu_2O single crystal backside can be screen printed on the Cu_2O wafers [185].

For actual validation and production of the cells, formation of front surface field and back surface field; FSF and BSF, at the contact-semiconductor interfaces should be evaluated. These fields can be formed by increasing the doping in the n- and p-emitter near the ohmic contacts [202, 203], and will minimize the surface recombination at these interfaces.

10.3 Example: Rooftop IBSC system in Oslo

Based on the results from the master's thesis by Nordahl [167] for the consulting company Multiconsult, an example of a complete IBSC system is given with the assumption that electrical components for Si-modules can be used for the IBSC modules designed in this thesis.

There are many uncertainties regarding this example system with IBSC instead of the Si-cells in the modules originally used by Nordahl, and the compatibility of the materials and expected performance from the chosen production route of the IBSCs will need more attention. However, as an example for the chosen location and other requirements from Chapter 7, the IBSCs are assumed compatible with the standard installation method for crystalline Si-cells.

10.3.1 PV modules

The most conventional production route with PECVD of the "simple cell" described in section 9.2.2 is chosen for the cell manufacturing. Each module will consist of 60 IBSCs of dimensions 156 x 156 mm encapsulated in EVA in 6 x 10 rows. The module dimensions will be 1 x 1.6 m after framing with aluminum frames. Tempered glass and Teflon will be used as a front and back protection sheet, respectively. This common encapsulation and framing of the IBSC modules in this system example enables the flow chart in section 8.2 to apply.

10.3.2 Site assessment

Since the location is set to Oslo, the most logical choice is the on-roof solution for flat roofs. There are a lot of old apartment and company buildings there, and many of them have suitable roofs for an additive rooftop PV system. As an example, the site and site assessment of the PV system designed in a thesis by Nordahl [167] is used. The roof area investigated in this thesis was approximately 1200 m^2, and the roof height was 22.5 m. In the surroundings there is a twelve floor building, and together with elements placed on the roof, the shadowing effect on the modules should be considered.

Tilt

The desired orientation and tilt of the modules are important to establish early on, to be able to design the number of modules in a string, and the pitch distance between the rows, i.e. the distance needed to avoid shadowing. The latitude-dependent tilt value of 45-50º found in section 8.1.1 should be further optimized. Other than the latitude, the tilt should be optimized for the local weather and the specific area for installation. Because of the large amount of clouds, more diffuse solar radiation and the large difference between summer and winter irradiation, the optimum tilt should be around 40-44º with south facing orientation [167]. Smaller tilt angles could also be investigated to ensure no shadowing.

Mounting structure

The choice of mounting system will have an effect on the module tilt and surrounding the edge zones, meaning the distance from the PV installation to the roof's edge. The five mounting systems evaluated in the thesis by Nordahl had an average edge zone requirement of approximately 2 meters. Only additive, non-penetrating roof systems were evaluated, to avoid penetration of the roof that could lead to insulation problems and water damages. The

issue of the total installation weight must also be evaluated, but large roof areas are usually designed to withstand heavy weight.

10.3.3 Inverter

The array of modules and the chosen inverter(s) must match in three areas; voltage, current and power. These three areas are unexplored for the IBSCs, since no complete IBSC device or module exist yet. To investigate the inverter choice based on location, it is assumed that the IBSC modules have similar electrical properties as the modules examined by Nordahl.

The module voltage is dependent on the temperature, as mentioned in section 2.6.3. The number of modules in a string is determined by the temperature-voltage relationship of the inverter. The extreme temperatures of winter and summer are chosen for inverter-array matching. Regarding the current, the highest module current has to be smaller than the maximum inverter current. The maximum PV array rated power and maximum DC input power are normally specified for the different inverter choices. These parameters must be examined for the IBSC modules in order to successfully pick a suitable inverter.

For a large PV system installed on a 1200 m^2 roof, several strings of modules are needed, and inverters with MPPT inputs should be considered to maximize the output for each string.

10.3.4 The PV system

Two systems were considered. First, a system with 100 modules, 10 modules in each string, connected to five inverters with two MPPT inputs each was simulated. Each string would then be operated at MPP. This PV system with a pitch distance of 2 m and a system with 72 modules and 2.5 meter pitch distance are shown in Figure 10.3. The edge zone is 2 m in both cases.

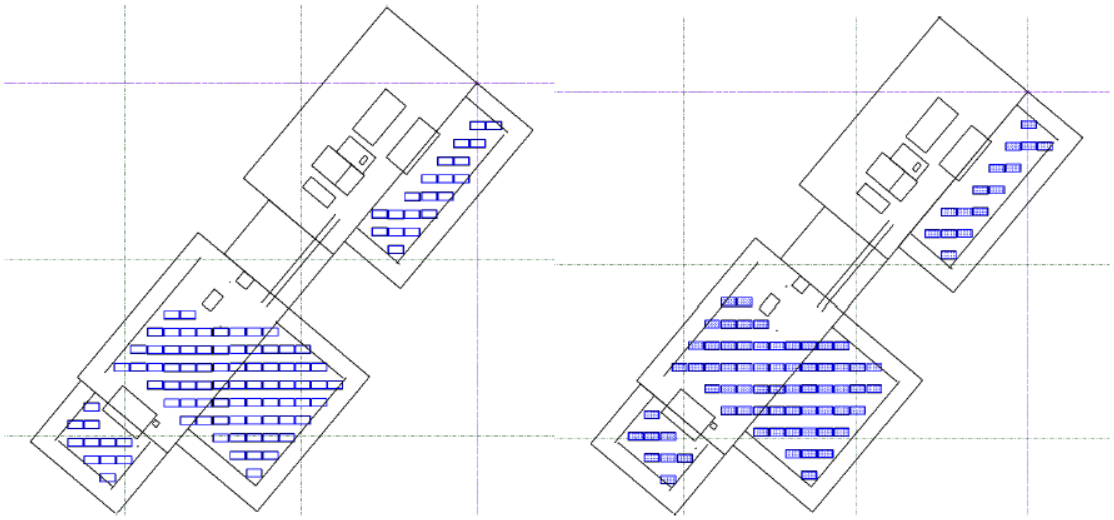

Figure 10.3: The roof with two cases; (left) 100 modules and 2 m pitch distance, and (right) 72 modules with 2.5 m pitch distance [167].

Considering the annual yield, the optimum tilt angle of the modules in Oslo was 40º. At this tilt, the 100 modules case produced 23.17 MWh/year with a performance ratio of 77.0 %. However, due to the limited amount of space on the roof it was found that the tilt angle

resulting in both an acceptable performance ratio and production was 20º. A pitch distance of approximately 2 m was the most optimal value. Increasing the pitch distance further would increase the performance ratio slightly, due to reduced shading, but the total amount of modules would decrease and, therefore, reduce the installed capacity of the installation.

The module efficiency in this example was 15.16 %, and considering the desired performance of the IBSCs, this system design would result in higher performance both in the optimistic and realistic case. However, the efficiency of 18 % in the realistic IBSC case is cell and not module efficiency.

A monocrystalline module was also studied for the PV system described above. This module had an efficiency of 20.1 %, and the PV installation with this module and 2 m pitch distance produced 31 MWh/year, which is approximately 50 % more than the electricity consumed in an average Norwegian household.

10.4 Discussion of the final results

The systems engineering process performed in this thesis involved a number of design choices for the PV system, and particularly the IBSC device. Materials and production of the cell were the main focus, and most of the design choices influenced the analysis of cell materials and production route. Many of the choices made regarding the cell design throughout this process have affected the other parts of the cell, and limited the design choices for other cell components. Here, the final results regarding materials, design and production routes of the cell are discussed.

10.4.1 Cell design

Based on the issues regarding the material challenges in Chapter 4, desired cell structure in section 7.4 and performance in Chapter 8, it seems that much research is still needed to reach a conclusion whether the Cu_2O/ZnO-based IBSC is a promising technology or should be dismisses in favor of other materials. There are numerous challenges yet to overcome before this cell can be realized with a promising performance for future large scale deployment. However, the discussed progress in heterojunction Cu_2O/ZnO cells in section 8.4.1, and the fact that Cu_2O:N is a promising IB material show that there is hope and room to overcome the remaining material challenges through further research.

10.4.2 Production

The cylindrical sc-Cu_2O rods grown by the floating zone method should at least have a diameter of 156-160 mm to obtain the desired 156 x 156 mm wafers. The existing floating zone melting furnaces for sc-Cu_2O growth might not be large enough, as discussed in section 4.5.2. The investigation of the techniques used for FZ-grown sc-Si wafers may aid further improvement of up-scaling of FZ-grown sc-Cu_2O.

If the issues regarding unwanted reactions in crucibles for single crystal Cu_2O-growth [129, 131] could be solved, conventional methods using large scale crucibles could be a sustainable alternative to the FZ method that results in less material loss. The FZ-rods must be cut into square wafers, while the ingots from crucibles usually are cube-shaped.

The two chosen deposition methods, PLD and PECVD, could serve different purposes. To facilitate further research of the unexplored production of Cu_2O/ZnO-based IBSCs high quality low-scale deposition like PLD could be a suitable technique combined with the FZ method. The two methods of this production route might even be industrialized in time for realization of IBSCs.

PECVD is as mentioned earlier already implemented into high quality Si-cell production. This technique combined with FZ sc-Cu_2O growth would be better suited for competition with existing Si-technology.

10.4.3 Example system

There are many uncertainties regarding this example system with IBSC instead of the Si-cells in the modules originally used by Nordahl. The electrical behavior of the designed IBSC modules may not be compatible with the electrical components chosen in the case example. Also, the materials in the simple cell alternative and desired performance from the chosen

production route were identified based on many assumptions, and would need further investigation.

If the system with 100 modules and a pitch distance of 2 meters can be used for the IBSC system with the “optimistic module efficiency” of 35.8 %, see section 8.1.2, the IBSC system would have a high output, considering the 31 MWh/year produced by sc-Si modules with 20.1 % efficiency.

11 Remarks on the method

The process of learning the SEP methodology while using it turned out to be challenging. A top-down approach is not in the nature of most materials scientists, who normally are more concerned with the detailed bottom-up perspective. However, after reading scientific articles, conducting a literary review and learning the SEP fundamentals, ideas on how to combine the IBSC technology and SEP methodology appeared.

11.1 The process performed

The needs, requirements and performance analyses in Chapters 6, 7 and 8, focused first on the system level before going into a more detailed analysis of the cell. Chapter 9 was only focused on the IBSC, but with the previous defined system parameters in mind. The material scenarios were found along with the two production routes for a simple and advanced cell, which facilitated the production route design in Chapter 10. The production technique analysis was solved according to the stated needs and requirements. Step 4 and 5 go hand in hand in the process of this thesis, and they could possibly be combined for further utilization of the method. When both the materials and production are investigated from a materials science point of view, materials cannot be selected without exploring possible production routes, and the other way around.

In Chapter 6 it was stated that the IBSC system should be sustainable. There has been a focus on environmentally friendly materials throughout this thesis, but step 6 of the SEP where the sustainability could have been verified was not conducted due to time constraints. The production routes identified could also be environmentally harmful, since not enough information on the sustainability of these techniques was available. Verification of the IBSC system could focus on sustainability by e.g. evaluation of environmental impacts through a LCA. In Chapter 13 Further work, an analysis of how this system sustainability can be evaluated at a later time is mentioned.

11.2 The combination of materials science and SEP

Looking at the whole IBSC system as one is an objective of the SoRoSol-project. The method combining materials science and SEP facilitated this way of thinking, and prevented the trap many materials scientists fall in; only focusing on optimizing the material and production parameters in the laboratory. A sustainable and socially robust technology usually requires attention to the surroundings and the parties interested in a final product.

To conduct a holistic SEP, an interdisciplinary group may be needed. As an alternative, other disciplines can be approached through interviews and literature searches. Interdisciplinary discussions are important to state needs and requirements that take all parts of the integrated system into account. The work conducted in this thesis would benefit from interactions with other fields and disciplines.

The reliability of the analysis and optimization in step 4 based on specified performance in step 3 are weakened when the decisions are made from a material and production perspective only, influenced by available, and often limited, literature and technology competence. However, with the main goal of unveiling challenges regarding materials and production of a Cu_2O/ZnO-based IBSC, the combined method was successful. With these materials as a case to test the IBSC concept for further research and possible implementation, this method could

be utilized for different IBSC host material scenarios. A wider utilization of the method could also be possible, as this thesis opened the door for other combinations between materials science and systems engineering principles.

11.3 System integration

To answer the question whether a future Cu_2O/ZnO-based IBSC system is realistic or not, other technologies than material science, such as electrical power, and other disciplines, such as economy and environmental studies, should be considered. Influence by some of the other disciplines could be:

- An economic point of view would influence system choices already from the initial need step based on e.g. research financing, development costs and installing costs.
- The bioware or social aspect could influence the system choices based on e.g. the publics demands and desires with respect to usability and design, and the governmental laws and regulations for PV installing and use.
- From an environmental perspective, existing environmental restrictions and future negotiations and bylaws could influence the demand of PV systems and set requirements to the system sustainability.
- Innovative information technology could open up new markets for PV systems, like the Smart Home example given in section 6.1.1.

A detailed configuration of the whole IBSC system through interdisciplinary analyses could give a holistic result which takes all the aspects mentioned above into account.

However, the material science may still be the most important technology for future realization of IBSC systems. Through further testing, the cell materials should be characterized and optimized for desired properties, the materials compatibility should be investigated and fabrication of the cell should be attempted.

Some of the future work that might be feasible to approach realization of the IBSC system is further discussed in Chapter 13.

12 Conclusions

A top-down approach based on systems engineering principles was simplified to match the detailed goals of this work, and a new approach that can solve combined materials technology and systems engineering assignments was developed. By utilizing this approach, challenges of possible IBSC host materials; ZnO and Cu_2O were identified. The most prominent material challenges were the high resistivity of Cu_2O and unwanted charge transport at the ZnO/IB-Cu_2O interface. Single crystal growth of Cu_2O and a tailored buffer layer and surface treatment at the ZnO/IB-Cu_2O junction can mitigate these challenges.

A conventional PV system was used as an example for rooftop mounting of the IBSC system in Oslo. The module dimensions, mounting structure and electrical components of the conventional PV system were assumed to be compatible with the IBSC cells investigated here. Two alternatives for the cell materials and production were provided; a simple cell that can be fabricated by conventional, high quality methods and an advanced cell with more complex materials and production route. Both cells consist of sustainable materials and aim at higher efficiency than conventional cells, but the advanced cell is assumed to have significantly higher efficiency than the simple cell. The best material composition available and the highest quality production predicted industrialized within years, makes the advanced cell most promising. With the increasing demand for clean energy, PV systems of these IBSCs could be a sustainable, high efficiency solution.

13 Further work

The sixth step of the SEP explained in Chapter 5 could be conducted to test and verify the cell and system results. Also, the sustainability of the cell materials and production could be evaluated through various analyses.

13.1 Systems engineering process step 6: Verify and test

The different stages of testing, see Figure 5.5, could be evaluated for system verification during the sixth step that was not covered in this thesis.

Cell research

The IBSC can be fabricated and optimized for different parameters, such as; O_2 flow during sc-Cu_2O growth, temperature, thickness of deposited layers, deposition rate, deposition method etc. To test Cu_2O parameters, different single crystals of varying purity could be purchased and tested for optimal deposition of buffer layer and AZO n-emitter. To be able to say for certain if the ZnO/IB-Cu_2O/Cu_2O will function as desired, optical and electrical properties must be tested.

If high quality cells with the desired electrical behavior are produced in the future, electrical components with the different I-V characteristics could be matched to IBSC modules, and a complete IBSC system could be designed in practice.

13.2 Sustainability verification

The IBSC system's sustainability can be verified from analyses with different perspectives, such as; life cycle assessment (LCA) with focus on environmental impacts or life cycle costing (LCC) with focus on economy.

A LCA conducted on the PV system developed in this master's thesis will give answers about the environmental impacts during the systems life cycle. The phase that contributes most to the total impact is the manufacturing phase, and the cell materials and production route identified in this thesis could then be evaluated.

The cost is not accounted for in any part of this thesis. The abundant and sustainable materials are though usually low-cost, since resource scarcity tends to lead to high cost. The economic challenges that were easily discovered throughout the process were taken into account, because the economic system part has such a large influence. E.g. the economic issues related to gold contacts were intentionally taken into account. A LCC could however give a detailed view of the economic challenges associated with designing a new PV system.

In addition, analyses based on LCA, like social life cycle assessment (S-LCA) would include the bioware part of the integrated system by assessing the social implications.

13.3 Redefining the needs

If a high quality and sustainable ZnO/IB-Cu_2O/Cu_2O cell cannot be produced, other materials identified as suitable IBSC host materials in the specialization project [17] can be evaluated.

Other needs can also be redefined to find a better solution for the new or improved IBSC system. To explore the system from a different starting point, the initial needs can be redefined in the first SEP step. This will probably change the whole process through the rest of the steps. As an example, the location of the PV system can be changed to get a more realistic energy mix and emission profile for locations without the hydro-dominated energy mix found in Norway. Other installation methods could also be evaluated, like inclined roofs for household installation.

14 Bibliography

1. Jaeger Waldau, A., *PV status: Research, Solar cell Production and Market Implementation of Photovoltaics.* Refocus, 2005. **6**(3): p. 20-23.
2. Alsema, E.A. and E. Nieuwlaar, *Energy viability of photovoltaic systems.* Energy policy, 2000. **28**(14): p. 999-1010.
3. Angelis-Dimakis, A., et al., *Methods and tools to evaluate the availability of renewable energy sources.* Renewable and Sustainable Energy Reviews, 2011. **15**(2): p. 1182-1200.
4. Brabec, C.J., et al., *Organic photovoltaics: concepts and realization*. Vol. 60. 2003: Springer.
5. Stoppato, A., *Life cycle assessment of photovoltaic electricity generation.* Energy, 2008. **33**(2): p. 224-232.
6. Green, M.A., *Third generation photovoltaics: Ultra-high conversion efficiency at low cost.* Progress in Photovoltaics: Research and Applications, 2001. **9**(2): p. 123-135.
7. Tsakalakos, L., *1.23 - Application of Micro- and Nanotechnology in Photovoltaics*, in *Comprehensive Renewable Energy*, S. Editor-in-Chief: Ali, Editor. 2012, Elsevier: Oxford. p. 515-531.
8. ASDReports. *Global Solar PV Market will Show Significant Growth up to 2020*. 2013 [01.03.2013]; Available from: http://www.csrwire.com/press_releases/35051-Global-Solar-PV-Market-will-Show-Significant-Growth-up-to-2020?tracking_source=rss.
9. Barnham, K., M. Mazzer, and B. Clive, *Resolving the energy crisis: nuclear or photovoltaics?* Nature materials, 2006. **5**(3): p. 161-164.
10. Wolf, M., *Limitations and possibilities for improvement of photovoltaic solar energy converters. I. Considerations for earth's surface operation.* Proceedings of the Institute of Radio Engineers, 1960. **48**(7): p. 1246.
11. Luque, A. and A. Martí, *Increasing the Efficiency of Ideal Solar Cells by Photon Induced Transitions at Intermediate Levels.* Physical Review Letters, 1997. **78**(26): p. 5014-5017.
12. Luque, A. and A. Marti, *A metallic intermediate band high efficiency solar cell.* Progress in photovoltaics: research and applications, 2001. **9**(2): p. 73-86.
13. Luque, A. and A. Martí, *The intermediate band solar cell: Progress toward the realization of an attractive concept.* Advanced Materials, 2010. **22**(2): p. 160-174.
14. Walukiewicz, W., et al., *Interaction of Localized Electronic States with the Conduction Band: Band Anticrossing in II-VI Semiconductor Ternaries.* Physical Review Letters, 2000. **85**(7): p. 1552-1555.
15. Luque, A., et al., *Intermediate bands versus levels in non-radiative recombination.* Physica B: Condensed Matter, 2006. **382**(1–2): p. 320-327.
16. Tanabe, K., et al., *High-efficiency InAs/GaAs quantum dot solar cells by metalorganic chemical vapor deposition.* Applied Physics Letters, 2012. **100**(19): p. 193905-193905-3.
17. Thorstensen, A.E., *Specialization project: New materials for intermediate band solar cells*, in *Department of Materials Science and Engineering* 2013, Norwegian University of Science and Technology (NTNU): Trondheim.
18. Ardente, F., et al., *Energy performances and life cycle assessment of an Italian wind farm.* Renewable and Sustainable Energy Reviews, 2008. **12**(1): p. 200-217.
19. *ISO 14040: Environmental management -- Life cycle assessment -- Principles and framework*, 2006, International Standard: Geneva. p. 20.

20. Leonard, J. and D.S.M.C. Press, *Systems Engineering Fundamentals: Supplementary Text*. 1999: Defense Systems Management College.
21. Fet, A.M., *Systems engineering methods and environmental life cycle performance within ship industry*, in *Doktor Ingeniøravhandling*1997, NTNU: Trondheim.
22. Green, M.A., *Third generation photovoltaics: advanced solar energy conversion*. 2003: Springer.
23. Simbolotti, G., M. Taylor and G. Tosato *Solar Photovoltaics Technology Brief*, in *IRENA-IEA-ETSAP Technology Briefs* 2013, The International Renewable Energy Agency (IRENA) and International Energy Agency's Energy Technology Systems Analysis Programme (IEA-ETSAP): Abu Dhabi, United Arab Emirates.
24. Despotou, E., *1.10 - Vision for Photovoltaics in the Future*, in *Comprehensive Renewable Energy*, S. Editor-in-Chief: Ali, Editor. 2012, Elsevier: Oxford. p. 179-198.
25. Deutsche_Gesellshaft_Fur_Sonnenenergie, *Chapter 2: PV system components*. Planning and installing photovoltaic systems: a guide for installers, architects and engineers. 2005: Earthscan.
26. Naval Research Laboratory, U.S. *NRL Designs Multi-Junction Solar Cell to Break Efficiency Barrier*. 2013; Available from: http://www.nrl.navy.mil/media/news-releases/2013/nrl-designs-multi-junction-solar-cell-to-break-efficiency-barrier.
27. Mezin, V. *Harness the Sun Toolbox*. UEE07 – Electrotechnology 2012; Available from: http://toolboxes.flexiblelearning.net.au/demosites/series13/13_02/content_sections/learn_about/08_solar_page_007.htm.
28. Wang, W., *Intermediate band solar cells based on ZnTeO*, 2010, The University of Michigan.
29. Antolín, E., A. Martí, and A. Luque, *1.29 - Intermediate Band Solar Cells*, in *Comprehensive Renewable Energy*, S. Editor-in-Chief: Ali, Editor. 2012, Elsevier: Oxford. p. 619-639.
30. Martí, A., et al., *Nanostructured Materials for Solar Energy Conversion, Chapter 17*. 2006: Elsevier Science.
31. Card, H.C. and E.S. Yang, *Electronic processes at grain boundaries in polycrystalline semiconductors under optical illumination.* Electron Devices, IEEE Transactions on, 1977. **24**(4): p. 397-402.
32. Ito, T., et al., *Single-crystal growth and characterization of Cu2O and CuO.* Journal of Materials Science, 1998. **33**(14): p. 3555-3566.
33. Markvart, T., *Chapter 3: Solar Cells*. Solar electricity. 2000: John Wiley & Sons.
34. Chopra, K.L. and S.R. Das, *Thin film solar cells*. 1983: Springer.
35. Seshan, K., *Handbook of Thin-Film Deposition Processes and Techniques - Principles, Methods, Equipment and Applications (2nd Edition)*, 2002, William Andrew Publishing/Noyes.
36. Eason, R., *Pulsed Laser Deposition of Thin Films: Applications-Led Growth of Functional Materials*. 2007: Wiley.
37. George, S.M., *Atomic layer deposition: an overview.* Chemical Reviews, 2009. **110**(1): p. 111-131.
38. Musselman, K.P., et al., *A Novel Buffering Technique for Aqueous Processing of Zinc Oxide Nanostructures and Interfaces, and Corresponding Improvement of Electrodeposited ZnO-Cu2O Photovoltaics.* Advanced Functional Materials, 2011. **21**(3): p. 573-582.
39. Green, M.A., *Solar cells: operating principles, technology, and system applications.* Englewood Cliffs, NJ, Prentice-Hall, Inc., 1982. 288 p., 1982. **1**.

40. Sze, S.M. and K.K. Ng, *Physics of Semiconductor Devices*. 2006: Wiley.
41. Brillson, L.J. and Y. Lu, *ZnO Schottky barriers and Ohmic contacts.* Journal of Applied Physics, 2011. **109**(12): p. 121301-121301-33.
42. Streetman, B.G. and S. Banerjee, *Solid state electronic devices*. Vol. 4. 2000: Prentice Hall New Jersey.
43. Aldous, S., Zeke Yewdall, Sam Ley *A Peek Inside a PV Cell*. 2007 9.9.2013]; Available from: http://www.homepower.com/articles/solar-electricity/equipment-products/peek-inside-pv-cell.
44. Deutsche_Gesellshaft_Fur_Sonnenenergie, *Chapter 3: Components of PV systems*. Planning and Installing Photovoltaic Systems: A Guide for Installers, Architects and Engineers. 2013: Taylor & Francis.
45. Arvizu, D., P. Balaya, L. Cabeza, T. Hollands, A. Jäger-Waldau, M. Kondo, C. Konseibo, V. Meleshko, W. Stein, Y. Tamaura, H. Xu, R. Zilles, *Direct Solar Energy*, in *IPCC Special Report on Renewable Energy Sources and Climate Change Mitigation*, R.P.-M. O. Edenhofer, Y. Sokona, K. Seyboth, P. Matschoss, S. Kadner, T. Zwickel, P. Eickemeier, G. Hansen, S. Schlömer, C. von Stechow (eds), Editor 2011, Cambridge University Press: Cambridge, United Kingdom and New York, NY, USA. p. 353-355.
46. Sumper, A., et al., *Life-cycle assessment of a photovoltaic system in Catalonia (Spain).* Renewable and Sustainable Energy Reviews, 2011. **15**(8): p. 3888-3896.
47. Deutsche_Gesellshaft_Fur_Sonnenenergie, *Chapter 8: Mounting systems and building integration*. Planning and Installing Photovoltaic Systems: A Guide for Installers, Architects and Engineers. 2013: Taylor & Francis.
48. Pacca, S., D. Sivaraman, and G.A. Keoleian, *Parameters affecting the life cycle performance of PV technologies and systems.* Energy Policy, 2007. **35**(6): p. 3316-3326.
49. Shockley, W. and H.J. Queisser, *Detailed balance limit of efficiency of p-n junction solar cells.* Journal of applied physics, 1961. **32**(3): p. 510-519.
50. Nelson, J., *The physics of solar cells*. Vol. 57. 2003: World Scientific.
51. Raugei, M., S. Bargigli, and S. Ulgiati, *Life cycle assessment and energy pay-back time of advanced photovoltaic modules: CdTe and CIS compared to poly-Si.* Energy, 2007. **32**(8): p. 1310-1318.
52. Azzopardi, B. and J. Mutale, *Life cycle analysis for future photovoltaic systems using hybrid solar cells.* Renewable and Sustainable Energy Reviews, 2010. **14**(3): p. 1130-1134.
53. Mason, J., et al., *Energy payback and life-cycle CO2 emissions of the BOS in an optimized 3· 5 MW PV installation.* Progress in Photovoltaics: Research and Applications, 2006. **14**(2): p. 179-190.
54. *Electrical Properties of PV Modules*. HK RE Net: Solar photovoltaic 2012; Available from: http://re.emsd.gov.hk/english/contactus/contactus.html.
55. SMA, *Performance ratio: Quality factor for the PV plant.* 2010.
56. Jahn, U. and W. Nasse, *Operational performance of grid-connected PV systems on buildings in Germany.* Progress in Photovoltaics: Research and Applications, 2004. **12**(6): p. 441-448.
57. Alsema, E. and M. de Wild-Scholten, *Environmental impacts of PV electricity generation-a critical comparison of energy supply options.* 2006.
58. Lorenzo, E., *Chapter 22: Energy collected and delivered by PV modules*. Handbook of photovoltaic science and engineering, ed. A. Luque and S. Hegedus. 2011: Wiley. com.

59. Reite, S., *Private communication: Efficiency of PV systems in Norway*, A.E. Thorstensen, Editor 2013: ZERO Conference 2013, Oslo.
60. Roy, P., et al., *A review of life cycle assessment (LCA) on some food products.* Journal of Food Engineering, 2009. **90**(1): p. 1-10.
61. Heijungs, R., G. Huppes, and J.B. Guinée, *Life cycle assessment and sustainability analysis of products, materials and technologies. Toward a scientific framework for sustainability life cycle analysis.* Polymer Degradation and Stability, 2010. **95**(3): p. 422-428.
62. Kramer, K.-L., *Chapter 4 - Pulling it All Together*, in *User Experience in the Age of Sustainability*. 2012, Morgan Kaufmann: Boston. p. 101-149.
63. Pennington, D.W., et al., *Life cycle assessment Part 2: Current impact assessment practice.* Environment International, 2004. **30**(5): p. 721-739.
64. Strømman, A.H., *Methodological Essentials of Life Cycle Assessment*, 2010 -. p. 83-85.
65. Nieuwlaar, E., E. Alsema, and B. van Engelenburg, *Using life-cycle assessments for the environmental evaluation of greenhouse gas mitigation options.* Energy Conversion and Management, 1996. **37**(6–8): p. 831-836.
66. Komiyama, H., et al., *Life cycle analysis of solar cell systems as a means to reduce atomospheric carbon dioxide emissions.* Energy Conversion and Management, 1996. **37**(6–8): p. 1247-1252.
67. Kato, K., A. Murata, and K. Sakuta, *An evaluation on the life cycle of photovoltaic energy system considering production energy of off-grade silicon.* Solar Energy Materials and Solar Cells, 1997. **47**(1–4): p. 95-100.
68. Dones, R. and R. Frischknecht, *Life-cycle assessment of photovoltaic systems: results of Swiss studies on energy chains.* Progress in Photovoltaics: Research and Applications, 1998. **6**(2): p. 117-125.
69. Kato, K., A. Murata, and K. Sakuta, *Energy pay-back time and life-cycle CO2 emission of residential PV power system with silicon PV module.* Progress in Photovoltaics: Research and Applications, 1998. **6**(2): p. 105-115.
70. Frankl, P. and M. Gamberale, *The methodology of Life-Cycle Assessment (LCA) and its application to the energy sector.* Advances in energy studies, energy flows in ecology and economy. Rome: MUSIS, 1998: p. 241-56.
71. Alsema, E., *Energy pay-back time and CO2 emissions of PV systems.* Progress in photovoltaics: research and applications, 2000. **8**(1): p. 17-25.
72. Oliver, M. and T. Jackson, *The evolution of economic and environmental cost for crystalline silicon photovoltaics.* Energy Policy, 2000. **28**(14): p. 1011-1021.
73. Greijer, H., et al., *Environmental aspects of electricity generation from a nanocrystalline dye sensitized solar cell system.* Renewable Energy, 2001. **23**(1): p. 27-39.
74. Kato, K., et al., *A life-cycle analysis on thin-film CdS/CdTe PV modules.* Solar Energy Materials and Solar Cells, 2001. **67**(1–4): p. 279-287.
75. Meier, P.J., *Life-cycle assessment of electricity generation systems and applications for climate change policy analysis*. 2002: University of Wisconsin--Madison.
76. Ito, M., et al., *A preliminary study on potential for very large-scale photovoltaic power generation (VLS-PV) system in the Gobi desert from economic and environmental viewpoints.* Solar Energy Materials and Solar Cells, 2003. **75**(3-4): p. 507-517.
77. Jungbluth, N., *Life cycle assessment of crystalline photovoltaics in the Swiss ecoinvent database.* Progress in Photovoltaics: Research and Applications, 2005. **13**(5): p. 429-446.

78. Battisti, R. and A. Corrado, *Evaluation of technical improvements of photovoltaic systems through life cycle assessment methodology.* Energy, 2005. **30**(7): p. 952-967.
79. Hondo, H., *Life cycle GHG emission analysis of power generation systems: Japanese case.* Energy, 2005. **30**(11-12 SPEC. ISS.): p. 2042-2056.
80. Tripanagnostopoulos, Y., et al., *Energy, cost and LCA results of PV and hybrid PV/T solar systems.* Progress in Photovoltaics: Research and applications, 2005. **13**(3): p. 235-250.
81. Raugei, M., S. Bargigli, and S. Ulgiati. *Energy and life cycle assessment of thin film CdTe photovoltaic modules*. in *Proceedings of the 20th European Photovoltaic Solar Energy Conference*. 2005.
82. Fthenakis, V. and E. Alsema, *Photovoltaics energy payback times, greenhouse gas emissions and external costs: 2004–early 2005 status.* Progress in Photovoltaics: Research and Applications, 2006. **14**(3): p. 275-280.
83. de Wild-Scholten, M., et al. *A cost and environmental impact comparison of grid-connected rooftop and ground-based PV systems*. in *21st European Photovoltaic Solar Energy Conference*. 2006.
84. Veltkamp, A. and M. de Wild-Scholten, *Dye sensitised solar cells for large-scale photovoltaics; the determination of environmental performances.* 2006.
85. Muneer, T., et al., *Life cycle assessment of a medium-sized photovoltaic facility at a high latitude location.* Proceedings of the Institution of Mechanical Engineers, Part A: Journal of Power and Energy, 2006. **220**(6): p. 517-524.
86. Kannan, R., et al., *Life cycle assessment study of solar PV systems: An example of a 2.7 kWp distributed solar PV system in Singapore.* Solar Energy, 2006. **80**(5): p. 555-563.
87. Fthenakis, V.M. and H.C. Kim, *Greenhouse-gas emissions from solar electric- and nuclear power: A life-cycle study.* Energy Policy, 2007. **35**(4): p. 2549-2557.
88. Ito, M., et al., *A comparative study on cost and life-cycle analysis for 100 MW very large-scale PV (VLS-PV) systems in deserts using m-Si, a-Si, CdTe, and CIS modules.* Progress in Photovoltaics: Research and Applications, 2008. **16**(1): p. 17-30.
89. SENSE, *Sustainability Evaluation of Solar Energy Systems, LCA Analysis* 2008, Wuerth Solar GmbH & Co.KG., Free Energy Europe SA, Zentrum fuer Sonnenenergie- und Wasserstoff-Forschung, Fraunhofer-Gesellschaft zur, Foerderung der Angewandten, Forschung e.V. , Ambiente Italia srl, Fundacion Gaiker: University of Stuttgart.
90. Fthenakis, V.M., H.C. Kim, and E. Alsema, *Emissions from photovoltaic life cycles.* Environmental science & technology, 2008. **42**(6): p. 2168-2174.
91. Ito, M., K. Komoto, and K. Kurokawa. *A comparative LCA study on potential of very-large scale PV systems in Gobi desert*. in *Photovoltaic Specialists Conference (PVSC), 2009 34th IEEE*. 2009. IEEE.
92. de Wild-Scholten, M. and M. Schottler. *Solar as an environmental product: Thin-film modules–production processes and their environmental assessment* in *Thin Film Industry Forum*. 2009. Berlin, Germany.
93. Fthenakis, V., et al. *Update of PV energy payback times and life-cycle greenhouse gas emissions*. in *24th European Photovoltaic Solar Energy Conference and Exhibition*. 2009.
94. Ito, M., K. Komoto, and K. Kurokawa, *Life-cycle analyses of very-large scale PV systems using six types of PV modules.* Current Applied Physics, 2010. **10**(2, Supplement): p. S271-S273.

95. Filippidou, F., et al., *A comparative analysis of a cdte and a poly-Si photovoltaic module installed in North Eastern Greece.* Applied Solar Energy, 2010. **46**(3): p. 182-191.
96. Dominguez-Ramos, A., et al., *Prospective CO2 emissions from energy supplying systems: photovoltaic systems and conventional grid within Spanish frame conditions.* The International Journal of Life Cycle Assessment, 2010. **15**(6): p. 557-566.
97. Ito, M., et al., *A comparative study on life cycle analysis of 20 different PV modules installed at the Hokuto mega-solar plant.* Progress in Photovoltaics: Research and Applications, 2011. **19**(7): p. 878-886.
98. de Wild-Scholten, M. *Environmental profile of PV mass production: globalization*. in *26th European Photovoltaic Solar Energy Conference, Hamburg, Germany*. 2011.
99. Held, M. and R. Ilg, *Update of environmental indicators and energy payback time of CdTe PV systems in Europe.* Progress in Photovoltaics: Research and Applications, 2011. **19**(5): p. 614-626.
100. de Wild-Scholten, M. and R. Gløckner, *Environmental footprint of Elkem Solar Silicon®.* 2012.
101. Westgaard, T., C. Olson, and T. Veltkamp, *Life cycle analysis of modules: A multicrystalline silicon case study.* Photovoltaics International, 2012: p. 136-140.
102. Mittiga, A., et al., *Heterojunction solar cell with 2% efficiency based on a Cu2O substrate.* Applied Physics Letters, 2006. **88**(16): p. -.
103. Loferski, J.J., *Theoretical Considerations Governing the Choice of the Optimum Semiconductor for Photovoltaic Solar Energy Conversion.* Journal of Applied Physics, 1956. **27**(7): p. 777-784.
104. Green, M.A. and M.J. Keevers, *Optical properties of intrinsic silicon at 300 K.* Progress in photovoltaics, 1995. **3**(3): p. 189-192.
105. Jeong, S., et al., *An analysis of temperature dependent current–voltage characteristics of Cu2O–ZnO heterojunction solar cells.* Thin Solid Films, 2011. **519**(19): p. 6613-6619.
106. Katayama, J., et al., *Performance of Cu2O/ZnO Solar Cell Prepared By Two-Step Electrodeposition.* Journal of Applied Electrochemistry, 2004. **34**(7): p. 687-692.
107. Ruiz, E., et al., *Electronic structure and properties of Cu2O.* Physical Review B - Condensed Matter and Materials Physics, 1997. **56**(12): p. 7189-7196.
108. Minami, T., et al., *Effect of ZnO film deposition methods on the photovoltaic properties of ZnO–Cu2O heterojunction devices.* Thin Solid Films, 2006. **494**(1–2): p. 47-52.
109. Dimitriadis, C.A., L. Papadimitriou, and N.A. Economou, *Resistivity dependence of the minority carrier diffusion length in in single crystals of Cu2O.* Journal of Materials Science Letters, 1983. **2**(11): p. 691-693.
110. Nolan, M. and S.D. Elliott, *The p-type conduction mechanism in Cu2O: A first principles study.* Physical Chemistry Chemical Physics, 2006. **8**(45): p. 5350-5358.
111. Abdu, Y. and A. Musa, *Copper (I) oxide (Cu 2) based solar cells -a review.* Bayero Journal of Pure and Applied Sciences, 2009. **2**(2): p. 8-12.
112. Hussain, S., et al., *Effect of electrodeposition and annealing of ZnO on optical and photovoltaic properties of the p-Cu2O/n-ZnO solar cells.* Electrochimica Acta, 2011. **56**(24): p. 8342-8346.
113. Jeong, S. and E.S. Aydil, *Heteroepitaxial growth of Cu2O thin film on ZnO by metal organic chemical vapor deposition.* Journal of Crystal Growth, 2009. **311**(17): p. 4188-4192.
114. Akimoto, K., et al., *Thin film deposition of Cu2O and application for solar cells.* Solar Energy, 2006. **80**(6): p. 715-722.

115. Minami, T., et al., *High-efficiency oxide solar cells with ZnO/Cu2O heterojunction fabricated on thermally oxidized Cu2O sheets.* Applied physics express, 2011. **4**(6): p. 2301.
116. Nishi, Y., T. Miyata, and T. Minami, *The impact of heterojunction formation temperature on obtainable conversion efficiency in n-ZnO/p-Cu2O solar cells.* Thin Solid Films, 2013. **528**(0): p. 72-76.
117. Milnes, A. and D. Feucht, *Heterojunctions and Metal-Semiconductor Junctions.* Academic Press, New-York and London, 1972.
118. Olsen, L.C., F.W. Addis, and W. Miller, *Experimental and theoretical studies of Cu2O solar cells.* Solar Cells, 1982. **7**(3): p. 247-279.
119. Herion, J., E.A. Niekisch, and G. Scharl, *Investigation of metal oxide/cuprous oxide heterojunction solar cells.* Solar Energy Materials, 1980. **4**(1): p. 101-112.
120. Miyata, T., et al. *Effect of a buffer layer on the photovoltaic properties of AZO/Cu2O solar cells*. 2005.
121. Bube, R.H., *Photoelectronic Properties of Semiconductors*. 1992: Cambridge University Press.
122. Zhang, D.K., et al., *The electrical properties and the interfaces of Cu2O/ZnO/ITO p-i-n heterojunction.* Physica B: Condensed Matter, 2004. **351**(1-2): p. 178-183.
123. McShane, C.M., W.P. Siripala, and K.-S. Choi, *Effect of Junction Morphology on the Performance of Polycrystalline Cu2O Homojunction Solar Cells.* The Journal of Physical Chemistry Letters, 2010. **1**(18): p. 2666-2670.
124. Li, B.S., K. Akimoto, and A. Shen, *Growth of Cu2O thin films with high hole mobility by introducing a low-temperature buffer layer.* Journal of Crystal Growth, 2009. **311**(4): p. 1102-1105.
125. Paul, G.K., et al., *Defects in Cu2O studied by deep level transient spectroscopy.* Applied Physics Letters, 2006. **88**(14): p. -.
126. Navruz, T.S. and M. Saritas, *Determination of the optimum material parameters for intermediate band solar cells using diffusion model.* Progress in Photovoltaics: Research and Applications, 2012.
127. Gao, F., et al., *Preparation of high transmittance ZnO:Al film by pulsed filtered cathodic arc technology and rapid thermal annealing.* Applied Surface Science, 2011. **257**(15): p. 7019-7022.
128. Lee, Y.S., *Defect engineering of cuprous oxide thin-films for photovoltaic applications*, 2013, Massachusetts Institute of Technology.
129. Cheng, K., et al., *Interface engineering for efficient charge collection in Cu2O/ZnO heterojunction solar cells with ordered ZnO cavity-like nanopatterns.* Solar Energy Materials and Solar Cells, 2013. **116**(0): p. 120-125.
130. Georgieva, V., A. Tanusevski, and M. Georgieva, *Low Cost Solar Cells Based on Cuprous Oxide.* Solar Cells – Thin Film Technologies, 2011: p. 55-76.
131. Papadimitriou, L. and N.A. Economou, *Preparation of bulk single crystals of Cu2O by the plastic flow method and investigation of their electrical properties.* Journal of Crystal Growth, 1983. **64**(3): p. 604-608.
132. Toth, R.S., R. Kilkson, and D. Trivich, *Preparation of large area single-crystal cuprous oxide.* Journal of Applied Physics, 1960. **31**(6): p. 1117-1121.
133. Ebisuzaki, Y., *Preparation of monocrystalline cuprous oxide.* Journal of Applied Physics, 1961. **32**(10): p. 2027-2028.
134. Zucker, R.S., *Growth of single crystal cuprous oxide from the melt and luminescence of cuprous oxide.* Journal of The Electrochemical Society, 1965. **112**(4): p. 417-420.

135. Chang, K.B., et al., *Removal of Copper Vacancies in Cuprous Oxide Single Crystals Grown by the Floating Zone Method.* Crystal Growth & Design, 2013. **13**(11): p. 4914-4922.
136. Trivich, D. and G.P. Pollack, *Preparation of Single Crystals of Cuprous Oxide in an Arc-Image Furnace.* Journal of The Electrochemical Society, 1970. **117**(3): p. 344-345.
137. Dhanaraj, G., et al., *Springer Handbook of Crystal Growth*. 2010: Springer.
138. Ohshima, E., et al., *Growth of the 2-in-size bulk ZnO single crystals by the hydrothermal method.* Journal of Crystal Growth, 2004. **260**(1–2): p. 166-170.
139. Nielsen, J.W. and E.F. Dearborn, *The growth of large single crystals of zinc oxide.* Journal of Physical Chemistry, 1960. **64**(11): p. 1762-1763.
140. Ohashi, N., et al., *Band-edge emission of undoped and doped ZnO single crystals at room temperature.* Journal of Applied Physics, 2002. **91**(6): p. 3658-3663.
141. Shiloh, M. and J. Gutman, *Growth of ZnO single crystals by chemical vapour transport.* Journal of Crystal Growth, 1971. **11**(2): p. 105-109.
142. Matsumoto, K. and K. Noda, *Crystal growth of ZnO by chemical transport using HgCl2 as a transport agent.* Journal of Crystal Growth, 1990. **102**(1-2): p. 137-140.
143. Look, D.C., et al., *Electrical properties of bulk ZnO.* Solid State Communications, 1998. **105**(6): p. 399-401.
144. Ntep, J.M., et al., *ZnO growth by chemical vapour transport.* Journal of Crystal Growth, 1999. **207**(1): p. 30-34.
145. Laudise, R.A., E.D. Kolb, and A.J. Caporaso, *Hydrothermal Growth of Large Sound Crystals of Zinc Oxide.* Journal of the American Ceramic Society, 1964. **47**(1): p. 9-12.
146. Sekiguchi, T., et al., *Hydrothermal growth of ZnO single crystals and their optical characterization.* Journal of Crystal Growth, 2000. **214**: p. 72-76.
147. Katsumi, M., et al., *Growth of 2 inch ZnO bulk single crystal by the hydrothermal method.* Semiconductor Science and Technology, 2005. **20**(4): p. S49.
148. Olsen, L.C., R.C. Bohara, and M.W. Urie, *Explanation for low-efficiency Cu2O schottky-barrier solar cells.* Applied Physics Letters, 1979. **34**(1): p. 47-49.
149. Meyer, B.K., et al., *Binary copper oxide semiconductors: From materials towards devices.* physica status solidi (b), 2012. **249**(8): p. 1487-1509.
150. Kim, H.-K., et al., *Electrical and Structural Properties of Ti/Au Ohmic Contacts to n - ZnO.* Journal of The Electrochemical Society, 2001. **148**(3): p. G114-G117.
151. Navruz, T.S. and M. Saritas. *Intermediate band solar cells*. 2005.
152. Olea, J., et al., *Titanium doped silicon layers with very high concentration.* Journal of Applied Physics, 2008. **104**(1): p. -.
153. Gonzalez-Díaz, G., et al., *Intermediate band mobility in heavily titanium-doped silicon layers.* Solar Energy Materials and Solar Cells, 2009. **93**(9): p. 1668-1673.
154. Antolín, E., et al., *Lifetime recovery in ultrahighly titanium-doped silicon for the implementation of an intermediate band material.* Applied Physics Letters, 2009. **94**(4): p. -.
155. Castán, H., et al., *Experimental verification of intermediate band formation on titanium-implanted silicon.* Journal of Applied Physics, 2013. **113**(2): p. -.
156. Malerba, C., et al., *Nitrogen doped Cu2O: A possible material for intermediate band solar cells?* Solar Energy Materials and Solar Cells, 2012. **105**(0): p. 192-195.
157. Zhao, Z., et al., *First-principles study on the doping effects of nitrogen on the electronic structure and optical properties of Cu2O.* RSC Advances, 2013. **3**(1): p. 84-90.
158. Sage, A.P., *Systems Engineering*. 1992: Wiley.

159. Fet, A.M., E.M. Schau, and C. Haskins, *A framework for environmental analyses of fish food production systems based on systems engineering principles.* Systems Engineering, 2010. **13**(2): p. 109-118.
160. Blanchard, B.S., *System Engineering Management*. 1991: Wiley.
161. Nähr, C., Sarah Römsch, Susanne Henkel, Anja Jasper. *Smart Home with Solar Electricity*. 2012; Available from: http://en.sma-sunny.com/2012/08/07/smart-home-with-solar-electricity/.
162. Nordahl, S.H., *Private communication: Installation of PV systems in Norway*, A.E. Thorstensen, Editor 2013: Multiconsult, Oslo.
163. Blanchard, B.S., *System engineering management*. 2003: Wiley.
164. Linge, C.A.R., *Master's thesis: Modeling of the Intermediate Band Tandem Solar Cell*, in *Department of Physics* 2011, Norwegian University of Science and Technology (NTNU): Trondheim.
165. Åm, H., *Report SoRoSol dialogue meetings*, 2013, NTNU: Trondheim.
166. Luque, A. and S. Hegedus, *Handbook of photovoltaic science and engineering*. 2011: Wiley. com.
167. Nordahl, S.H., *Master's thesis: Design of Roof PV Installation in Oslo*, in *Department of Electrical Power Engineering* 2012, NTNU: Trondheim.
168. Gholami, M.M., *Private communication: Calculation of intermediate band solar cell efficiency as a function of band gaps*, 2013: NTNU, Trondheim.
169. Kinoshita, T., et al., *The approaches for high efficiency HIT solar cell with very thin (< 100 μm) silicon wafer over 23%.* 26th EUPVSC Proceedings, 2011: p. 871-874.
170. Green, M.A., et al., *Solar cell efficiency tables (version 42).* Progress in Photovoltaics: Research and Applications, 2013. **21**(5): p. 827-837.
171. Swanson, D. *The role of modeling in SunPower's commercialization efforts*. in *Challenges in PV Science, Technology, and Manufacturing: A workshop on the role of theory, modeling and simulation*. 2012. Purdue University, United States.
172. Reenaas, T.W., *Private communication: Efficiency of intermediate band solar cells*, A.E. Thorstensen, Editor 2013: NTNU, Trondheim.
173. *ZERO Conference 2013, Topic: Expanding the electricity grid to England and Germany*, A.E. Thorstensen, Editor 2013: Oslo.
174. Hodby, J., et al., *Cyclotron resonance of electrons and of holes in cuprous oxide, Cu2O.* Journal of Physics C: Solid State Physics, 1976. **9**(8): p. 1429.
175. Carel, C., M. Mouallem-Bahout, and J. Gaude, *Re-examination of the non-stoichiometry and defect structure of copper(II) oxide or tenorite, Cu1 +/- zO or CuO1 +/-epsilon - A short review.* Solid State Ionics, 1999. **117**(1-2): p. 47-55.
176. Yang, W.-Y. and S.-W. Rhee, *Effect of electrode material on the resistance switching of Cu2O film.* Applied Physics Letters, 2007. **91**(23): p. 232907-3.
177. Kikuchi, S., Y. Takahashi, and T. Sakata, *Measurement on Work Function of Polycrystalline Zinc Oxide Covered by Organic Dye.* Applied optics, 1969. **8**(101): p. 42-44.
178. Fonash, S., *Solar Cell Device Physics*. 1981: Elsevier Science.
179. Eremets, M.I., et al., *Superconductivity in boron.* Science, 2001. **293**(5528): p. 272-274.
180. Michaelson, H.B., *The work function of the elements and its periodicity.* Journal of Applied Physics, 1977. **48**(11): p. 4729-4733.
181. Wilson, R., *Vacuum Thermionic Work Functions of Polycrystalline Nb, Mo, Ta, W, Re, Os, and Ir.* Journal of Applied Physics, 1966. **37**(8): p. 3170-3172.
182. Park, Y., et al., *Work function of indium tin oxide transparent conductor measured by photoelectron spectroscopy.* Applied Physics Letters, 1996. **68**(19): p. 2699-2701.

183. Cheng Siah, S., et al., *Low contact resistivity of metals on nitrogen-doped cuprous oxide (Cu2O) thin-films.* Journal of Applied Physics, 2012. **112**(8): p. -.
184. Georgieva, V. and M. Ristov, *Electrodeposited cuprous oxide on indium tin oxide for solar applications.* Solar Energy Materials and Solar Cells, 2002. **73**(1): p. 67-73.
185. Hanafusa, A., T. Aramoto, and A. Morita, *Performance of Graphite Pastes Doped with Various Materials as Back Contact*. 2001.
186. Young Kim, S., et al., *Low-resistance Ti/Al ohmic contact on undoped ZnO.* Journal of Electronic Materials, 2002. **31**(8): p. 868-871.
187. Madelung, O., U. Rössler, and M. Schulz, *Zinc oxide (ZnO) refractive index*, in *II-VI and I-VII Compounds; Semimagnetic Compounds*. 1999, Springer Berlin Heidelberg. p. 1-12.
188. Ramanathan, K., et al., *Properties of 19.2% efficiency ZnO/CdS/CuInGaSe2 thin-film solar cells.* Progress in Photovoltaics: Research and Applications, 2003. **11**(4): p. 225-230.
189. Dodge, M.J., *Refractive properties of magnesium fluoride.* Applied optics, 1984. **23**(12): p. 1980-1985.
190. Kishore, R., S.N. Singh, and B.K. Das, *Screen printed titanium oxide and PECVD silicon nitride as antireflection coating on silicon solar cells.* Renewable Energy, 1997. **12**(2): p. 131-135.
191. Nagel, H., A.G. Aberle, and R. Hezel, *Optimised antireflection coatings for planar silicon solar cells using remote PECVD silicon nitride and porous silicon dioxide.* Progress in Photovoltaics: Research and Applications, 1999. **7**(4): p. 245-260.
192. Shannon, R.D., et al., *Refractive index and dispersion of fluorides and oxides.* Journal of physical and chemical reference data, 2002. **31**(4): p. 931-970.
193. Chin, A.K., et al., *Al2O3 as an antireflection coating for InP/InGaAsP LEDs.* Journal of Vacuum Science & Technology B, 1983. **1**(1): p. 72-73.
194. Wang, Y., et al., *Facile synthesis, enhanced field emission and photocatalytic activities of Cu2O–TiO2–ZnO ternary hetero-nanostructures.* Journal of Physics D: Applied Physics, 2013. **46**(17): p. 175303.
195. Deng, M., et al., *Screen-printed Cu2S-based Counter Electrode for Quantum-dot-sensitized Solar Cell.* Chemistry Letters, 2010. **39**(11): p. 1168-1170.
196. Delft, J.A.v., D. Garcia-Alonso, and W.M.M. Kessels, *Atomic layer deposition for photovoltaics: applications and prospects for solar cell manufacturing.* Semiconductor Science and Technology, 2012. **27**(7): p. 074002.
197. Honsberg, C. and S. Bowden. *Screen Print Rear Aluminium*. PVEducation.org 2013 [cited 2013; Available from: http://www.pveducation.org/pvcdrom/manufacturing/screen-print-rear-aluminium].
198. Hofmann, M., et al. *High-Power-Plasma PECVD of SiNx and Al2O3 for industrial solar cell manufacturing*. 2013. This conference.
199. Henini, M., *Molecular Beam Epitaxy: From Research to Mass Production*. 2012: Elsevier Science.
200. Aziz, M.J., *Film growth mechanisms in pulsed laser deposition.* Applied Physics A, 2008. **93**(3): p. 579-587.
201. Kidowaki, H., T. Oku, and T. Akiyama. *Fabrication and characterization of CuO/ZnO solar cells*. in *Journal of Physics: Conference Series*. 2012. IOP Publishing.
202. Zouari, A. and A. Ben Arab, *Effect of the front surface field on crystalline silicon solar cell efficiency.* Renewable Energy, 2011. **36**(6): p. 1663-1670.
203. von Roos, O., *A simple theory of back surface field (BSF) solar cells.* Journal of Applied Physics, 1978. **49**(6): p. 3503-3511.

204. Kalogirou, S.A., *Chapter two - Environmental Characteristics*, in *Solar Energy Engineering*. 2009, Academic Press: Boston. p. 49-762.
205. Datas, A. and C. Algora, *Detailed balance analysis of solar thermophotovoltaic systems made up of single junction photovoltaic cells and broadband thermal emitters.* Solar Energy Materials and Solar Cells, 2010. **94**(12): p. 2137-2147.

Appendix A: Solar cell fundamentals

A solar cell is essentially a p-n junction of p- and n-type semiconductors illuminated by solar radiation. A brief introduction to solar radiation, the basic operation of solar cells, and the major loss mechanisms in solar cells are described in this appendix.

Solar radiation

This section is based on solar radiation description by M. Green [Green, 2003]. A black body is a perfect absorber and emitter of black body radiation. The sun emits radiation like a black body. The sun emits light from its entire surface, and only a small fraction of this light will reach the earth. Through the earth's atmosphere, parts of the sunlight are scattered and absorbed. This affects the intensity and spectral distribution of the solar radiation that eventually reaches the surface of the earth. The path of the sunlight through the atmosphere is compared to the minimum path length when the sun's position is perpendicular to the surface of the earth. This minimum length is called air mass one, or AM1. The air mass index is calculated as follows:

$$\text{Air mass} = \frac{1}{\cos\phi} \tag{A.1}$$

ϕ is the angle of the sun in relation to the surface of the earth; see Figure A 1 [Kalogirou, 2009].

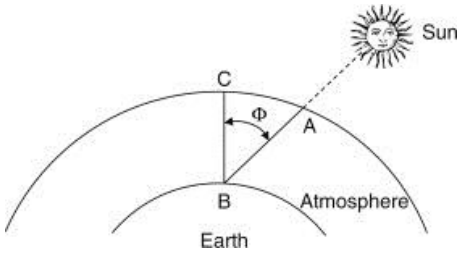

Figure A 1: Air mass definition [204].

The air mass zero spectrum, or AM0, is the solar spectrum just outside the atmosphere of the earth. Figure A 2 shows the solar spectrum for various air mass indexes [Richards, 2006].

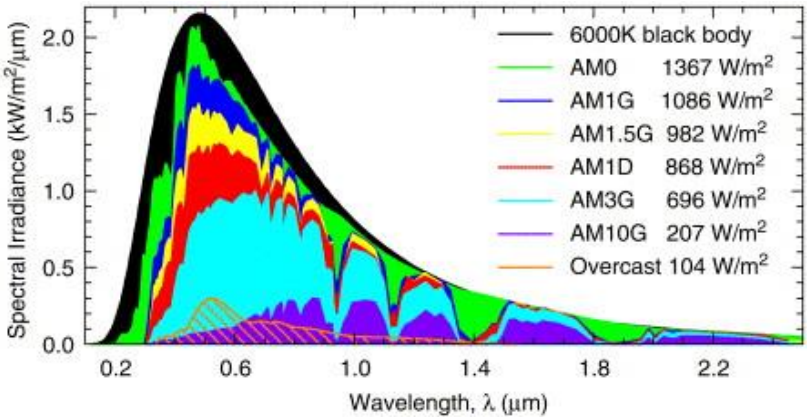

Figure A 2: The incident solar spectrum for various air mass indices and a black-body spectrum (black) [Richards, 2006].

Semiconductors and the p-n junction

The simplest solar cells consist of p- and n-type semiconductors and contacts as shown in Figure A 3 to the left [Datas, 2010] [205]. The n-type semiconductor is doped with donor atoms to achieve a high concentration of electrons, while the acceptor-doped p-type is high in hole concentration. Semiconductors have a valence band (VB) and conduction band (CB). The two energy bands are separated by the band gap, E_g (ε_{gap} in Figure A 3).

Absorption of photons of energy higher than the band gap allows electrons to transfer from the VB to the CB [Luque, 2010]. This process is referred to as carrier generation. Recombination is the opposite process, where electrons in the CB "fall" down to the VB and energy is emitted as phonons or photons. The electrons of high energy (in the CB) will flow through the contact to an external circuit, and form an electric current. The potential (or voltage) over the cell equals the energy difference between the CB and VB quasi-Fermi-levels (QFLs) on each side: $qV = \varepsilon_{fc} - \varepsilon_{fv}$, see Figure A 3, left. Outside of the cell, the electrons lose their potential energy to a load. At a lower energy, the electrons are then fed to the VB through another contact.

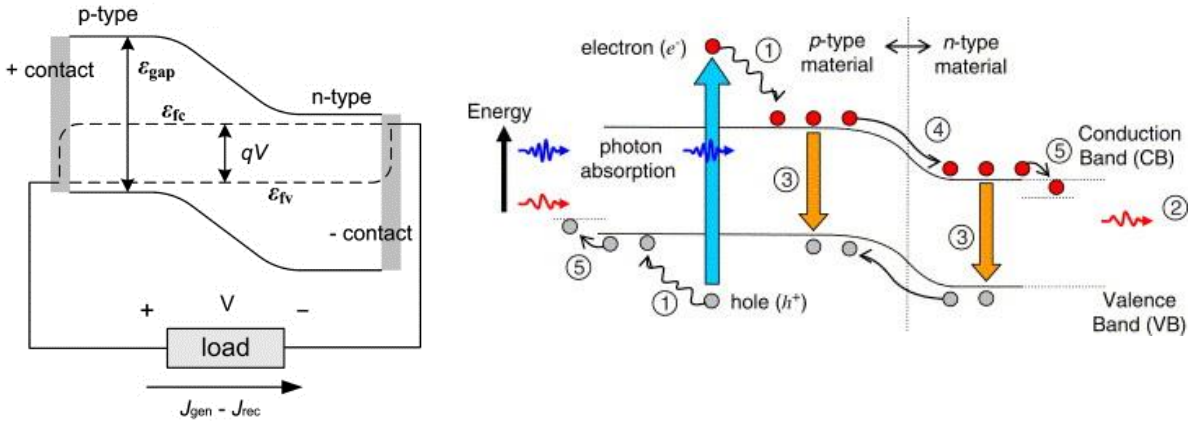

Figure A 3: Left: Schematic drawing of the band diagram of a single junction solar cell under illumination, connected to a load. J_{gen} is the photogenerated current, and J_{rec} the total recombination current (loss) [Datas, 2010]. Right: The energy processes in a solar cell (p-n junction under illumination) [Richards 2006].

Figure A 3 to the right [Richards, 2006] shows energy loss processes in a conventional single-junction solar cell. The different losses illustrated in the figure are: lattice thermalization loss (1); transparency loss (2); recombination loss (3), junction loss (4), and contact loss (5). Each of these losses contributes to reduced efficiency of the solar cell. These losses are further explained below:

1. Thermalization loss: A photon with high energy creates an electron–hole (e–h) pair far above the band edge. The e-h pair quickly loses energy in excess of the band gap via collisions with the lattice, and the extra energy is lost as heat within the device.
2. Transparency loss: The transparency (no absorbance) of the semiconductor to sub-band gap photons.
3. Recombination of e–h pairs; can be minimized by elimination of energy levels in the band gap. Radiative recombination will always occur.
4. Junction loss: The built-in potential causes an energy loss, but the loss is reduced as the voltage over the cell increases.
5. Contact loss: The Fermi-level of the contacts is typically slightly lower than in the p- and n-layers, and this results in a small energy loss.

References

Datas, A. and C. Algora, *Detailed balance analysis of solar thermophotovoltaic systems made up of single junction photovoltaic cells and broadband thermal emitters*. Solar Energy Materials and Solar Cells, 2010. **94**(12): p. 2137-2147.

Green, M.A., *Third generation photovoltaics: advanced solar energy conversion*. 2003: Springer.

Kalogirou, S.A., *Chapter two - Environmental Characteristics*, in Solar Energy Engineering. 2009, Academic Press: Boston. p. 49-762.

Luque, A. and A. Martí, *The intermediate band solar cell: progress toward the realization of an attractive concept*. Advanced Materials, 2010. **22**(2): p. 160-174.

Richards, B.S., *Enhancing the performance of silicon solar cells via the application of passive luminescence conversion layers*. Solar Energy Materials and Solar Cells, 2006. **90**(15): p. 2329-2337.

Appendix B: Theory of IBSC material properties

The main purpose of the IB material is to absorb light, and the band gap and absorption coefficient are thus the most important parameters for this material. The most important properties for the n- and p-emitters are the mobility, effective mass and resistivity.

Band gap

IBSCs with high efficiencies can be achieved for wide band gap ranges. The main (host material) band gap equals $E_g = E_H + E_L$, since the IB is assumed to have zero energy width in the ideal case. The maximum efficiency for 1 sun is 46.8 %, and for fully concentrated light 62.3 %, and based on the results from the master's thesis by Linge [Linge, 2011], the efficiency was calculated for two different light intensities; 1 sun (X=1) and fully concentrated light (X=46050) [Gholami, 2013]: The main band gap ranges 1.7 - 3.2 eV for X = 1, and 1.3 - 2.8 eV for X = 46050, results in efficiencies equal to 90 % of the maximum or higher.

If the IBSCs are combined in multi-junction (MJ) cells in the same way as for ordinary single band gap solar cells, the band gap ranges are wider than for single IBSCs. A tandem cell (2J) has a maximum efficiency of 53.9 % if the upper cell has a main band gap of 3.3 eV and the lower cell 1.35 eV at light intensity of 1 sun. Band gaps in the range 2.5 – 3.7 eV for the top cell with a 1.35 eV bottom IBSC, and 0.8 – 1.5 eV for the bottom cell with a 3.3 eV top IBSC, results in efficiencies within 90 % of the maximum; η = 48.5 – 53.9 %.

Absorption coefficient

Absorption spectra are obtained by using an absorption spectrophotometer, which compares the intensity of a light beam impinging on a sample with the intensity of the same beam after traversing the sample [Di Bartolo, 2006]:

$$I_0(\lambda) = I_i(\lambda)e^{-\alpha(\lambda)L} \tag{B.1}$$

$I_0(\lambda)$ and $I_i(\lambda)$ are the intensity at wavelength λ of output and input beam, respectively. $\alpha(\lambda)$ is the absorption coefficient of the material at wavelength λ, and L is the sample thickness.

The absorption coefficient reference value or 10^4 cm^{-1}, is typical for solar cell materials, and it is commonly used in IBSC efficiency calculations [Luque, 1997; Navruz, 2008].

Mobility and effective mass

There is not much literature on optimal mobility for IBSCs, but Navruz [Navruz, 2010] recently described how the efficiency of an IBSC material can vary with mobility. For X = 46000 the efficiency as a function of IB energy levels for an IBSC material (E_g = 1.95 eV) are shown at two different mobility and effective density of states values in Figure B 1. This figure shows that effective carrier density ($N_{C,V}$) is a more important property for the IBSC material than the mobility to reach high efficiency. From an article on optimum IB material parameters [Navruz, 2012], a mobility reference value of 200 cm^2/Vs should be suitable for IBSC materials. A desired carrier concentration for IBSC host materials is around $10^{19}cm^{-3}$, as seen from the figure.

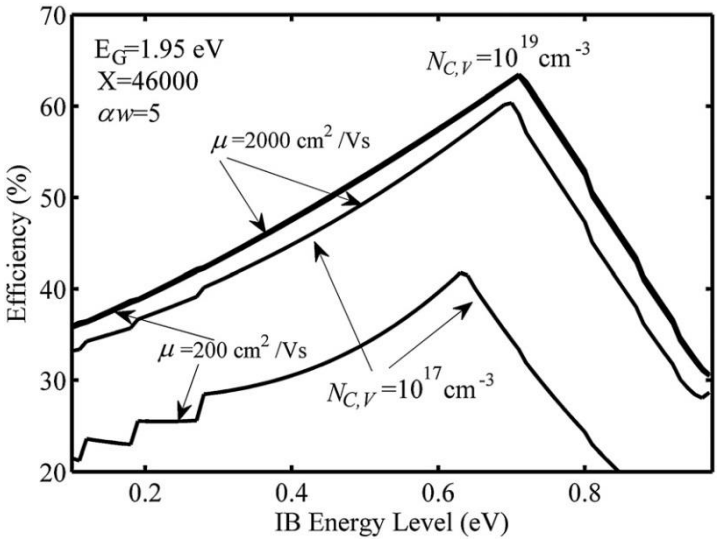

Figure B 1: Efficiency versus intermediate band energy level curves for two different effective carrier density and mobility values [Navrus, 2012].

Conductivity is a function of the mobility, and for a semiconductor the conductivity is the sum of the n-type and p-type conductivity:

$$\sigma = n\mu_e q + p\mu_h q \tag{B.2}$$

where μ_e and μ_h are carrier mobilities, defined as their average drift velocity in an electric field of unit strength, n and p are the charge carrier concentrations, and q is the elementary charge [Cox, 2010]. The purpose of the n- and p-emitters is to collect the photogenerated carriers, and transport them to the electrodes. The IB-layer is assumed to be in the depletion region of the p-n junction formed in the device, and it is assumed that carriers are effectively collected from the IB-layer to the emitters.

Electronic band structure

For intrinsic materials without defects or impurities, the carrier mobilities can be obtained from the electronic band structure of the material. The mobility of the charge carriers are related to the width (or curvature) of the conduction and valence bands.

Wide bands that are strongly curved result in high charge carrier mobility. The effective mass of the charge carriers, electrons and holes, is defined as:

$$m^* = \frac{h^2}{\left(\frac{\delta^2 E}{\delta k^2}\right)} \tag{B.3}$$

where the curvature is the denominator. Equation (B.4) shows that high curvature will give a low effective carrier mass. Low effective carrier masses will result in high carrier mobilities:

$$\mu = \frac{q\tau}{m^*}. \tag{B.4}$$

Here, τ is the lifetime of carriers that is strongly dependent on the recombination processes in the material. The lifetime depends on the crystalline quality and the purity of the material. The mobility of a material will thus decrease with increasing recombination.

In addition to the electron and hole mobilities, the carrier concentrations n and p play a role in achieving high conductivity, see Equation (B.2). The carrier concentrations n and p are functions of the density-of-states effective electron and hole masses, m_e^* and m_h^*, via the effective carrier densities N_C and N_V:

$$n = N_C e^{-(E_C - E_F)/kT} \quad \text{where} \quad N_C = 2\left(\frac{2\pi m_e^* kT}{h^2}\right)^{3/2}, \tag{B.5}$$

$$\text{and} \quad p = N_V e^{-(E_F - E_V)/kT} \quad \text{where} \quad N_V = 2\left(\frac{2\pi m_h^* kT}{h^2}\right)^{3/2}. \tag{B.6}$$

Snyder *et al.* [Snyder, 2008] explained that large effective masses produce low electrical conductivity, and the density-of-states effective masses increases in flat, narrow bands with high density of states at the Fermi surface. Heavy carriers will move at slower velocities, and lower mobility, that will result in decreased electrical conductivity, see Equation (B.2) and (B.4). High mobility and low effective mass is typically found in materials made from elements with small electronegative differences, whereas high effective masses and low mobilities are found in materials with narrow bands such as ionic compounds.

Resistivity

Resistivity is an important performance indicator in solar power generation because it shows the degree to which a material tends to impede the flow of electrical current [Brown, 2010] The resistivity is a bulk material property that determines the electrical resistance of a specific sample, regardless of how that material is eventually processed into an electrical component. There is not much literature on typical resistivity values for IBSCs, but for Si in typical solar applications, the resistivity value is commonly around 1 ohm cm [Brown 2010]. This value will be used as a reference for literature search on resistivity in this project.

Defects and impurities

To fully understand a material's optical and electronic properties, the defects present should be investigated. Defects will affect the performance of the material, and the ability to understand and predict the relationship between dopants and defect concentrations. This relationship is important for the IBSC materials and design. The simplest models for ionic materials are based on point defects [Cox, 2010], which involves two major types of point defects; Schottky and Frenkel defects [West, 1999]. The Schottky defect is a pair of vacant sites, one anion and one cation vacancy. To compensate for these vacancies, there are two atoms for each Schottky defect at the surface of the material. The Frenkel defect involves an atom displaced off its lattice site into an otherwise empty interstitial site. For non-ionic compounds, single vacancies or interstitials can occur.

In addition to the defects described above, impurities are present in almost all materials. In the case of an impurity, the usually unwanted atoms are often incorporated at regular atomic sites in the host crystal structure. This is neither vacant nor interstitial sites, and is called a substitutional defect [Askeland, 2009].

Aliovalent substitution [West, 1999], where ions are substituted by ions of different charge, involves creation of vacancies or interstitials (ionic compensation), or creation of electrons and holes (electronic compensation). Ionic compensation gives no electronic conductivity, while electronic compensation leads to semiconducting, metallic, or even superconducting products. Donors induce creation of excess electrons while acceptors create excess holes, and they both carry a net charge opposite to that of the defect they generate in the lattice.

A defect chemistry approach can be used to predict how a material will behave and change properties upon doping. The prediction of extrinsic behavior is important for p-, n-, and IB materials to achieve the wanted material properties. The knowledge of defect chemistry is important to understand why published results for a material vary in different research. Defect chemistry can for example indicate if the materials can be used to form an intermediate band.

Crystal structure

The crystal structure and lattice parameters are important material characteristics when the defect reactions taking place should be predicted. This is largely because the formation of interstitials or vacancies depends on the size of atoms or ions, packing of these elements, and the holes between elements at lattice sites. In addition, knowledge about the crystal structure and lattice parameters is important in fabrication of IBSCs, as the substrate and deposited materials should have similar lattice parameters.

A crystal of an element or a compound is constructed by repeating structural elements; atoms, molecules or ions [Shriver, 2006]. These structural elements have respective lattice points that form a crystal lattice consisting of repeating units called unit cells. The angles and lengths that define the unit cell are called lattice parameters. There are seven different crystal systems defined by the relationship between the lattice parameters in three dimensions: Cubic, tetragonal, orthorhombic, monoclinic, triclinic, trigonal, and hexagonal.

References

Askeland, D.R., P.P. Fulay, and D.K. Bhattacharya, *Essentials of Materials Science and Engineering: SI Edition*. 2009: Cengage Learning.

Brown, P., *Silicon Resistivity: Key to Solar Efficiency.* Novus Media Today, 2010.

Cox, P.A., *Transition metal oxides: an introduction to their electronic structure and properties*. 2010: Oxford Univ Pr.

Di Bartolo, B. and J. Collins, *Luminescence Spectroscopy*, in *Handbook of Applied Solid State Spectroscopy*. 2006, Springer. p. 509-575.

Gholami, M.M., *Private communication: Calculation of intermediate band solar cell efficiency as a function of band gaps*, 2013: NTNU, Trondheim.

Linge, C.A.R., *Master's thesis: Modeling of the Intermediate Band Tandem Solar Cell*, in *Department of Physics* 2011, Norwegian University of Science and Technology (NTNU): Trondheim.

Luque, A. and A. Martí, *Increasing the Efficiency of Ideal Solar Cells by Photon Induced Transitions at Intermediate Levels.* Physical Review Letters, 1997. **78**(26): p. 5014-5017.

Navruz, T.S. and M. Saritas, *Efficiency variation of the intermediate band solar cell due to the overlap between absorption coefficients.* Solar Energy Materials and Solar Cells, 2008. **92**(3): p. 273-282.

Navruz, T.S. and M. Saritas, *Determination of the optimum material parameters for*

intermediate band solar cells using diffusion model. Progress in Photovoltaics: Research and Applications, 2012.
Shriver, D. and P. Atkins, *Inorganic Chemistry*. 2006: W. H. Freeman.
Snyder, G.J. and E.S. Toberer, *Complex thermoelectric materials.* Nature materials, 2008. **7**(2): p. 105-114.
van de Krol, R., *Principles of Photoelectrochemical Cells.* Photoelectrochemical Hydrogen Production, 2011. **102**: p. 13.
West, A.R., *Basic solid state chemistry*, 1999, John Wiley & Sons (New York). p. 213-218, 230-236.

Appendix C: Values for IBSC material properties

In the specialization project where new possible host materials for IBSCs were identified [Thorstensen, 2013], reference values were found and used to indicate how suitable the individual materials were for single and tandem IBSCs, see Table C 1.

Table C 1: Reference values from the material properties studied in the specialization project.

Layer	Property	Reference value	Ref.
IB-layer	Band gap range Single IBSC	1.7 - 3.2 eV (X = 1)	Gholami, 2013
		1.3 - 2.8 eV (X = 46050)	
	Band gap range Two terminal IBSC	2.5 – 3.7 eV (top cell, X = 1) 0.8 – 1.5 eV (bottom cell, X = 1)	Linge, 2011
	Absorption coefficient	10^4 cm^{-1}	Navruz, 2008
n- and p-emitter layers	Mobility	200 cm^2/Vs	Navruz, 2012
	Resistivity	1 ohm cm	Brown, 2010

Table C 2 lists the five best alternatives for IBSC host materials found in the specialization project [Thorstensen, 2013]. The given references in the table can be found in the reference list of the specialization project.

Table C 2: The most important material properties of the five possible intermediate band host materials from the specialization project. For references, please see the specialization project.

	Bandgaps [eV]	Abs. coeff. [1/cm]	Structure	Electron mobility [cm^2/Vs]	Hole mobility [cm^2/Vs]	Resistivity [Ω cm]
Ag_2O	1.2-1.5 [47, 57, 58]	All in the range of 10^4	Cubic	128 [97]	67 [97]	$\geq 2\times10^{-5}$ [97]
Cu_2O	2.0-2.7 [47, 60, 61]		Cubic	159 [99]	130 [100]	10, 43, 120 [131-133]
SnO_2	2.5-3.5 [47, 60]		Tetragonal rutile	260 [114]	n.a.	2.8×10^{-2} [134]
ZnO	3.2-3.4 [47, 60, 61]		Cubic zincblende and tetragonal wurtzite	205 [122]	180 [123]	$\geq 3.0\times10^{-2}$ [135]
Zn_3N_2	1.2-3.2 [69, 70, 71]		Cubic	156 [128]	n.a.	$\geq 1.5\times10^{-3}$ [69]

References

Brown, P., *Silicon Resistivity: Key to Solar Efficiency*. Novus Media Today, 2010.

Gholami, M.M., *Private communication: Calculation of intermediate band solar cell efficiency as a function of band gaps*, 2013: NTNU, Trondheim.

Linge, C.A.R., *Master's thesis: Modeling of the Intermediate Band Tandem Solar Cell, in Department of Physics 2011*, Norwegian University of Science and Technology (NTNU): Trondheim.

Navruz, T.S. and M. Saritas, *Efficiency variation of the intermediate band solar cell due to the overlap between absorption coefficients*. Solar Energy Materials and Solar Cells, 2008. **92**(3): p. 273-282.

Navruz, T.S. and M. Saritas, *Determination of the optimum material parameters for intermediate band solar cells using diffusion model*. Progress in Photovoltaics: Research and Applications, 2012.

Thorstensen, A.E., *Specialization project: New materials for intermediate band solar cells*, in Department of Materials Science and Engineering 2013, Norwegian University of Science and Technology (NTNU): Trondheim.

Appendix D: Irradiation values

Irradiation values for different locations around the world are given in Table D 1.

Table D 1: Irradiation values of different locations and latitudes.

Country/*region*	City/*average*	Solar radiation [kWh/m^2/yr]	Reference
Australia	Sydney	1614	Stoppato, 2008
Austria	Vienna	1108	Stoppato, 2008
Belgium	Brussels	946	Stoppato, 2008
Canada	Ottawa	1377	Stoppato, 2008
China	Gobi dessert	1702	Ito *et al.*, 2003; Ito *et al.*, 2008; Ito *et al.*, 2009; Ito *et al.*, 2010
Czech Republic	Prague	1000	Stoppato, 2008
Denmark	Copenhagen	985	Stoppato, 2008
Finland	Helsinki	956	Stoppato, 2008
France	Paris	1057	Stoppato, 2008
France	Marseille	1560	Stoppato, 2008
Germany	Berlin	999	Stoppato, 2008
Germany	Munich	1143	Stoppato, 2008
Germany	Frankfurt	1200	SENSE, 2008; Held and Ilg, 2011
Greece	Athens	1563	Stoppato, 2008
Greece	Xanthi	1420	Filippidou, 2010
Hungary	Budapest	1198	Stoppato, 2008
Ireland	Dublin	948	Stoppato, 2008
Italy	Rome	1700	SENSE, 2008; Held and Ilg, 2011
Italy	Rome	1552	Stoppato, 2008
Italy	Milan	1251	Stoppato, 2008
Japan	Tokyo	1168	Stoppato, 2008
Japan	Hokuto	1725 (tilted)	Ito *et al.* 2011
Republic of Korea	Seoul	1215	Stoppato 2008
Luxenbourg	Luxenbourg	1035	Stoppato 2008
Middle Europe	*Average*	1000	Alsema et al. 2006
Netherlands	Amsterdam	1045	Stoppato 2008
New Zealand	Wellington	1412	Stoppato 2008
Norway	Oslo	967	Stoppato 2008
Portugal	Lisbon	1682	Stoppato 2008
Portugal	*Average*	1900	Held and Ilg 2011
Spain	Madrid	1660	Stoppato, 2008
Spain	Sevilla	1754	Stoppato, 2008
Spain	*Average*	1825	Dominguez-Ramos *et* al., 2010

Spain	*Average*	1900	Held and Ilg, 2011
Solar belt	*Average*	2200	SENSE, 2008
Southern Europe	*Average*	1700	Alsema *et al*., 2006
Sweden	Stockholm	980	Stoppato, 2008
Switzerland	Bern	1117	Stoppato, 2008
Switzerland	*Average*	1100	Jungbluth, 2005
Turkey	Ankara	1697	Stoppato, 2008
United Kingdom	London	955	Stoppato, 2008
United Kingdom	Edinburgh	890	Stoppato, 2008
United States	Washington	1487	Stoppato, 2008

References

Alsema, E. and M. de Wild-Scholten, *Environmental impacts of PV electricity generation-a critical comparison of energy supply options*. 2006.

Dominguez-Ramos, A., et al., *Prospective CO2 emissions from energy supplying systems: photovoltaic systems and conventional grid within Spanish frame conditions*. The International Journal of Life Cycle Assessment, 2010. **15**(6): p. 557-566.

Filippidou, F., et al., *A comparative analysis of a cdte and a poly-Si photovoltaic module installed in North Eastern Greece*. Applied Solar Energy, 2010. **46**(3): p. 182-191.

Held, M. and R. Ilg, *Update of environmental indicators and energy payback time of CdTe PV systems in Europe*. Progress in Photovoltaics: Research and Applications, 2011. **19**(5): p. 614-626.

Ito, M., et al., *A preliminary study on potential for very large-scale photovoltaic power generation (VLS-PV) system in the Gobi desert from economic and environmental viewpoints*. Solar Energy Materials and Solar Cells, 2003. **75**(3-4): p. 507-517.

Ito, M., et al., *A comparative study on cost and life-cycle analysis for 100 MW very large-scale PV (VLS-PV) systems in deserts using m-Si, a-Si, CdTe, and CIS modules*. Progress in Photovoltaics: Research and Applications, 2008. **16**(1): p. 17-30.

Ito, M., K. Komoto, and K. Kurokawa. *A comparative LCA study on potential of very-large scale PV systems in Gobi desert. in Photovoltaic Specialists Conference (PVSC)*, 2009 34th IEEE. 2009. IEEE.

Ito, M., K. Komoto, and K. Kurokawa, *Life-cycle analyses of very-large scale PV systems using six types of PV modules*. Current Applied Physics, 2010. **10**(2, Supplement): p. S271-S273.

Ito, M., et al., *A comparative study on life cycle analysis of 20 different PV modules installed at the Hokuto mega-solar plant*. Progress in Photovoltaics: Research and Applications, 2011. **19**(7): p. 878-886.

Jungbluth, N., *Life cycle assessment of crystalline photovoltaics in the Swiss ecoinvent database*. Progress in Photovoltaics: Research and Applications, 2005. **13**(5): p. 429-446.

SENSE, *Sustainability Evaluation of Solar Energy Systems, LCA Analysis* 2008, Wuerth Solar GmbH & Co.KG., Free Energy Europe SA, Zentrum fuer Sonnenenergie- und Wasserstoff-Forschung, Fraunhofer-Gesellschaft zur, Foerderung der Angewandten, Forschung e.V. , Ambiente Italia srl, Fundacion Gaiker: University of Stuttgart.

Stoppato, A., *Life cycle assessment of photovoltaic electricity generation*. Energy, 2008. **33**(2): p. 224-232.

Appendix E: Toxicity and material availability

During the specialization project [Thorstensen, 2013], toxicity and availability of the possible IBSC materials were considered. Other than the radioactive elements that also were disregarded, the toxic elements found were: Pb, Cd, Hg, As, Sb, Se, Te, Bi, Cr, Ni, Co, Ba and Tl [Kyle, 2011; Stohs, 2001; Seregin, 2006; Domingo, 1989; Deepthiraju, 2012; Sangvanich, 2010].

The European Commission [European Commission, 2010] has listed all the critical elements in terms of availability. These are found in Table E 1.

Table E 1: The critical elements, including all rare earths, listed by the European Commission.

Critical elements		Critical rare earth elements	
Symbol	**Name**	**Symbol**	**Name**
Sb	Antimony	Y	Yttrium
Be	Beryllium	Sc	Scandium
Co	Cobalt	La	Lanthanum
Ga	Gallium	Ce	Cerium
Ge	Germanium	Pr	Praseodymium
C	Graphite	Nd	Neodymium
In	Indium	Pm	Promethium
Mg	Magnesium	Sm	Samarium
Nb	Niobium	Eu	Europium
Pt	Platinum	Gd	Gadolinium
Pd	Palladium	Tb	Terbium
Ir	Iridium	Dy	Dysprosium
Rh	Rhodium	Ho	Holmium
Ru	Ruthenium	Er	Erbium
Os	Osmium	Tm	Thulium
Ta	Tantalum	Yb	Ytterbium
W	Tungsten	Lu	Lutetium

References

Deepthiraju, B. and P. Varma, *Barium toxicity—a rare presentation of fireworks ingestion.* Indian Pediatrics, 2012. **49**(9): p. 762-762.

Domingo, J.L., *Cobalt in the environment and its toxicological implications.* Reviews of environmental contamination and toxicology, 1989. **108**: p. 105.

European Commission, *Critical raw materials for the EU-Report of the Ad-hoc Working Group on defining critical raw materials*. European Commission (EC), 2010: p. 36-38.

Kyle, J., et al., *Review of trace toxic elements (Pb, Cd, Hg, As, Sb, Bi, Se, Te) and their deportment in gold processing. Part 1: Mineralogy, aqueous chemistry and toxicity.* Hydrometallurgy, 2011. **107**(3): p. 91-100.

Sangvanich, T., et al., *Selective capture of cesium and thallium from natural waters and*

simulated wastes with copper ferrocyanide functionalized mesoporous silica. Journal of hazardous materials, 2010. **182**(1): p. 225-231.

Seregin, I. and A. Kozhevnikova, *Physiological role of nickel and its toxic effects on higher plants.* Russian Journal of Plant Physiology, 2006. **53**(2): p. 257-277.

Stohs, S.J., et al., *Oxidative mechanisms in the toxicity of chromium and cadmium ions.* Journal of environmental pathology, toxicology and oncology: official organ of the International Society for Environmental Toxicology and Cancer, 2001. **20**(2): p. 77.

Thorstensen, A.E., *Specialization project: New materials for intermediate band solar cells*, in Department of Materials Science and Engineering 2013, Norwegian University of Science and Technology (NTNU): Trondheim.